CHEMICAL ENGINEERING SCIENCE
GENIE CHIMIQUE

VOL. 3 JUNE 1954 No. 3

The gas flow characteristics of the disc absorption column

N. A. WARNER

School of Chemical Engineering, N.S.W. University of Technology, Broadway, N.S.W.

(*Received 5 February* 1954)

Summary—The gas flow characteristics of the disc column designed by STEPHENS and MORRIS [4] are studied by means of pressure drop determinations across the column. Water is run down the column with a range of gases passing countercurrent through the column. The gases studied are hydrogen, air, vinyl chloride and dichlorodifluoromethane.

Correlations for pressure drop across the column, with and without liquid flowing over the discs, and across the empty column, are presented, which enable a correlation of data for pressure drop across a single disc to be made.

The pressure drop data and gas film coefficients of mass transfer for the disc column are compared in order to show the relationship between mass transfer characteristics and gas flow characteristics. Changes in gas flow characteristics as indicated by break points in graphs relating pressure drop and gas velocity were found to be consistent with changes in the mass transfer data. Equations which enable a prediction of the location of changes in the gas flow characteristics are developed.

Data are also presented for the flooding velocities of the disc column with the system air-water.

Résumé—Au moyen de mesures de pertes de charge au travers d'une colonne à disques de STEPHENS et MORRIS, l'auteur étudie les caractéristiques de l'écoulement gazeux. On fait couler de l'eau dans la colonne où des gaz divers passent à contre-courant : hydrogène, air, chlorure de vinyle, dichlorodifluoremethane.

L'auteur présente des corrélations pour la perte de charge au travers de la colonne, avec ou sans écoulement de fluide sur les disques, avec la colonne vide, et en déduit une corrélation pour la perte de charge correspondant au disque unique.

L'auteur compare dans le cas de la colonne à disques, les résultats sur la perte de charge et ceux sur le coefficient d'échange dans le gaz de façon à établir l'interdépendance des caractéristiques du phénomène d'échange et de l'écoulement gazeux. On trouve que des changements dans le caractère de l'écoulement qui ne manifestent pas une brisure sur les courbes : perte de charge/vitesse d'écoulement, concordent avec des altérations dans le phénomène d'échange de matière. L'auteur développe des équations prédisant les altérations dans les caractéristiques de l'écoulement.

Données sur les vitesses d'inondation de la colonne à disque dans le système air-eau.

INTRODUCTION

The disc column as introduced by STEPHENS and MORRIS [4] has to date been used primarily for the investigation of gas absorption systems in which the liquid film is the major resistance. To evaluate the liquid film coefficients, the overall coefficients of mass transfer are corrected to take into account the effect of gas film resistance.

To establish the characteristics of the column with respect to the gas film, STEPHENS and MORRIS [4] applied a liquid film correction to overall coefficients obtained for the absorption of ammonia in water from dilute mixtures with air. These results were then applied to other gas mixtures by means of a general correlation applicable to wetted-wall columns [1], [2], viz.:

$$\frac{M_d k_g}{v \rho_d} = \beta \left(\frac{Dv\rho}{\mu}\right)^{-n} \left(\frac{\mu}{\rho D_v}\right)^{-m} \frac{P}{P_{BM}}$$

ROPER [3] reported data for the evaporation of water and carbon tetrachloride by air in a disc column. These data and the gas film coefficients for the absorption of ammonia in water from dilute mixtures with air were well correlated by an equation of the same form as used by STEPHENS and MORRIS.

The use of a general correlation applicable to wetted wall columns for the determination of gas film coefficients in a disc column is not entirely justified on the basis of the experimental work reported. No data have been published for gas film coefficients in a disc column for any other gas phase except air or dilute mixtures with air as the diluent.

Theoretical and experimental developments in the three fields of fluid friction, heat and mass transfer indicate that they are all closely related. It was therefore considered that an investigation of the gas flow characteristics of the disc column would provide data useful in the interpretation of gas film mass transfer coefficients. It is reasonable to expect comparable changes in the mass transfer coefficients and the conditions of gas flow. STEPHENS and MORRIS observed a change in slope of the line obtained when the gas film coefficients for a particular liquid rate were plotted against relative velocity of the air stream. The existence of such a discontinuity or " break point " in the graph is an indication that the gas flow characteristics of the disc column also undergo a change at a definite air velocity.

The gas flow characteristics of the disc column were conveniently studied by pressure drop measurements across the discs of the column. By selecting a range of gases which had extremely different physical properties it was possible to establish relationships which showed the positions of discontinuities observed in the gas flow conditions and enabled the pressure drop measurements to be correlated with the velocity and physical properties of the gas phase.

A knowledge of the limiting capacity is useful in the design of experimental work using the disc column. The air velocities at which the column ceased to function due to entrainment of the liquid were determined.

VOL. 3 1954

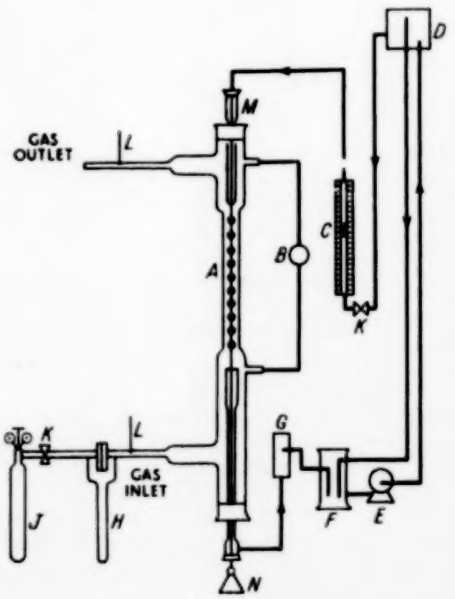

Fig. 1. Diagram of apparatus.

A—Disc column
B—Micromanometer
C—Liquid rotameter
D—Constant head tank
E—Circulating pump
F—Pump sump
G—Liquid seal arrangement
H—Calibrated orifice plate
J—Compressed gas source
K—Needle control valve
L—Thermometer
M—Liquid flow nozzle
N—Disc supporting weight

EXPERIMENTAL PROCEDURE AND RESULTS

Apparatus

The laboratory column used was developed by STEPHENS and MORRIS [4] and consisted of 27 carbon discs, 1·45 to 1·5 cm diameter, 0·44 to 0·45 cm thick, threaded edgeways on a 16 B.S.W. wire. The discs were maintained mutually at right angles by means of a plastic cement. The disc assembly forming the liquid flow path was mounted vertically inside a 2·5 cm bore glass tube through which the gas was passed. The manometer tappings for determining the pressure drop across the discs were located a short distance from each end of the disc assembly.

Table 1. *Principal dimensions of disc column*

Number of discs	= 27
Disc diameter	= 1·475 cm
Disc thickness	= 0·45 cm
Tube diameter	= 2·5 cm
Mean perimeter for liquid flow	= 0·122 ft.
Equivalent diameter for gas flow	= 0·052 ft.
Free space (dry)	= 89%
Absorption surface (dry)	= 0·1605 sq. ft.

The pressure drop readings were measured using a micromanometer graduated to read to one hundredth of a millimetre water gauge pressure differential.

The general layout of the apparatus is shown in Fig. 1 and the principal dimensions are shown in Table 1.

Procedure

The total pressure drop across the column was obtained for different liquid and gas flow rates for a wide range of gases. The gases studied were hydrogen (mol. wt. = 2), air (mol. wt. = 29), vinyl chloride (mol. wt. = 62·5) and dichlorodifluoromethane (mol. wt. = 121). As the investigation was centred on the gas phase characteristics, the liquid phase flowing over the discs was not varied and water was used in all runs.

Due to the construction of the column used it was considered necessary to determine the pressure drop over the column without the discs in position with the same range of gases. These readings enabled an estimate of the pressure drop over the discs to be made as distinct from the pressure drop over the complete column, including column walls and entrance and exit losses.

The maximum air velocities at which the column could be operated without the water being blown from the discs and the column flooding, were also investigated for different liquid rates. The liquid rate was kept constant and the gas velocity slowly increased until flooding occurred.

Results

(a) *Pressure drop across column*

The data for pressure drop across the whole column for the range of gases : hydrogen, air, vinyl chloride and dichlorodifluoromethane are shown in Table 2. The data are well correlated when ΔP_t is plotted against $v\rho^{0.41}\ \Gamma^{0.22}$ on a log-log scale as shown in Fig. 2.

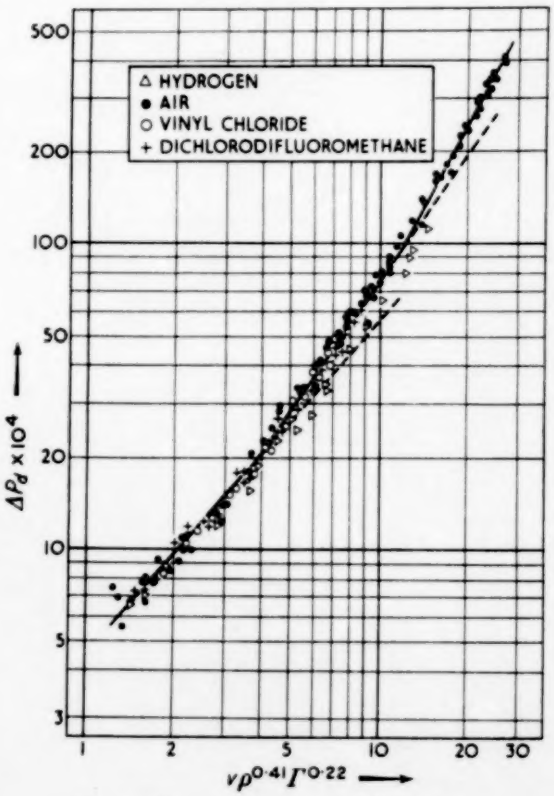

Fig. 2. Pressure drop across the column.

Table 2. Data for pressure drop across the column.

Liquid Rate lb./hr.ft.	*Gas Velocity ft./sec.*	*Gas Re*	ΔP_f *lb./ft.²*
	Air – Water		
408	5·13	1650	0·1580
408	6·90	2210	0·2420
408	8·35	2680	0·3195
408	8·83	2835	0·3490
408	10·8	3470	0·4920
408	13·6	4370	0·6940
408	15·6	5000	0·8740
408	16·5	5290	0·9625
408	17·7	5680	1·0970
408	20·6	6620	1·4430
335	1·05	337	0·0226
335	1·28	411	0·0266
335	1·42	456	0·0308
335	1·75	562	0·0368
335	2·37	761	0·0492
335	2·85	916	0·0636
335	3·70	1190	0·0944
335	4·90	1573	0·1394
335	7·35	2360	0·2440
335	8·80	2820	0·3078
188	4·23	1360	0·1043
188	6·30	2020	0·1763
188	7·40	2380	0·2214
188	9·40	3020	0·3074
188	10·7	3430	0·3996
188	13·0	4175	0·5280
188	14·4	4620	0·6425
188	16·2	5190	0·7560
	Dichlorodifluoromethane – Water		
253	3·96	7700	0·1970
253	3·41	6630	0·1620
253	2·76	5370	0·1150
253	2·16	4190	0·0818
253	1·67	3244	0·0594
253	1·34	2608	0·0432
253	0·96	1865	0·0328
166·5	3·97	7720	0·1663
166·5	3·34	6500	0·1393
166·5	2·78	5400	0·1044
166·5	2·26	4390	0·0779
166·5	1·82	3540	0·0574
166·5	1·32	2570	0·0410
166·5	0·92	1780	0·0256
	Vinyl Chloride – Water		
253	4·27	5080	0·1457
253	3·93	4680	0·1270
253	3·52	4180	0·1087
253	3·03	3600	0·0862
253	2·70	3210	0·0717
253	2·36	2810	0·0594
253	1·94	2310	0·0493
253	1·50	1785	0·0369
253	1·16	1605	0·0269

Liquid Rate lb./hr.ft.	*Gas Velocity ft./sec.*	*Gas Re*	ΔP_f *lb./ft.²*
	Air – Water		
368	4·95	1590	0·1438
358	6·20	1990	0·1926
368	7·40	2380	0·2566
368	8·50	2730	0·3080
368	11·30	3630	0·4955
368	12·8	4120	0·6060
368	13·5	4330	0·6600
368	14·7	4720	0·7675
368	17·2	5530	1·0030
368	19·0	6100	1·1690
368	19·7	6330	1·2730
368	21·1	6780	1·4390
166·5	0·96	296	0·0144
166·5	1·35	433	0·0239
166·5	1·53	491	0·0246
166·5	1·80	577	0·0308
166·5	2·16	693	0·0369
166·5	2·70	867	0·0470
166·5	4·05	1300	0·0881
166·5	5·60	1797	0·1294
166·5	6·95	2230	0·01890
166·5	9·04	2900	0·02650
188	18·2	5840	0·9415
188	20·2	6480	1·1320
188	21·2	6810	1·2475
188	22·0	7060	1·3225
355	3·93	7640	0·2113
355	3·37	6550	0·1725
355	2·82	5480	0·1330
355	2·03	3940	0·0882
355	1·47	2860	0·0575
355	1·01	1963	0·0369
355	0·665	1293	0·0226
355	4·22	5020	0·1636
355	3·94	4690	0·1475
355	3·52	4180	0·1250
355	3·00	3570	0·1006
355	2·43	2900	0·0718
355	1·92	2280	0·0512
355	1·62	1930	0·0410
355	1·29	1537	0·0328

Liquid Rate lb./hr.ft.	*Gas Velocity ft./sec.*	*Gas Re*	ΔP_f *lb./ft.²*
	Air – Water		
281	4·43	1425	0·1187
281	6·55	2100	0·2032
281	8·20	2630	0·2870
281	10·8	3470	0·4372
281	13·0	4175	0·5930
281	16·0	5130	0·8322
281	18·7	6000	1·1100
281	20·7	6650	1·3350
255	1·05	337	0·0238
255	1·35	433	0·0266
255	1·80	578	0·0328
255	1·90	611	0·0390
255	2·40	772	0·0471
255	3·16	1015	0·0737
255	4·60	1477	0·1187
255	6·40	2055	0·1826
255	7·10	2280	0·2177
255	8·10	2760	0·2784
378	1·05	337	0·0188
378	1·35	433	0·0266
378	1·70	546	0·0350
378	2·32	745	0·0492
378	3·22	1035	0·0782
378	4·30	1381	0·1169
378	5·80	1860	0·1725
378	6·90	2210	0·2210
378	8·50	2730	0·2996
	Hydrogen – Water		
255	13·6	630	0·0964
255	15·2	704	0·1087
255	17·2	795	0·1312
255	20·5	950	0·1745
255	23·5	1090	0·2112
255	26·5	1230	0·2544
255	29·5	1365	0·3060
255	16·2	750	0·1250
255	33·0	1530	0·3510
255	38·0	1760	0·4325
255	33·6	1560	0·3670
255	3·65	169	0·0226
255	4·1	190	0·0246
255	4·8	222	0·0308
255	7·3	338	0·0452
255	9·3	430	0·0595
255	12·5	579	0·0881
255	10·0	463	0·0696
255	14·0	648	0·1024

VOL. 3 1954

The three straight lines of Fig. 2 and the location of the " break points " are better illustrated by plotting the dimensional group $\frac{\Delta P_t}{v^2\rho}$ against gas velocity. A comparison between the two methods of plotting is shown in Fig. 3, in which ΔP_t and $\frac{\Delta P_t}{v^2\rho}$ are plotted against gas velocity for data of one of the air-water runs shown in Table 2.

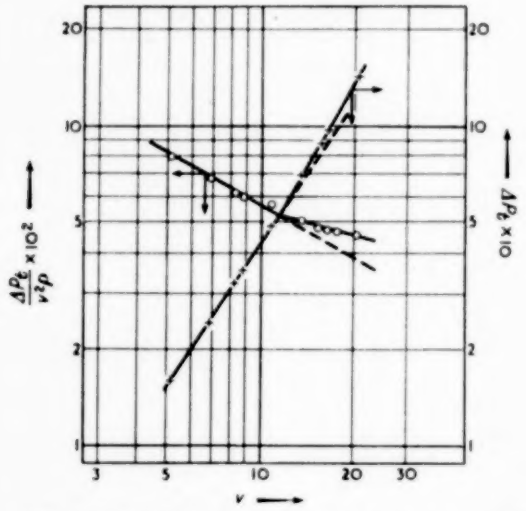

Fig. 3. Comparison of methods of plotting data

$\frac{\Delta P_t}{v^2\rho}$ versus v

ΔP_t versus v

Air-water system ($\Gamma = 408$ lb./(hr.)(ft.).

The method of plotting $\frac{\Delta P}{v^2\rho}$ was adopted for all runs to determine the " break points " but it was considered more fundamental to present final empirical correlations in terms of the pressure drop ΔP.

(b) *Pressure drop across column with zero liquid rate*

Flow through the dry column is equivalent to flow through porous media with a single fluid phase. Such data are best correlated by plotting a friction factor against Reynolds Number on log-log paper.

However, it is unnecessary to use the complete Fanning friction factor for purposes of illustrating the flow characteristics of a particular column.

The dimensional group $\frac{\Delta P_t}{v^2\rho}$ has been plotted against Re in Fig. 4 for data on the pressure drop across the dry column as shown in Table 3.

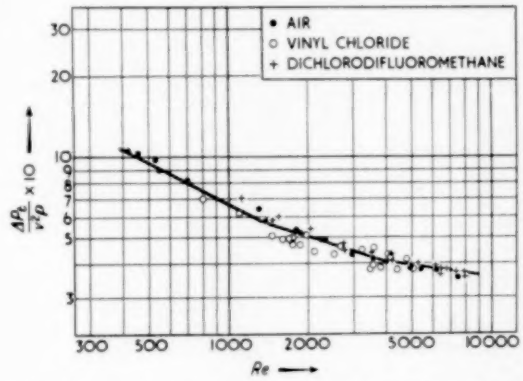

Fig. 4. Pressure drop across column at zero liquid rate.

(c) *Pressure drop across the empty column*

To evaluate the pressure drop due to the disc assembly it was considered necessary to determine the pressure drop due to the glass column itself without the discs in place.

Correlation of the data shown in Table 4 is obtained by plotting the dimensional group $\frac{\Delta P_e}{v^2\rho}$ against Re on a log-log graph as shown in Fig. 5.

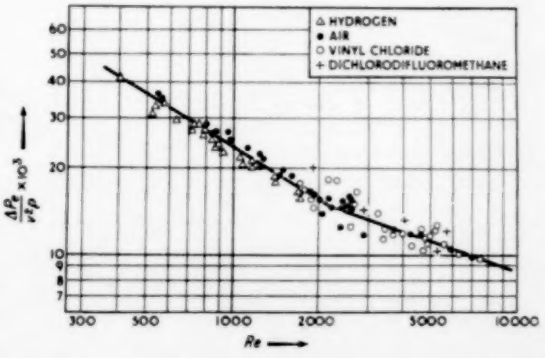

Fig. 5. Pressure drop across the empty column (discs removed).

Table 3. Pressure drop across the column at zero liquid rate.

Gas Velocity ft./sec.	*Gas Re*	ΔP_t *lb./ft.*^{2}	*Gas Velocity ft./sec.*	*Gas Re*	ΔP_t *lb./ft.*^{2}	*Gas Velocity ft./sec.*	*Gas Re*	ΔP_t *lb./ft.*^{2}
	Air			*Vinyl Chloride*			*Dichlorodifluoromethane*	
1·35	417	0·0143	4·17	4960	0·1067	4·03	7850	0·1822
1·67	537	0·0205	3·72	4420	0·0839	3·46	6730	0·1413
4·30	1380	0·0800	3·20	3800	0·0635	3·09	6000	0·1169
5·75	1845	0·1290	2·96	3520	0·0553	2·70	5250	0·0922
7·2	2310	0·1886	2·11	2510	0·0307	2·15	4175	0·0594
9·08	2920	0·2642	1·47	1750	0·0164	1·42	2760	0·0307
2·17	698	0·0286	1·23	1463	0·0123	1·04	2020	0·0185
1·42	457	0·0154	0·68	950	0·0051	0·75	1460	0·0103
1·67	537	0·0184	3·5	4160	0·0822	4·02	7820	0·1887
6·20	1990	0·1683	3·0	3570	0·0656	3·73	7250	0·1620
8·20	2630	0·2420	2·68	3190	0·0513	3·30	6420	0·1313
10·7	3430	0·3852	2·23	2660	0·0369	2·97	5770	0·1067
14·2	4560	0·5980	1·66	1973	0·0226	2·53	4920	0·0800
16·3	5230	0·7155	1·35	1605	0·0143	2·14	4160	0·0615
19·2	6160	0·9665	0·91	1082	0·0082	1·82	3540	0·0452
20·7	6650	1·0975	4·0	4760	0·1064	1·42	2760	0·0287
22·2	7130	1·2310	3·45	4110	0·0821	0·80	1566	0·0123
24·0	7700	1·3975	3·07	3650	0·0635	0·57	1108	0·0072
			2·50	2980	0·0430			
			2·10	2500	0·0307			
			1·78	2120	0·0225			
			1·47	1750	0·0174			
			1·44	1713	0·0164			
			1·56	1855	0·0185			

(d) *Corrected pressure drop due to discs*

The pressure drop across the column due to the discs was obtained by substracting the pressure drop due to the empty column (as determined from Fig. 5) from the pressure drop data due to the assembled column.

An example of the method of calculation used to approximate the pressure drop across a single disc in a disc column is shown in Table 5.

The estimated pressure drop ΔP_d due to a single disc is well correlated by plotting ΔP_d against $v\rho^{0.41}\ \Gamma^{0.22}$ on a log-log graph.

The dimensional equations for this correlation are

Let $v\rho^{0.41}\ \Gamma^{0.22} = \phi$

(a) Above $\phi = 12$

$$\Delta P_d = 9{\cdot}8 \times 10^{-5}\ \phi^{1.84}$$

(b) Between $\phi = 12$ and $\phi = 4$

$$\Delta P_d = 2{\cdot}94 \times 10^{-4}\ \phi^{1.41}$$

(c) Below $\phi = 4$

$$\Delta P_d = 4{\cdot}5 \times 10^{-4}\ \phi^{1.09}$$

(e) *Flooding characteristics*

The "flooding velocity" of the column with water flowing over the discs at various liquid rates and air passing up the column was determined visually. The first visual appearance of flooding occurred when small drops of water were blown off the periphery of the wetted discs. The column became unstable at this point and as the gas velocity was increased or the liquid rate was increased, slugs of liquid were blown off the discs and surged upward through the column.

Due to the unstable nature of the column when

VOL. 3 1954

Table 4. Pressure drop across the empty column (discs removed).

Gas Velocity ft./sec.	*Gas Re*	ΔP_e *lb./ft.²*
	Hydrogen	
8·7	402	0·0164
11·3	522	0·0205
15·8	730	0·0369
19·0	880	0·0451
23·0	1065	0·0595
25·2	1165	0·0675
30·3	1400	0·0863
37·0	1710	0·1150
11·5	532	0·0225
12·3	570	0·0266
16·3	755	0·0389
17·2	797	0·0410
19·7	913	0·0451
23·0	1065	0·0573
25·0	1157	0·0677
30·3	1400	0·0862
36·5	1690	0·1128
13·8	638	0·0287
15·6	722	0·0348
18·2	843	0·0431
14·7	680	0·0318
17·2	796	0·0410
19·0	880	0·0451
	Air	
1·77	568	0·0082
2·68	860	0·0144
3·1	995	0·0184
4·04	1297	0·0267
5·10	1637	0·0369

Gas Velocity ft./sec.	*Gas Re*	ΔP_e *lb./ft.²*
	Air	
6·10	1958	0·0451
6·85	2199	0·0553
7·60	2440	0·0676
8·30	2664	0·0758
1·73	555	0·0082
2·50	803	0·0133
2·74	880	0·0154
3·55	1140	0·0225
3·95	1268	0·0266
4·70	1509	0·0327
5·85	1878	0·0429
6·95	2230	0·0532
7·70	2472	0·0655
8·20	2632	0·0820
2·50	803	0·0164
3·02	969	0·0184
3·85	1236	0·0225
4·60	1477	0·0308
5·10	1637	0·0369
6·35	2038	0·0472
7·9	2536	0·0697
8·2	2632	0·0800
5·9	1895	0·0410
8·1	2600	0·0614
10·6	3400	0·0944
15·2	4870	0·1907
17·7	5670	0·2560

Gas Velocity ft./sec.	*Gas Re*	ΔP_e *lb./ft.²*
	Air	
19·6	6280	0·2890
23·5	7540	0·4020
5·45	1155	0·0328
6·40	2060	0·0431
7·40	2380	0·0513
9·10	2920	0·0717
11·5	3680	0·1190
13·2	4230	0·1558
14·5	4650	0·1865
18·6	5960	0·2682
22·3	7150	0·3668
	Vinyl Chloride	
1·62	1928	0·0061
2·30	2737	0·0144
2·90	3451	0·0164
3·35	3987	0·0210
4·10	4879	0·0307
4·00	4760	0·0266
1·46	1737	0·0061
1·84	2190	0·0103
2·25	2678	0·0123
2·70	3213	0·0164
3·12	3713	0·0185
3·62	4311	0·0226
3·90	4641	0·0297
4·16	4950	0·0317
4·45	5296	0·0389
4·40	5236	0·0389
1·95	2321	0·0113
1·50	1785	0·0061
	Dichlorodifluoromethane	
2·75	5350	0·0246
0·98	1907	0·0061
1·50	2920	0·0103
2·1	4080	0·0184
2·93	5700	0·0328

the flooding point is approached it was found difficult to determine accurately the flooding point.

Data based on the visual determination of the flooding velocity for different liquid rates are shown in Table 6.

Table 5. Determination of pressure drop across a disc.

Liquid rate lb./(hr.)(ft.)	*Gas velocity* ft./sec.	*Gas* R_e	ΔP_t lb./ft.^{2}	ΔP_e lb./ft.^{2} (*from Fig. 5*)	$\Delta P_t - \Delta P_e$ lb./ft.^{2}	ΔP_d lb./ft.^{2}
368	4·95	1590	0·1438	0·0328	0·1110	0·00411
368	6·20	1990	0·1926	0·0450	0·1476	0·00547
368	7·40	2380	0·2566	0·0597	0·1969	0·00729
368	8·50	2730	0·3080	0·0755	0·2325	0·00853
368	11·3	3630	0·4955	0·1200	0·3755	0·01389
368	12·8	4120	0·6060	0·1482	0·4578	0·01695
368	13·5	4330	0·6600	0·1606	0·4994	0·01851
368	14·7	4720	0·7675	0·1857	0·5818	0·02153
368	17·2	5530	1·0030	0·2400	0·7630	0·02820
368	19·0	6100	1·1690	0·2846	0·8844	0·03272
368	19·7	6330	1·2730	0·3030	0·9700	0·03590
368	21·1	6780	1·4390	0·3380	1·1010	0·04075

Table 6. Air velocities which initiate flooding.

(Flooding visually determined.)

Liquid rate lb./(hr.)(ft.)	*Air velocity* ft./sec.
101	32·0
141	27·0
188	26·5
234	23·5
281	22·5
325	21·0
368	21·5
408	20·0

DISCUSSION

The correlation for pressure drop across a disc, in which ΔP_d is plotted against $v\rho^{0.41} \Gamma^{0.22}$ on a log scale shows that the graph obtained is discontinuous and is characterised by two break points over the range studied. These break points are at $v\rho^{0.41} \Gamma^{0.22} = 4$ and $v\rho^{0.41} \Gamma^{0.22} = 12$. The positions of the break points for a particular system are not fixed exactly by these equations, as they tend to give high values of the critical velocities for the air runs and low values for the hydrogen and dichlorodifluoromethane runs. However, they do give an indication of the gas phase velocities, near which changes in the gas flow conditions can be expected.

The existence of these critical points is better illustrated by plotting $\frac{\Delta P_t}{v^2\rho}$ against gas Reynolds Number Re for individual runs with

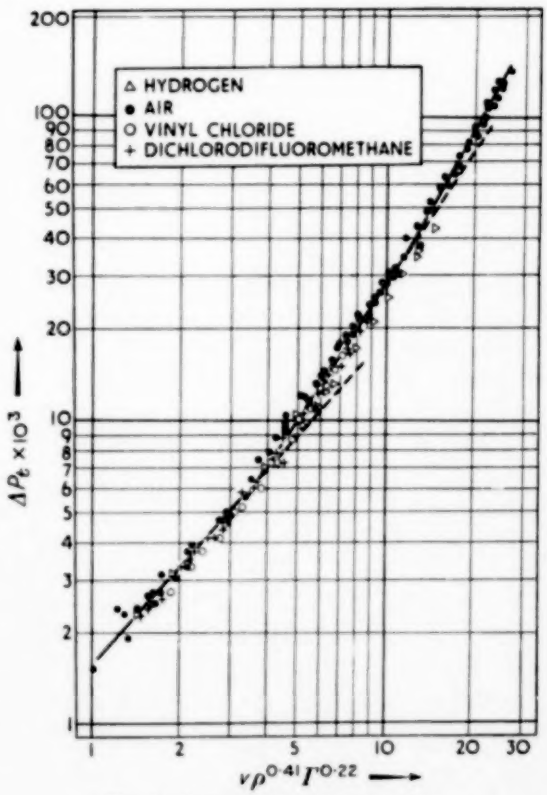

Fig. 6. Pressure drop across a disc.

VOL. 3 1954

liquid rates as parameters. Such a series of graphs is presented in Fig. 7.

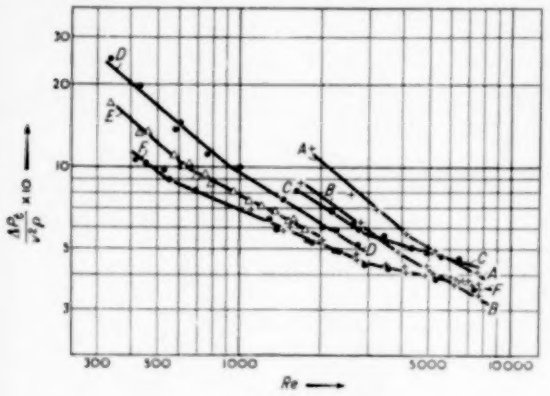

Fig. 7.

AA	dichlorodifluoromethane-water	$\Gamma = 255$ lb./(hr.)(ft.)
BB	dichlorodifluoromethane-water	$\Gamma = 131$ lb./(hr.)(ft.)
CC	air-water	$\Gamma = 408$ lb./(hr.)(ft.)
DD	air-water	$\Gamma = 255$ lb./(hr.)(ft.)
EE	hydrogen-water	$\Gamma = 255$ lb./(hr.)(ft.)
FF	air and dichlorodifluoromethane	$\Gamma = 0$ lb./(hr.)(ft.)

Referring to Fig. 7 the lines *AA* and *BB* are typical of a group of lines obtained for a particular gas phase with different liquid rates showing the existence of a break point at a Reynolds Number of approximately 4000. This break point corresponds to the lower break point of the correlation shown in Fig. 2. Lines *AA*, *DD* and *EE* are for different gas phases with the same liquid rate. The break points for these lines are approximately $Re = 4000$, $Re = 950$ and $Re = 600$ respectively. These break points all correspond to the lower break points of the correlation shown in Fig. 2. A break point corresponding to the higher break point of the correlation shown in Fig. 2 is indicated by the line *CC* at $Re = 3000$.

The inclusion in Fig. 7 of the data for the dry column shows that the flow conditions can be well correlated by graphing $\frac{\Delta P_t}{v^2\rho}$ against Re as shown by line *FF*. However, once the column is operating with liquid flowing over the discs the gas flow characteristics at a constant liquid rate can no longer be correlated by a Reynolds Number alone.

This can be clearly seen from the lines *EE*, *DD* and *AA*, which are for constant liquid rate with different gas phases. Hence it appears that the use of a gas Reynolds Number together with some functions of liquid rate as adopted by STEPHENS and MORRIS [4] and ROPER [3] for a correlation of gas film mass transfer coefficients, is not sufficient for a general correlation applicable to all gaseous systems.

As can be seen from Fig. 7, the line for zero liquid rate is found to intersect the line *BB* for dichlorodifluoromethane at a high Reynolds Number and then continues above the low liquid rate line. A similar effect was noticed if the low liquid rates of the air runs were plotted. The higher pressure drop of the dry column at the high Reynolds Number could be attributed to the increase in impact pressure losses on the square edges of the dry discs. The effect of liquid flowing is to round off the discs and thereby reduce the impact pressure losses. However, the liquid flowing over the discs will greatly increase skin friction and hence the general trend that pressure drop is increased with increased liquid rate.

The fact that break points are observed indicate that flow conditions in the gas phase change at definite critical points. Hence it is reasonable to expect some comparable change in the gas film coefficient under similar conditions. The data of ROPER [3] and STEPHENS and MORRIS [4] were critically examined for discontinuity in the gas film coefficient at gas velocities corresponding to the break points indicated by pressure drop measurements.

The bulk of the data reported by ROPER [3] on the evaporation of water in a disc column was for air velocities which are below the first break point on the pressure drop relations. However, data for liquid rates of 121 lb./(hr.)(ft.) and 81 lb./(hr.)(ft.) extend on both side of the first break point observed in the pressure drop relation investigated. These data have been plotted in Fig. 8 in which the pressure drop data for a low liquid rate of the air-water system are also shown.

The break point in the gas film mass transfer coefficient graph compares well with the observed break point in the pressure drop data. The data of STEPHENS and MORRIS [4] for the gas film

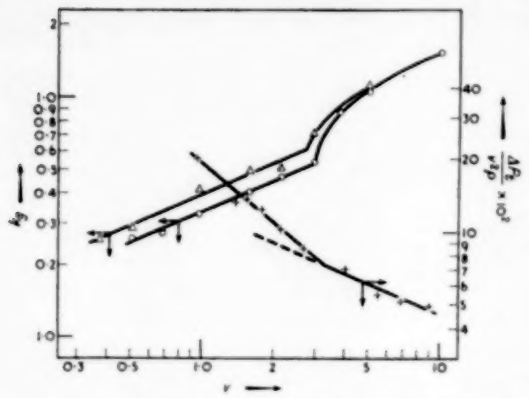

Fig. 8. Comparison of pressure and mass transfer characteristics.

● Γ = 121 lb./(hr.)(ft.) } Data of ROPER [3]
○ Γ = 81 lb./(hr.(ft.) } For gas film mass transfer coefficients in the evaporation of water in streams of air.
+ Γ = 166·5 lb./(hr.)(ft.) Pressure drop data for air-water system.

coefficient in the absorption of dilute ammonia-air mixtures by water, when plotted in the same manner, also show a break point which is consistent with that observed for pressure drop data.

ACKNOWLEDGMENTS

Acknowledgment is made to Professor J. P. BAXTER and Mr. G. H. ROPER, School of Chemical Engineering, N.S.W. University of Technology, for helpful discussion and interest in this work. Acknowledgment is also made to the *Monsanto Chemical Company (Aust.)* for the provision of the research scholarship which made this investigation possible.

NOTATION

D = equivalent diameter for gas flow, ft.
D_v = diffusivity, ft.^{2}/hr.
k_g = gas film mass transfer coefficient, lb./(hr.)(ft.^{2})(atm.)
M_d = molecular weight of the diffusing gas
P_{BM} = logarithmic mean of the partial pressure of the inert gas at the phase boundary and in the bulk of the gas stream, atm.
P = total pressure, atm.
ΔP = pressure drop, lb./ft.^{2}
ΔP_t = pressure drop across the whole column, lb./ft.
ΔP_e = pressure drop across the empty column (discs removed), lb./ft.^{2}
ΔP_d = pressure drop due to a single disc in a disc column, lb./ft.^{2}
Re = Reynolds Number for the gas phase, $Dv\rho/\mu$
v = velocity of the gas stream, ft./sec.
Γ = liquor rate, lb./(hr.)(ft.)
β = a function of liquid rate
μ = absolute viscosity of the gas stream, lb. mass./(ft.)(hr.)
ρ = density of the gas stream, lb./ft.^{3}
ρ_d = density of the diffusing gas, lb./ft.^{3}
ϕ = the dimensional function $v\rho^{0.41}\,\Gamma^{0.22}$
n = exponent of Reynolds Number
m = exponent of the Schmidt Number

REFERENCES

[1] GILLILAND, E. R. and SHERWOOD, T. K.; Ind. Eng. Chem. 1934 **26** 516.
[2] JOHNSTONE, H. F. and PIGFORD, R. L.; Trans. Amer. Inst. Chem. Engrs. 1942 **38** 25.
[3] ROPER, G. H.; Chem. Eng. Sci. 1953 **2** 18.
[4] STEPHENS, E. J. and MORRIS, G. A.; Chem. Eng. Progr. 1951 **47** 232.

Chemical Engineering Science, 1954, Vol. 3, pp. 87 to 96. Pergamon Press Ltd.

Hydroextraction IX: Studies of flow through incompressible cakes

M. M. Haruni,** K. H. Todhunter* and J. Anderson Storrow

Chemical Engineering Laboratory, College of Technology, Manchester, England

(*Received* 13 *November* 1952)

Summary—Hydroextraction and filtration tests on rigid beds of particles, consisting of either sintered metal or ceramic material, have proved conclusively the mechanism and flow equations for hydroextraction postulated in previous communications.

Résumé—Les auteurs ont procédé à des essais de centrifugation et de filtration sur les couches rigides de particules constituées soit de métaux frittés soit de matériaux céramiques. Ces essais ont définitivement prouvé l'exactitude du mécanisme et des équations imaginés dans leurs communications précédentes sur la centrifugation.

Previous work has shown that the flow mechanism of hydroextraction is covered adequately by equations proposed from this laboratory [1, 2]. The discrepancies between hydroextraction permeabilities derived from these equations and filtration permeabilities measured without disturbance of the centrifuge cake are still significant, though probably due to causes discussed in the previous communications. To confirm the validity of the hydroextraction equations, by attaining a close agreement with filtration relations, tests were justified on cakes which were incompressible and invariable in permeability under the experimental range of centrifugal fields. The following account describes tests on porous ceramic cylinders which represented complete cakes and on sintered metal plugs representing a radial element of a cake.

Tests have been made using metal dust, e.g. zinc, to make incompressible beds. The characteristics of such beds are satisfactory in purely centrifuging studies, but they are difficult to test in filtration within the hydroextractor basket. Such beds were thus of limited value in the present work.

Ceramic Cylinders

Experimental Technique

The ceramic cylinders were of a form directly comparable to the hydroextractor cakes discussed earlier. The hydroextraction tests for permeability K_c were obtained by carrying the cylinder between top and bottom circular plates which provided the appropriate ends of a hydroextractor ' basket ' (Fig. 1a). The cylinder was spun about a vertical axis by a direct-coupled motor, the speed of rotation being measured by a D.C.-generator tachometer on the motor shaft. The control and measurement of the apparatus were capable of the same accuracy as those on the centrifuges used in the associated tests [2]. Water was fed to the spinning cylinder as an " instantaneous " charge of specified volume V'_L, and the time t' measured for the vertical liquid surface to attain the inner surface of the ceramic cylinder as the water drained through the cylinder wall.

The analytical technique involving the measurement of drainage time has been described as Method III earlier [2]. It is useful so long as two major requirements are met. The addition of the initial charge V'_L at $t = 0$ must be rapid but not slow the basket appreciably. The liquid will soon attain the selected radial velocity of the basket but the time required represents an error in the following analysis and it must be small compared to the total drainage time, t'. The time t' must be measured accurately and detection

Present address : *Simon Carves Ltd., Research Department, Cheadle Heath, Stockport, England.
Present address : **Institute of Technology, Alexandria University, Alexandria, Egypt.

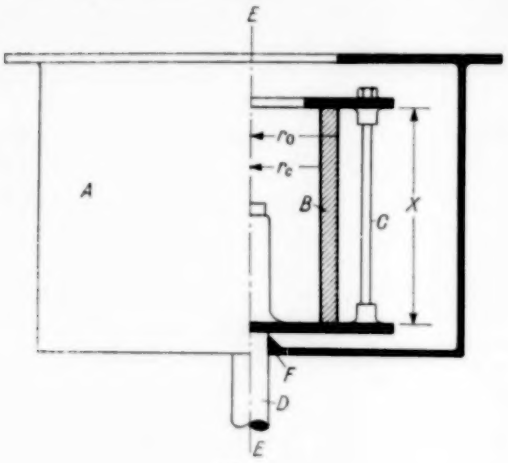

Fig. 1a.

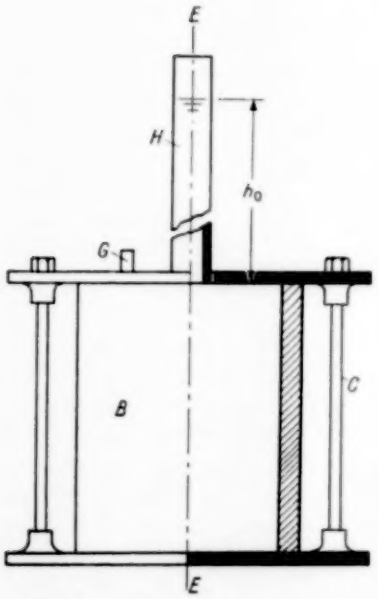

Fig. 1b.

Fig. 1. Ceramic cylinder : (*a*) in position for hydroextraction test; (*b*) in position for filtration test.
***X*, height of cylinder ; r_0, outside radius ; r_c, inside radius ; *B*, cylinder ; *C*, one of four connecting bolts ; *D*, driving shaft ; *F*, felt packing ; *G*, vent ; *H*, feed tube of cross section $a = 0.754$ cm^2 ; h_0, height of water in *H* above top surface of cylinder.**

of the coincidence of r_L with r_c when the liquid surface attains the inner ceramic surface is best carried out with a photoelectric detector [5]. The shielded light ray from the lamp *L* in Fig. 2 is reflected away from the shielded photoelectric cell *C*, when a water layer is maintained at $r_L < r_c$. When the ceramic surface is not covered by water, it reflects as a diffuse reflector and the maximum illumination reaches the cell.

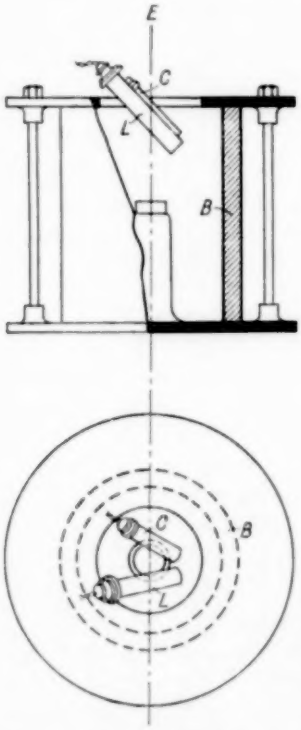

Fig. 2. Elevation and plan showing lamp *L* and photoelectric cell *C* in position for detection of critical wetting condition when $r_L = r_c$.

The graphs in Fig. 3 exemplify the data obtained from a sensitive galvanometer taking the barrier cell output, the ordinates being in arbitrary units. As the water layer becomes thinner as the liquid charge drains through the ceramic wall, the cell output increases until a sharp breakpoint is attained. " Rounding-off " at the break occurs only when the surface is covered by gelatinous deposit, as mentioned earlier [5]. The cell output may rise slightly after the breakpoint and this may be attributed to further air-drying of the ceramic surface, after the liquid layer at r_L has entered the ceramic ($r_L > r_c$). The photoelectric

VOL. 3 1954

method gives a clear breakpoint when $r_L = r_c$ and is far more reliable than visual observation, particularly in tests requiring immediate recognition of the critical wetting condition. The galvanometer readings were taken at appropriately spaced time intervals after the addition of the liquid V_L', and the time t' for attaining the critical condition taken from the extrapolation of the lines around the breakpoint.

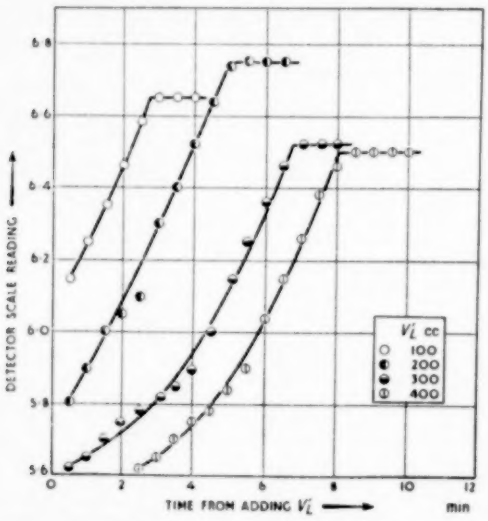

Fig. 3. Typical result of a photo-electric detection experiment. Break points are the critical times.

The analysis of the experimental data for various volumes V_L' and rotation speeds n was based on the flow rate equation

$$q = \frac{4\pi^3 n^2 K_c X}{\mu g} \cdot \frac{(r_0^2 - r_L^2)}{\log_e r_0/r_c} \qquad (1)$$

This equation is valid so long as a liquid layer remains on the cake, i.e. $r_L < r_c$, and the liquid fills the pores of the cake throughout the cake thickness $(r_0 - r_c)$. The liquid is in streamline motion and viscous resistance to this motion is the only significant resistance.

Equation (1) obtains at any moment from $t = 0$ to $t = t'$, assuming that throughout that time the liquid layer rotates at the basket speed n, i.e. does not take an appreciable time to be accelerated after the addition of V_L' and rotates at the same angular velocity at all points in the fluid. The assumption is made that the pores of the cake are already filled with liquid and do not require filling with liquid from V_L'. Thus for accuracy when the volume of the cake is comparable to the volume V_L', the technique should include the attainment of the critical wetting condition $(r_L = r_c)$ just prior to the addition of the charge V_L'.

The momentary drainage rate at time t is related to V_L the volume of liquid between radii r_L and r_c :

$$q = -\frac{dV}{dt} = \frac{4\pi^2 n^2 K_c}{\mu g \,.\, \log_e r_0/r_c} \,.\, (V_c + V_L) \qquad (2)$$

$$= \gamma (V_c + V_L) \qquad (2a)$$

where $\gamma = 4\pi^2 n^2 K_c/\mu \,.\, g \,.\, \log_e r_0/r_c$

$$V_c = \pi X (r_0^2 - r_c^2)$$

$$V_L = \pi X (r_c^2 - r_L^2)$$

whence :

$$\int_0^{V_L'} \frac{dV}{(V_C + V_L)} = \int_0^{t'} \gamma \, dt$$

$$\log_e \left[\frac{V_c + V_L'}{V_c}\right] = \gamma t' \qquad (3)$$

For a given speed of revolution n and cylinder dimensions, the terms γ and V_c are constant. Thus a plot of $\log (V_c + V_L')$ against t' should give a straight line of gradient γ and intercept of $\log V_c$, when $t' = 0$ corresponding to the use of a zero charge volume, $V_L' = 0$. The gradient $\gamma/2{\cdot}303$ may be analysed to find K_c. For various rotational speeds, γ should be proportional to n^2. The line obtained from a plot of $\log \gamma$ against $\log n$, thus should have a gradient of 2·0 and an ordinate when $n = 1$ of $\log (4\pi^3 K_c X/\log_e r_0/r_c)$. This plot, or its equivalent, can thus be used to obtain an average K_c from a series of sets of tests at different n, each set being at constant n and having variable V_L'.

To test filtration permeability K_F, the ceramic cylinders were held between top and bottom plates with appropriate connections for water input and air venting to make sure that an air lock did not form in the head of the space within

the cylinder (Fig. 1b). The techniques used included the measurement of flow rate to maintain a constant head of liquid above the cylinder, and also the measurement of the rate of fall of water in a vertical feed tube above the cylinder.

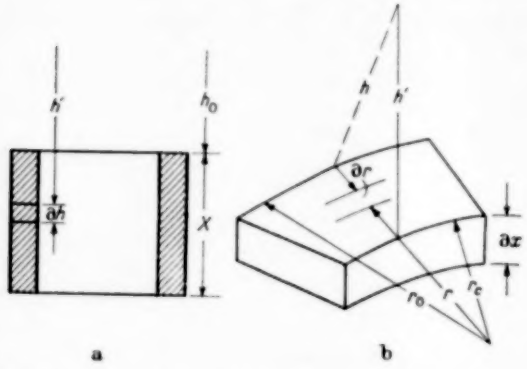

Fig. 4. Diagrams illustrating the derivation of an expression for filtration through a cylinder (equations 4-9).

The conditions at a depth h' below the free surface of the water in the feed tube are shown in Fig. 4. The flow through the cylinder is assumed to fill all the pores of a material of constant permeability and atmospheric pressure is assumed at the vertical wall on the outside of the cylinder. Flow through the annulus of the cylinder is assumed to be radial and horizontal. This is a reasonable approximation in the present tests, where with the heads h_0 of 35-150 cm and approximate cylinder dimensions of $(r_0 - r_c) =$ 1 cm, then $\partial p/\partial h$ is only 1-3% of $\partial p/\partial r$. For a precise solution the flow through the cylinder walls would be best analysed by relaxation methods. The desirable accuracy of 1% in the present investigations does not warrant such endeavour, though it is proper to focus attention on data obtained at high heads, where it is most reasonable to neglect $\partial p/\partial h$ in comparison with $\partial p/\partial r$.

The radial flow through the annulus of thickness ∂r at radius r is assumed to be given by an equation for streamline motion

$$q' = -\frac{K_F\, 2\pi r\, \delta x}{\mu} \cdot \frac{\partial h}{\partial r} \qquad (4)$$

The flow resistance due to frictional force is assumed to be the only significant resistance.

The head h available to produce flow varies from $h = h'$ at $r = r_c$ to $h = 0$ at $r = r_0$. Then for the annulus at constant depth h', with q constant at all radii

$$h' = \frac{q'\,\mu}{2\,\pi\, K_F \,.\, \delta x} \log_e r_0/r_c \qquad (5)$$

whence

$$q' = \frac{2\pi\, K_F \,.\, h' \,.\, \delta x}{\mu \log_e r_0/r_c} \qquad (6)$$

Then to obtain the total flow rate q from the whole cylinder over its height X, considering δx as $\delta h'$, we may integrate equation (6) between the limits $h' = h_0$ and $h' = (h_0 + X)$: whence,

$$q = \int_0^X q'\, dx = \frac{2\pi\, X\, K_F}{\mu \log_e r_0/r_c} \cdot \left(h_0 + \frac{X}{2}\right) \qquad (7)$$

$$= B\left(h_0 + \frac{X}{2}\right) \qquad (7a)$$

where $$B = \frac{2\pi\, X\, K_F}{\mu \,.\, \log_e r_0/r_c}$$

The flow rate from the cylinder thus varies linearly with the mean head $(h_0 + X/2)$, and from an arithmetic plot of q against $(h_0 + X/2)$ the permeability may be obtained from the constant gradient B.

If the flow is allowed without a feed to maintain a head h_0, then the equation (7) is appropriate to an instant as the head h_0 falls. If the head tube has a cross-sectional area a and no water is fed to the tube, the water level and hence h_0 will fall as time t increases from $t = 0$ at $h_0 = h_1$ to $t = t'$ at $h_0 = h_2$.

Then :

$$q = -a \,.\, \frac{dh_0}{dt} = B\left(h_0 + \frac{X}{2}\right) \qquad (8)$$

whence :

$$\log_e \left[\frac{h_1 + \frac{X}{2}}{h_2 + \frac{X}{2}}\right] = \frac{B}{a} \,.\, t' \qquad (9)$$

VOL. 3 1954

Thus using a calibrated glass tube above the cylinder, K_F may be obtained from B by plotting the semi-logarithmic equation (9) for measured t' values as head h_0 falls to various h_2, in the form of $\log (h_2 + X/2)$ against t'. As h_1 is the same for all the values of h_2 and t', then the data should lie on a straight line of gradient $-B/2{\cdot}303\,a$.

EXPERIMENTAL DATA

The two ceramic cylinders tested [6] are described in Table 1, and it will be noted that their permeabilities should differ considerably according to the pore sizes.

The hydroextraction results for Cylinder I are shown in Fig. 5. The lines representing the data for various V'_L at constant n should pass through the log $(V_c + V_L)$ axis at ordinate log V_c which is known. The actual lines concur

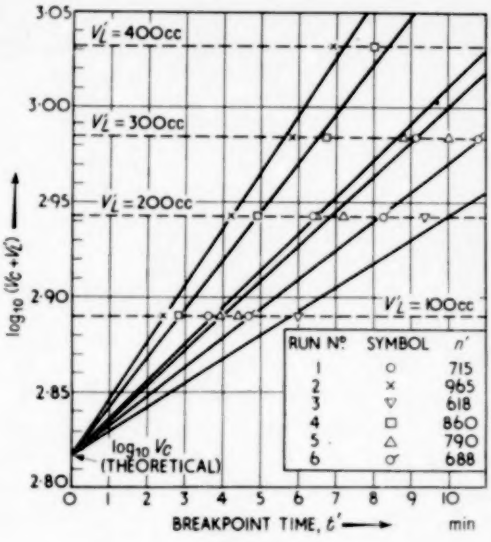

Fig. 5a.

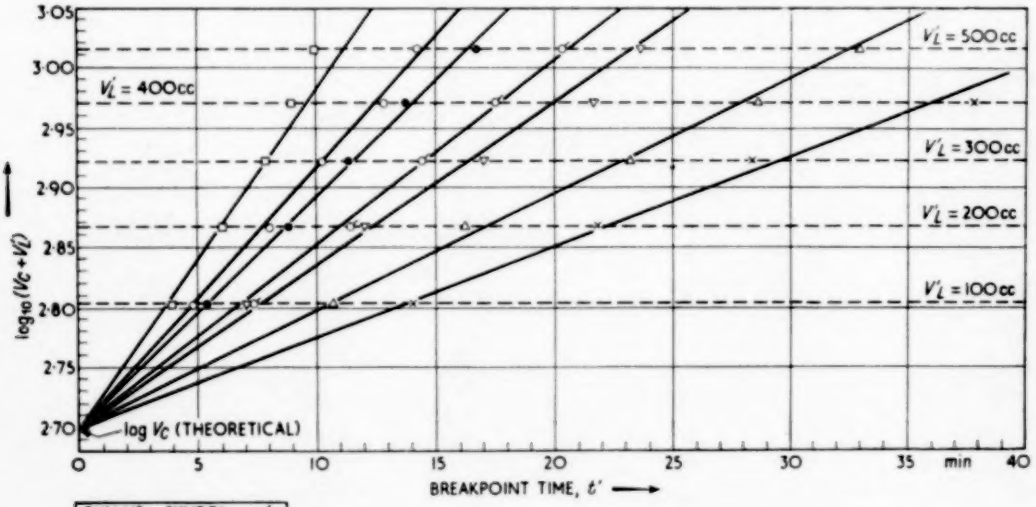

RUN Nº	SYMBOL	n'
1	□	1930
2	▽	1285
3	×	1020
4	●	1610
5	○	1770
6	△	1160
7	♂	1480

Fig. 5b.

Fig. 5. Data from hydroextraction tests, (*a*) on cylinder I, (*b*) on cylinder II.

at an intercept where $V_c = 658$ cc instead of the theoretical 676 cc, and were accepted as satisfactory. The gradients γ of these and similar lines are shown as a function of n on Fig. 6, confirming the expected power 2·0. From the mean line shown, the permeability K_c was found to be $2{\cdot}46 \times 10^{-7}$ g/sec².

The constant head filtration data shown in Fig. 7 were obtained using a rotameter to measure the rates q to maintain a steady head $(h_1 + X/2)$

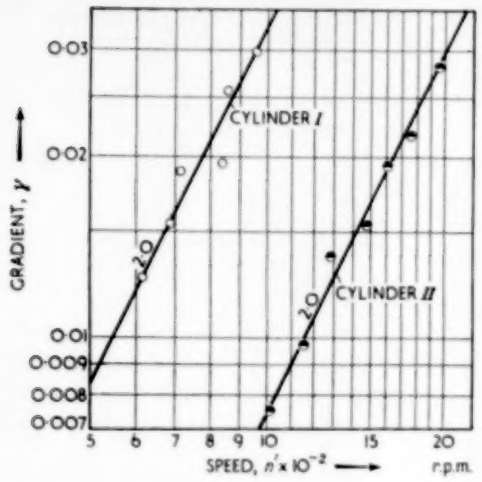

Fig. 6. Agreement between experimental results and equation (2).

in the glass head tube, the rotameter discharging freely into the head tube. The gradient B of the arithmetic plot of q against $(h_0 + X/2)$ was constant, confirming the assumption of a streamline flow in which the only significant resistance was that due to viscous resistance. From the gradient B in equation (7a) the filtration permeability was found to be $2{\cdot}16 \times 10^{-7}$ g/sec².

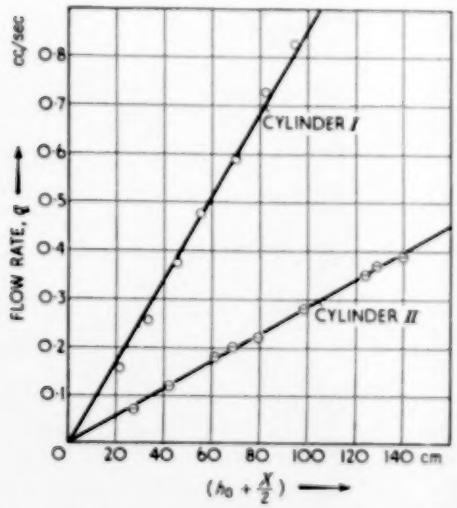

Fig. 7. Agreement between experimental results and equation (7).

Table 1. *Data on Ceramic Cylinders**

	Cylinder I	*Cylinder II*
Manufacturer's grade	S.P. (Sand pot)	P6A Porcelain
Nominal maximum pore size	35	2 microns
Mean dimensions :		
height, X	15·20	15·32 cm
outside diameter	12·22	14·98 cm
inside diameter	9·86	13·41 cm
r_0	6·11	7·49 cm
r_c	4·93	6·70 cm
Cylinder volume ; V_c	676	570 cc

* The ceramic cylinders used were made by *Doulton and Co. Ltd.*, Albert Embankment, Lambeth, London, S.E.1.

The filtration tests under falling head from $h_1 = 150$ cm at $t' = 0$ are plotted in Fig. 8. The gradient $(-B/2{\cdot}303\,a)$ of the straight line from equation (9) gave a permeability of $K_F = 2{\cdot}36 \times 10^{-7}$ g/sec². These data from falling head tests are generally more reliable than those at constant head due to the time anomalies in flow, which can occur at these low permeabilities, being less in the falling head tests. The agreement between K_c and K_F is probably within 5%.

The hydroextraction data for Cylinder II are shown in Fig. 5, 6, leading to a permeability $K_c = 0{\cdot}29 \times 10^{-7}$ g/sec² from the mean line on Fig. 6.

The constant head filtration data for Cylinder II are shown in Fig. 7, the gradient of the line giving $K_F = 0{\cdot}31 \times 10^{-7}$ g/sec².

The falling head filtration data for Cylinder II in Fig. 8 lead to a value of $K_F = 0{\cdot}30 \times 10^{-7}$ g/sec².

The data show a satisfactory agreement between hydroextraction permeability K_c and filtration

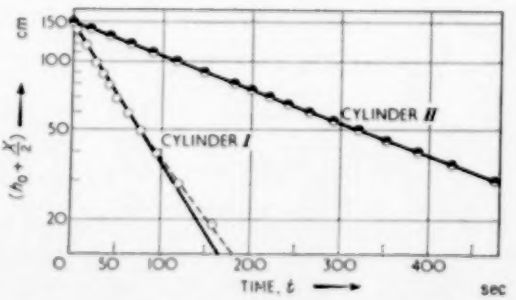

Fig. 8. Agreement between experimental results and equation (9).

permeability K_p, confirming the equations proposed. Since the ceramic cylinders readily available were limited in dimensions, porosity and evenness of porosity distribution, further tests were carried out with sintered metal plugs. It was hoped that these would provide data in closer agreement than those from the ceramic cylinders in view of the success of small cell experiments (3) wherein the liquid level could be maintained at $r_L = 0$, independently of time. This technique was expected to be superior to the time tests used on the ceramic cylinders (6), and it was expected that with small metal samples more uniform material would be available in greater widths $(r_0 - r_c)$ in a wide porosity range. It should also be emphasised that in tests of the present type the cylinders must be regarded as "expendable." After relatively short time of immersion in water algae growth and slight gelatinous films on the ceramic made the cylinders unsuitable for further work. All water used in the batch tests was treated with either thymol or mercuric chloride but some of the continuous tests required volumes of filtered sterilised water beyond the laboratory capacity. The series of tests on small plugs were expected to be very much quicker and thus more satisfactory than the long series discussed above.

Sintered Metal Plugs

The sintered metal plugs used in these tests are described in Table 2. The material consisted of small metal spheres moulded and sintered together without much deformation. The plugs were produced without machining the circular end faces of the rods. The cylindrical surface was sealed by filing and soldering when necessary. The bulk of the plug was not affected by this, the circular ends remaining fully permeable, appropriate to the pore dimensions, and flow being possible only through the length of the plug. These plugs were held in an appropriate carrier, which is shown in Fig. 9a. The carrier was whirled about the vertical axis at a constant speed of rotation. Flow rates q were controlled to maintain the water level at G in the feed tube over the experimental range of speeds n. The carrier was then held with the plug vertical (Fig. 9b) and the filtration test was conducted under suction with a constant feed of distilled water to keep the water level at G.

Table 2. Data on Sintered Bronze Plugs

Plug No.	*Length, L*	*Diameter, d*	*Sinter grade**
	cm	*cm*	
1 A	3·80	1·75	A
1 B	3·80	1·75	B
1 C	3·80	1·75	C
2 A	2·04	1·21	A
2 B	2·10	1·20	B
2 C	2·10	1·20	C
3 A	5·08	0·90	A
3 C	5·00	0·85	C
4 A	3·81	1·81	A

* The sinter grades are classified as follows according to the manufacturers, *Sintered Products Ltd.*, Sutton Coldfield, Notts, England :

Grade	*Maximum particle to pass (thousandths of an inch)*
A	0·1
B	0·2
C	0·5

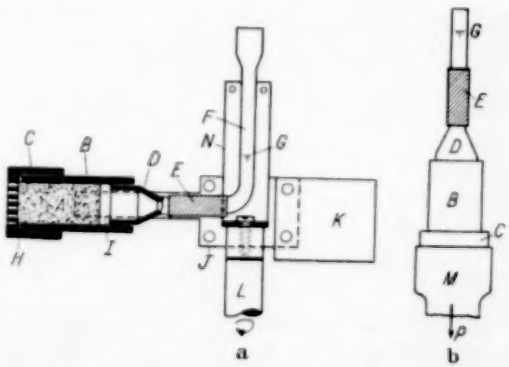

Fig. 9. Plug carrier, (*a*) in position for hydroextraction test ; (*b*) in position for filtration test.

A, bronze plug ; *B*, plug jacket ; the common surface between *A* and *B* is sealed ; *C*, a perforated base cap tightly screwed on *B* ; *H*, rubber gasket ; *D*, tapered brass connection tightly screwed in *B* ; *E*, rubber tube connecting *D* and glass feed tube *F* ; *G*, level of water in feed tube ; *L*, driving shaft ; *K*, counterbalancing weight ; *IJN*, back brass plates connecting *B*, *L*, and *K*, and securing tube *F* (the similar front plates are not shown) ; *M*, rubber tube ; *P*, to suction pump.

The hydroextraction permeability was assessed as K_c in the flow equation :

$$q = \frac{2\pi^2 n^2 A K_c}{\mu \cdot g} \cdot \frac{r_0^2}{r_0 - r_c} \qquad (10)$$

The filtration permeability K_F was calculated from the corresponding equation :

$$q = \frac{AH \cdot K_F}{\mu (r_0 - r_c)} \qquad (11)$$

The relation between K_c and K_F could be directly assessed as :

$$\frac{K_c}{K_F} = \frac{q_c}{q_j} \cdot \frac{H}{P_c} \qquad (12)$$

where P_c = centrifugal head = $\frac{1}{2} \cdot \frac{(2\pi n)^2}{g} \cdot r_0^2$.

Metal plugs with permeability of the order of 10^{-7} g/sec^2 showed a continuous decrease in flow rate when tested for filtration under constant hydrostatic heads. The application of suction below the plug reduced the effect but did not eliminate it. The flow rates might decrease to one fifth of the original within a few minutes in spite of using distilled water and maximum precautions to ensure cleanliness. Use of electrolyte solutions did not alter the results. Vibration and intermittent suction of air had a large effect, even up to temporary elimination of the phenomenon. This vibration may be the reason why the time effects are far less noticeable in hydroextraction.

Plugs of permeability of 10^{-3} g/sec^2 showed negligible time effects when tested under the same hydrostatic conditions over a considerable length of time, whereas with similar plugs of permeability of 10^{-5} g/sec^2, the effect was so quick that it was impossible to obtain reproducible results with aqueous solutions. With $K = 10^{-7}$ g/sec^2 the test had to be done as quickly as possible to attain the initial maximum flow rate, whereas plugs of permeability 10^{-6} and 10^{-5} g/sec^2 were more convenient to test. Flow rates through plugs of permeability 10^{-4} and 10^{-3} g/sec^2 were so high that the hydroextraction tests were difficult due to air being sucked into the feeding tube. The range of K around 10^{-5} to 10^{-6} g/sec^2 was the optimum for comparison between permeabilities in hydroextraction and filtration with the present apparatus.

Experimental Data

Fig. 10 is a typical plot of the q, n relationship for the case of plugs of permeability near 10^{-6} g/sec^2. The gradient 2·0 was also obtained with

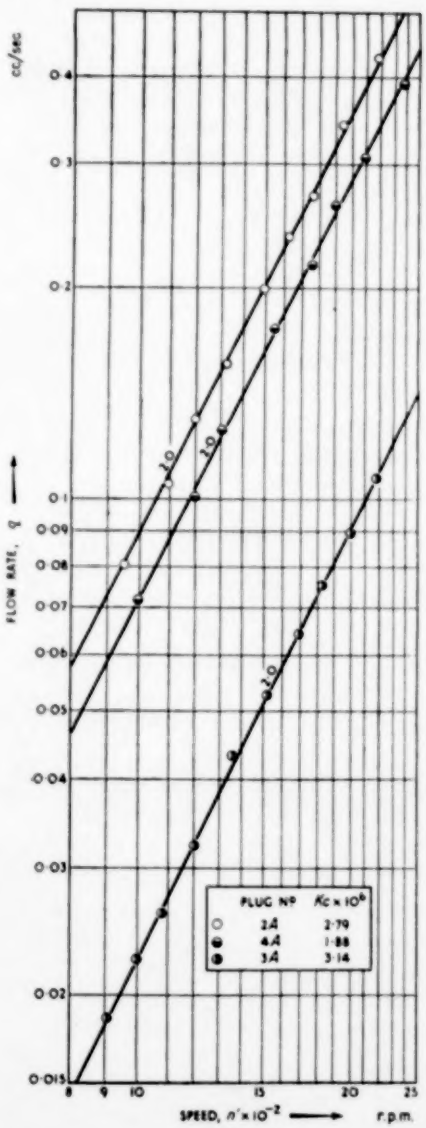

Fig. 10. Agreement between experimental results and equation (10).

VOL. 3 1954

Table 3 Relation between K_c and K_F for Sintered Bronze Plugs

Plug No.	*Filtration Test*			*Hydroextraction Test**			K_c/K_F
	P *cm Hg.*	q_F *cc/min.*	$K_F \times 10^6$ *g/sec²*	n' *r.p.m.*	q_c *cc/min.*	$K_c \times 10^6$ *g/sec²*	
1 A	73·0	6·60	2·02	1350	7·80	2·08	1·03
1 B	73·4	25·20	7·61	1260	25·10	7·70	1·01
1 C	69·5	58·80	18·72	1120	48·00	18·68	1·00
2 B	72·0	20·40	7·38	1250	20·40	7·45	1·01
2 C	71·6	57·00	20·7	960	33·00	20·5	0·99
3 C	73·5	7·50	12·6	1330	8·40	12·9	1·02
						Mean	1·01

* $r_0 = 10{\cdot}50$ cm

all plugs of other permeabilities given in Table 2. Clean connecting tubes and distilled water are essential in these tests, as the least contamination on the surface directly leads to erroneous results and lower q, n gradients.

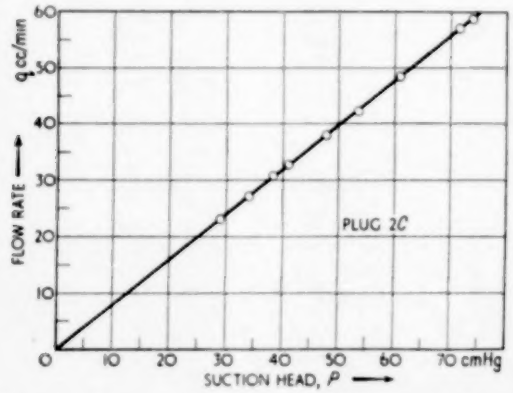

Fig. 11. Agreement between experimental results and equation (11).

Fig. 11 illustrates the linear proportionality between q and H for a filtration test on a plug of permeability $2{\cdot}07 \times 10^{-5}$ g/sec². The linearity could not be illustrated for lower permeabilities because of the time effects discussed above. Thus the range of permeability 10^{-5} and 10^{-6} g/sec² was chosen for comparison data for performance under hydrostatic and centrifugal heads. Table 3 exemplifies the results obtained. The ratio K_c/K_F is very near to unity with an average difference less than $\pm 1\%$.

Conclusion

Though the agreement between K_c and K_F for the ceramic cylinders was only within 5%, it is conceivable that the discrepancies were due to inaccuracies in technique rather than in the postulated mechanism for equation (1). The probable lack of uniformity in the cylinders, assumptions of negligible acceleration times in the batch tests, and similar approximations led to the 5% discrepancy, just as the hydroextraction reproducibility on Fig. 6 is shown to be $\pm 5\%$. The method used for the measurement of K_c with the metal plugs is more accurate than the batch technique [2].

The agreement to 1% between K_c and K_F with the metal plugs is considered to prove conclusively the mechanism of hydroextraction embodied in equation (1). The mean differences of 10-20% between K_c and K_F in tests on cakes of chalk and starch in hydroextractors and in a small filtration cell [3] are thus likely to be caused by variations in cake porosity and interface resistance as postulated earlier [4].

Notation

A = cross-sectional area of plugs (cm²)
a = cross-sectional area of feed tube in filtration tests (cm²)
B = constant in equation (7a)
g = gravitational acceleration (cm/sec²)
H = hydrostatic head in filtration tests on plugs (cm water)

h = hydrostatic head in filtration tests on cylinders (cm water) ; h' at $r = r_c$, h_0 at $X = 0$, h_1 and h_2 are limits of h.

K = permeability ; K_c from hydroextraction tests, K_F from filtration tests (g/sec^2)

n = speed of rotation (rev/sec) n' (r.p.m.)

p = pressure (dynes/cm^2)

P_c = centrifugal head (cm water)

q = rate of flow ; q' flow through a circular element of cylinder, q_c and q_F for flow under centrifugal and hydrostatic heads respectively (cc/sec)

r = radius from axis of rotation ; r_L for internal surface of liquid, r_c for internal surface of bed, r_0 for external surface of bed (cm)

t = time (sec), t' time for the flow of V''

V = volume (cc) ; $V_L = \pi X (r_c^2 - r_L^2)$ for liquid, V''_L for liquid initially added to cylinder, $V_c = \pi X (r_0^2 - r_c^2)$ for cylinder

x = height ; X height of cylinder (cm)

γ = gradient in equation (2a)

μ = viscosity of liquid (poise)

References

[1] Burak, N. and Storrow, J. A.; J. Soc. Chem. Ind. 1950 **69** 8.

[2] Haruni, M. M. and Storrow, J. A.; Hydroextraction I, Ind. Eng. Chem. 1952 **44** 2751.

[3] Haruni, M. M. and Storrow, J. A.; Hydroextraction II, Ind. Eng. Chem. 1952 **44** 2756.

[4] Haruni, M. M. and Storrow, J. A.; Hydroextraction IV, Chem. Eng. Sci. 1952 **1** 154.

[5] Inglesent, H. and Storrow, J. A.; Ind. Chem. 1951 **76**.

[6] Todhunter, K. H.; M.Sc.Tech. thesis (Manchester) 1950.

VOL. 3 1954

Chemical Engineering Science, 1954, Vol. 3, pp. 97 to 109. Pergamon Press Ltd.

Heat and mass transfer at high humidities in a wetted wall column

R. C. Cairns and G. H. Roper

School of Chemical Engineering, N.S.W. University of Technology, High Street, Kensington, N.S.W.

(*Received* 14 *January* 1954)

Summary—Simultaneous heat and mass transfer data were obtained from the operation of an adiabatic wetted-wall column with countercurrent flow of air and water. The runs were made over a limited range of Reynolds numbers 2390 to 9095 and from 0·03 to 0·85 mol fraction of the diffusing vapour in the gas film. The data were compared with the equation of previous investigators obtained at low humidities. Correlation of the data by means of a Nusselt-type equation gave

$$(k_G RTd/D)\,(p_{BM}/P)^{0.83} = 0.021\ Re^{0.83}\ Sc^{0.44}$$

at a liquor rate of 77 lb./hr. This equation differs from the Gilliland-Sherwood equation mainly by the exponent 0·83 on the group p_{BM}/P. Comparison with the Chilton-Colburn equation showed that their heat and mass transfer factors did not apply at high humidities. Correlation by new heat and mass transfer factors gave

$$\begin{aligned} j_H &= (h/cG)\ .\ Pr^{2/3}\,(p_{BM}/P)^{-0.27} \\ &= j_D = (k_G p_{BM} M_m/G)\,Sc^{2/3}\,(p_{BM}/P)^{-0.17} \\ &= 0.025\ Re^{-0.2} \end{aligned}$$

The theory of Colburn and Drew for the effect of simultaneous mass transfer on the heat transfer coefficients was unable to explain the data.

Résumé—Résultats des mesures simultanées d'échanges de chaleur et de matière dans une colonne adiabatique à parois mouillées avec écoulements opposés d'air et d'eau.

Expériences avec des nombres de Reynolds variant entre 2390 et 9095, et des concentrations molaires pour la vapeur diffusant au travers du film gazeux variant entre 0,03 et 0,85. Comparaison avec les formules proposées par d'autres expérimentateurs pour de faibles humidités. La corrélation conduit à formule du type de Nusselt :

$$(k_G\ RT\ d/D)\,(P_{BM}/P)^{0.83} = 0.021\ Re^{0.83}\ Sc^{0.44}$$

pour un débit liquide de 77 lb./hr. x ft. Cette équation diffère de celle de Gilliland et Sherwood par l'exposant 0,83 pour le groupe p_{BM}/P. La comparaison avec l'équation de Chilton - Colburn montre que leurs facteurs d'échanges pour la chaleur et pour la matière ne sont plus applicables aux humidités élevées.

La corrélation des nouveaux coefficients d'échange conduit aux égalités :

$$\begin{aligned} j_H &= (h/cG).\ Pr^{2/3}\,(p_{BM}/P)^{-0.27} \\ &= j_D = (k_G\,p_{BM}\,M_m/G)\,Sc^{2/3}\ (p_{BM}/P)^{-0.17} \\ &= 0{,}025\ Re^{-0.2} \end{aligned}$$

La théorie de Colburn et Drew pour l'effet d'un transfert simultané de matière sur le coefficient de transfert thermique ne peut expliquer les résultats des auteurs.

Introduction

A limited number of papers have reported experimental results for mass transfer occurring at high concentrations of the diffusing vapour. The mean mol fraction of the diffusing vapour has not exceeded 0·5 in any of the investigations previously published. The first paper to examine the effect of these high concentrations is that of Hanks and McAdams [9] who reported the measurements of Hemeon [10] of the rates of absorption of ammonia from air by water in a single contact chamber stirred at 350 r.p.m. in both the liquid and gas phases. A series of runs were made in which the total pressure of the gas was constant (1 atm) and the composition of the gas in the chamber was varied between 0·06 and 0·65 mol fraction ammonia. Hanks and McAdams correlated these results on the basis of the theory and the Stefan equation

$$N_A = DP\Delta p/RTxp_{BM} \qquad (1)$$

where x is the stagnant gas film thickness. The liquid film resistance was neglected, so that the gas film coefficient was assumed to be equal to the overall coefficient, viz.

$$K_G = k_G = \frac{DP\Delta p}{RTxp_{BM}} \qquad (2)$$

The experimental coefficients were correlated by

$$k_G = 0{\cdot}257/p_{BM} \qquad (3)$$

The correlation is unsatisfactory, but it does indicate that k_G is influenced by p_{BM}/P. It is probable that the liquid film resistance is not negligible and that the reaction in the liquid appreciably affects the liquid film coefficient.

Hinchley and Himus [11] varied the ratio p_{BM}/P from 0·55 to 0·99 in their study of the evaporation of water from open pans by natural and forced convection. The mass transfer coefficient for forced convection was not affected by variations in p_{BM}/P. The results for natural convection indicate the mass transfer coefficient to be approximately inversely proportional to this ratio. Wade [13] evaporated seven different liquids from a pan 3·5 in. square into a tunnel 4·72 in. × 2·36 in. The evaporations were made into still air (natural convection) and into air streams 4·4 to 13·1 ft. per sec. The ratio p_{BM}/P was varied between 0·68 and 0·99. The gas film coefficient, k_G was independent of p_{BM}/P for forced convection, and was inversely proportional to p_{BM}/P for natural convection.

Boelter, Gordon and Griffin [2] working with a 1 ft. diameter pan found that the mass transfer coefficients for the evaporation of water into air at 1 atm total pressure were best correlated by

$$k_G = 0{\cdot}14/p_{BM} \qquad (4)$$

for natural convection. They also correlated the data by the dimensionless equation

$$k_G RTd/D = 0{\cdot}643\,(Gr.Sc)^{0{\cdot}25} \qquad (5)$$

in which the ratio of p_{BM}/P does not enter. Their data may be better correlated by the dimensionless equation (6) than by equation (5), viz.,

$$k_G RTd/D = 0{\cdot}61\,(Gr.Sc.p_{BM}/P)^{0{\cdot}25} \qquad (6)$$

The ratio of p_{BM}/P was varied from 0·5 to 0·99 and the water temperature from 75°F to 202°F. The influence of p_{BM} in equation (4) is due to the close relationship between the modified Grashof number, Gr, and p_{BM}, and is not due to the effect predicted by the film theory and the Stefan equation.

Neither Hinchley and Himus, nor Wade give sufficient experimental details to recalculate their data in terms of the dimensionless equations, so that it is not possible to decide whether their data for natural convection can be correlated in accordance with equations (5) or (6).

Gilliland and Sherwood [8] studied the evaporation of nine different liquids in a wetted-wall tower 1·05 in. i.d. operating at pressures from 0·145 to 3·06 atm. They correlated their experimental results on the basis of the Stefan equation (1) and the film theory. For Reynolds numbers greater than 2000 and a constant liquor rate of 790 cc/min. (104 lb/hr. for water) their results were correlated by the dimensionless equation

$$(k_G RTd/D)\,(p_{BM}/P) = 0{\cdot}023\,Re^{0{\cdot}83}\,Sc^{0{\cdot}44} \qquad (7)$$

No variation of the left-hand side of equation (7)

VOL. 3 1954

with pressure was found, from which the authors concluded that k_G was inversely proportional to p_{BM} as indicated by the Stefan equation (1). However as Sherwood and Pigford [14, p. 77] point out, the ratio p_{BM}/P was varied only slightly. Hence no conclusions may be drawn for the effect of p_{BM} and P on k_G. Gilliland and Sherwood also measured the heat transfer coefficients for heating air in upward and downward flow in the column without liquid circulating. The experimental heat transfer data agreed closely with the McAdams [12, p. 168] equation (8) for heating air in turbulent flow in a pipe

$$Nu = 0{\cdot}023\ Re^{0{\cdot}8}\ Pr^{0{\cdot}4} \qquad (8)$$

Their mass transfer data are about 35% greater than their data for heat transfer.

Barnet and Kobe [1] studied heat and mass transfer in a wetted-wall column 1·049 in. i.d. For the evaporation of water into air streams at low humidities, their mass transfer data were correlated by the Sherwood-Gilliland type equation

$$(k_G RTd/D)\,(p_{BM}/P) = 0{\cdot}016\ Re^{0{\cdot}83} \qquad (9)$$

at liquor rates varying between 10 and 100 lb/hr. Taking the value of the Schmidt number under the conditions of their experiments as 0·60 equation (9) becomes

$$(k_G RTd/D)\,(p_{BM}/P) = 0{\cdot}020\ Re^{0{\cdot}83}\ Sc^{0{\cdot}44} \qquad (10)$$

Their mass transfer values are approximately 13% less than those of Gilliland and Sherwood; about 3% out of the 13% difference could be attributed to the different liquor rates used. Their mass and heat transfer data were also correlated in the form of the Chilton-Colburn dimensionless groupings, as follows

$$(k_G p_{BM} M_m/G)\ Sc^{2/3} = 0{\cdot}025\ Re^{-0{\cdot}2} \qquad (11)$$

and

$$(h/cG)\ Pr^{2/3} = 0{\cdot}031\ Re^{-0{\cdot}2} \qquad (12)$$

The heat transfer data without simultaneous mass transfer are 24% greater than the mass transfer data.

Colburn and Drew [6] have considered the effect of the sensible heat carried out by the diffusing molecules during simultaneous heat and mass transfer. Based on the film theory and in the absence of condensation in the gas phase, they developed the relation

$$q_C/A\Delta t = h = h_0 a/(1 - e^{-a}) \qquad (13)$$

where h_0 is the heat transfer coefficient in the absence of simultaneous mass transfer. The dimensionless group, a, is the ratio between the nett sensible heat carried by the diffusing vapours, and the heat transfer in the absence of mass transfer. For one diffusing component, a is $w_1 c_1/h_0$ and is positive if the mass transfer is in the same direction as the heat transfer. For two diffusing components, a is $(w_1 c_1 + w_2 c_2)/h_0$. If the heat transfer is in the same direction as the mass transfer, h is greater than h_0 and conversely if the heat transfer is in the opposite direction to the mass transfer h is less than h_0.

There is still some confusion in the literature concerning the effect of the inert gas concentration on the rate of diffusion of a vapour through a gas film. The effect of p_{BM}/P indicated by the Gilliland-Sherwood correlation and by the Chilton-Colburn correlation is retained purely on the basis of its appearance in the theoretical equation (1). There appears to be no definite attempt in the literature to show the influence of large variation of p_{BM}/P on the rate of mass transfer, and in view of the importance of p_{BM}/P in such cases as the condensation of vapour from non-condensable gas [4], [7] and in the condensation of mixed vapours, this investigation was made.

Apparatus, Procedure and Results

An outline of the apparatus is given in Fig. 1. The column and procedure were similar to those used by Gilliland and Sherwood. Air from a blower was passed through a glass-wool filter, and metered by a Fischer and Porter rotameter. The humidity of the incoming air was measured by wet- and dry-bulb thermometers before it entered an electric preheater where its temperature was controlled by a variac. The temperature of the air leaving the preheater was normally in the range 220-240°F. After preheating, the air was mixed with steam from the boiler. The boiler, of 6 gallons capacity, was heated with a 3-kW

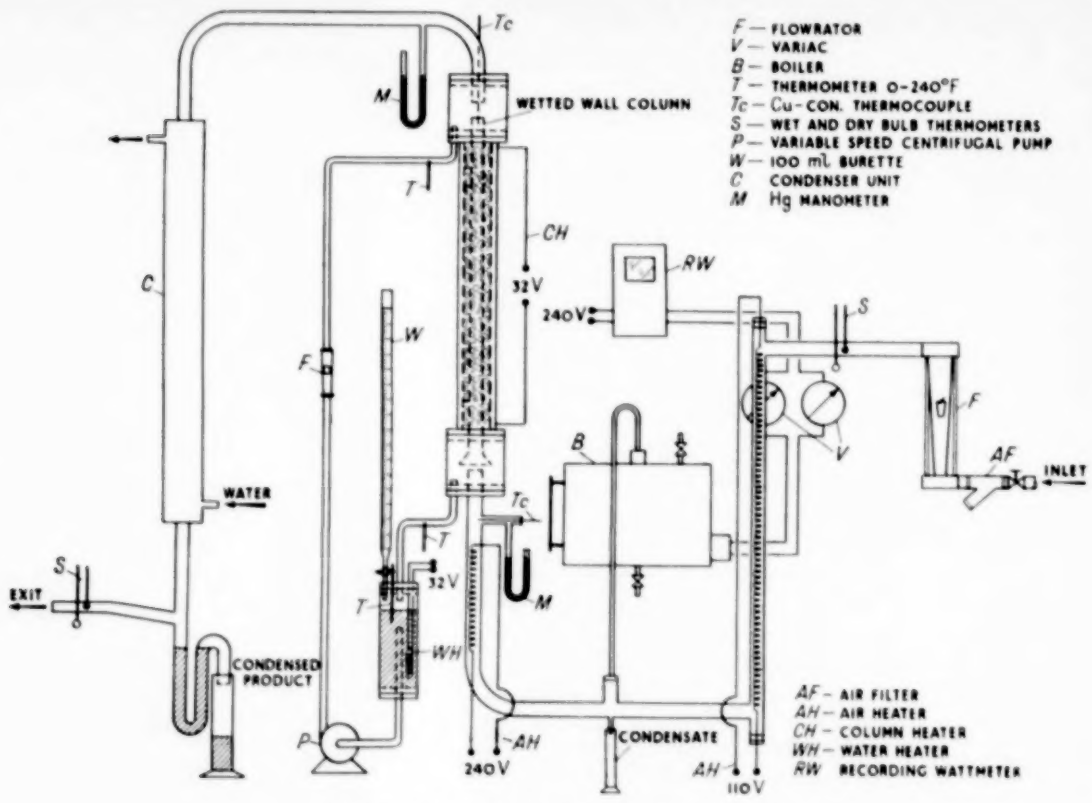

Fig. 1. Outline of the experimental apparatus.

Helicoil A.G.E. twin element immersion heater sealed into the side of the boiler and was lagged with 1 in. asbestos sheet. Power input was controlled by a variac on each element and recorded on an Evershed and Vignoles recording wattmeter. The steaming rate of the boiler was determined from the power input and a calibration curve determined under the conditions of the experiments. A correction was made for the condensation in the line from the boiler to the point where the steam and air mixed. The steam-air mixture was further heated electrically to the temperature at which it entered the column. The wetted-wall column was a glass tube 0·90 in. i.d. × 37¼ in. long. The column was enclosed in another glass tube 1·5 in. i.d. around which was wound an electrical heater. The column heater was controlled by a variac adjusted to maintain the operation as adiabatic as possible as determined by a heat balance. The heater was enclosed by a third glass tube. This arrangement allowed the water film to be seen at all times so that a check was kept to ensure that complete wetting occurred during all runs. The temperature of the water leaving the separator at the base of the column was measured. The water from the separator passed to a vessel with a controlled electrical heater. The water level in this vessel was maintained constant by additions from a 100 ml. burette. The water was recirculated by a small centrifugal pump, the water temperature entering the top of the column being adjusted to the temperature at the base by the controlled heater. The rate of water recirculation was measured by a rotameter.

The air-vapour mixture from the top of the column passed to a condenser except for those runs in which the load on the condenser was

excessive. The product which was condensed was collected and measured. The humidity of the cooled air-vapour mixture was determined by wet- and dry-bulb thermometers. The temperatures of the air-vapour mixtures entering and leaving the column were measured by copper-constantan thermocouples and a Cambridge thermocouple potentiometer. The lines at these two points were well lagged so that the radiation correction was negligible.

Manometers at the inlet and outlet of the column were used to determine the total pressure in the column.

Methods of Calculation

The runs were interpreted by comparing the experimental values of dimensionless groups with the values predicted by the correlations of Gilliland and Sherwood, Chilton and Colburn and Colburn and Drew. The experimental data is shown in Table 1. The water vapour entering the column is the sum of the water vapour from the boiler and in the incoming air corrected for the condensate from the steam line. The water vapour leaving the column in runs 1-19 was calculated from the amount entering the column and the amount added to the circulating water (make up). In runs 20-27 the water vapour leaving the column was calculated from the humidity of the exit air and the condensed product. In these runs the amount of make-up was small and the latter method was considered more accurate. The rate of evaporation was determined from the make-up in runs 1-19

Table 1. Experimental data

Run No.	*Dry Air rate lbs./hr.*	*H air lb./lb. dry air*		*Boiler rate lbs./hr.*	*Condensate lbs./hr.*	*Product rate lbs./hr.*	*Make up rate lbs./hr.*	*Mixture Temp. at Column °F.*		*Column Pressure atm.*	*Liquor rate lbs./hr.*	*Water Temp. at Column °F*	
		In	*Out*					*In*	*Out*			*In*	*Out*
1	3·93	·0075	·015	2·39	0·15	2·76	0·51	629	336	1·007	77	183·9	184·1
2	7·04	·007	·019	2·39	0·13	2·93	0·78	617	332	1·008	83	174·3	174·4
3	17·34	·012	–	5·73	0·07	–	1·56	581	358	1·019	77	175·4	175·6
4	11·68	·010	–	5·73	0·12	–	1·40	634	383	1·017	77	182·0	182·8
5	7·75	·010	·029	5·73	0·11	6·47	1·06	604	370	1·017	77	188·8	189·0
6	3·91	·009	·016	5·73	0·17	6·49	0·87	630	379	1·007	77	198·2	198·0
7	12·18	·007	–	2·39	0·12	–	1·13	613	351	1·008	77	164·1	164·3
8	17·48	·008	–	2·39	0·13	–	1·41	604	352	1·008	77	158·9	158·7
9	24·40	·007	–	2·39	0·13	–	1·77	592	338	1·005	77	152·3	151·9
10	1·89	·0095	·014	5·84	0·24	6·51	0·89	808	442	1·008	151	204·9	204·7
11	2·25	·006	·025	5·84	0·24	6·57	0·87	777	435	0·987	136	202·5	202·8
12	2·92	·007	·028	5·84	0·19	6·70	1·12	810	446	0·992	111	200·8	200·9
13	3·34	·008	·022	5·84	0·14	6·85	1·16	813	454	0·992	111	200·0	200·0
14	4·79	·007	·035	5·84	0·12	6·78	1·16	766	437	0·995	105	195·7	195·6
15	5·72	·007	·033	5·84	0·12	6·77	1·28	738	424	1·001	111	193·3	193·5
16	5·24	·007	·034	5·84	0·12	6·87	1·37	784	442	1·000	111	195·2	195·0
17	4·34	·007	·031	5·84	0·16	6·85	1·29	806	444	1·000	111	197·1	197·3
18	6·69	·006	·042	5·84	0·11	6·79	1·30	736	421	1·000	111	191·2	191·3
19	6·32	·006	·039	5·84	0·12	6·80	1·32	761	430	1·000	111	192·5	192·4
20	7·70	·0068	·015	0·0	0·0	0·14	–	302	184	1·007	24	101·9	101·9
21	7·71	·0075	·016	0·0	0·0	0·16	–	301	171	1·007	143	102·0	102·0
22	7·71	·0082	·015	0·0	0·0	0·15	–	297	176	1·005	42	101·6	101·6
23	7·72	·0078	·015	0·0	0·0	0·16	–	297	172	1·005	111	102·0	102·0
24	7·73	·0077	·016	0·0	0·0	0·15	–	298	174	1·005	77	101·5	101·5
25	6·73	·0061	·014	0·0	0·0	0·12	0·17	271	156	0·999	77	98·5	98·3
26	11·50	·0083	·033	0·0	0·0	0·0	0·31	263	167	1·008	77	102·5	102·6
27	24·07	·0062	·021	0·0	0·0	0·0	0·34	205	145	1·011	77	89·9	89·8

and from the difference between the entering and exit water vapour in runs 20-27. The inlet and outlet humidities were calculated from the water vapour entering or leaving the column and the dry air rate. The driving force, Δp, was taken as the difference between the vapour pressure corresponding to the liquid temperature and the partial pressure of water vapour in the gas phase. In calculating the gas film coefficients of mass transfer, the logarithmic mean between the driving force at the top and bottom of the column was used. The true mean driving force as determined by graphical integration differed by no more than 1% from the logarithmic mean in any of the runs. The values of the gas film coefficient of mass transfer were calculated from

$$k_G = N_A / A\ \Delta p_{\text{l.m.}}$$

In evaluating the Reynolds number the arithmetic mean of the mass rate of flow at the top and bottom of the column was calculated. The viscosity was determined at the mean film conditions by the method of Bromley and Wilke [3] using the viscosity data of Perry [13, p. 370]. The diffusivities were calculated from Spalding's equation [14, p. 10] for the same conditions. The temperature used in the dimensionless groups was the mean film temperature. The value of p_{BM} was taken as the arithmetic mean between the logarithmic mean partial pressures of air in the gas film at each end of the column. The Schmidt numbers were calculated for each run, and as the variation was slight an average value of 0·55 was taken. In calculating the dimensionless groups for correlating with p_{BM}/P, the values of these groups were corrected to a liquor rate of

Table 2. Calculated mass transfer data

Run No.	H at column lb./lb. dry air		N_A lb. moles/hr	$(\Delta p)_{\text{l.m.}}$ atm.	k_G	Re	$\frac{(k_G RTd)}{D}$	$\left(\frac{k_G RTd}{D}\right) . Re^{-0.83}$ at 77 lbs./hr.	$\frac{p_{BM}}{P}$	$\left(\frac{k_G p_{BM}}{G/M_m}\right) . Sc^{\frac{1}{3}} . Re^{0.2}$ at 77 lbs./hr.	Mass balance %
	In	Out									
1	0·578	0·707	0·0283	0·043	0·90	2389	18·7	0·0294	0·469	0·0210	+ 7·8
2	0·328	0·439	0·0433	0·061	0·97	3417	20·4	0·0236	0·587	0·0219	− 3·8
3	0·339	0·428	0·0867	0·071	1·67	8517	35·4	0·0194	0·583	0·0187	–
4	0·491	0·610	0·0778	0·059	1·81	6520	37·4	0·0253	0·501	0·0209	–
5	0·735	0·872	0·0589	0·044	1·83	5304	38·2	0·0310	0·413	0·0206	+ 6·6
6	1·432	1·655	0·0483	0·036	1·84	3987	37·6	0·0386	0·269	0·0166	− 9·2
7	0·193	0·286	0·0628	0·071	1·21	5100	25·5	0·0214	0·685	0·0228	–
8	0·137	0·218	0·0783	0·087	1·23	6826	26·1	0·0172	0·735	0·0199	–
9	0·0996	0·172	0·0983	0·081	1·66	9095	35·3	0·0183	0·779	0·0234	–
10	2·974	3·444	0·0494	0·020	3·50	3137	67·1	0·0760	0·153	0·0172	− 3·4
11	2·493	2·880	0·0484	0·025	2·64	3273	49·9	0·0555	0·175	0·0146	− 17·2
12	1·942	2·325	0·0623	0·027	3·16	3511	59·7	0·0651	0·212	0·0216	+ 0·9
13	1·716	2·063	0·0644	0·034	2·59	3662	48·6	0·0511	0·230	0·0185	− 2·6
14	1·200	1·443	0·0644	0·037	2·39	4157	45·9	0·0438	0·301	0·0209	− 3·4
15	1·007	1·231	0·0712	0·0408	2·39	4531	46·8	0·0413	0·337	0·0222	+ 6·3
16	1·099	1·361	0·0762	0·0404	2·58	4301	49·5	0·0455	0·315	0·0228	+ 5·8
17	1·316	1·613	0·0717	0·0357	2·75	3995	52·6	0·0515	0·280	0·0228	+ 1·6
18	0·863	1·057	0·0723	0·0426	2·32	4828	45·4	0·0380	0·371	0·0226	0·0
19	0·911	1·120	0·0734	0·0481	2·09	4641	40·6	0·0350	0·355	0·0197	+ 2·3
20	0·0068	0·0338	0·0117	0·0323	0·496	2814	12·6	0·0187	0·951	0·0273	–
21	0·0075	0·0363	0·0128	0·0297	0·590	2822	15·0	0·0187	0·949	0·0271	–
22	0·0082	0·0350	0·0117	0·0299	0·534	2822	13·6	0·0196	0·950	0·0284	–
23	0·0078	0·0363	0·0122	0·0297	0·562	2831	14·4	0·0187	0·949	0·0270	–
24	0·0077	0·0349	0·0117	0·0311	0·516	2831	13·1	0·0179	0·950	0·0260	–
25	0·0061	0·0312	0·0095	0·0290	0·446	2508	11·6	0·0175	0·955	0·0254	0·0
26	0·0083	0·0330	0·0156	0·0345	0·619	4293	16·1	0·0156	0·950	0·0187	+ 9·7
27	0·0062	0·0212	0·0200	0·0237	1·16	8925	31·3	0·0165	0·966	0·0244	− 5·9

77 lb./hr. from the relations of Fig. 2. The mass balances are expressed as an error in closure defined by

$$\% \text{ error in closure} = \frac{\text{total vapour in} - \text{total vapour out}}{\text{make-up}} \times 100$$

for those runs in which the complete data could be obtained. In some runs the condenser was unable to handle the load, and in others the amount of make-up was too small to measure accurately.

The calculated mass transfer data are given in Table 2.

Only those runs in which the error in closure of the heat balance was less than 10% were used in calculating the heat transfer data. For these runs the heat transferred across the gas-liquid interface is the product of the mass of water evaporated and its latent heat of vaporisation at the water temperature. Some of this heat (never more than 15%) is transferred by radiation and the rest is transferred by convection. The heat transferred by convection was taken as the difference between the total heat transferred and the heat transferred by radiation as calculated by the approximate method of Perry [13, p. 490]. In calculating the convective heat transfer coefficients, h, the log-mean temperature difference was used. The true mean temperature difference by graphical integration differed by less than 2% from the log-mean in any of the runs. The specific heat data for air and water vapour were taken from Wenner [16]. The variation of the Prandtl number was slight and the average value of 0·76 was taken in the calculations. The dimensionless group, a, derived

Table 3. *Calculated heat transfer data*

Run No.	q_T *BTU/hr.*	q_C *BTU/hr.*	$(\Delta t)_{\text{l.m.}}$ °*F.*	h	*St at 77 lbs./hr.*	$St \cdot Pr^{\frac{1}{3}} \cdot Re^{0.2}$ *at 77 lbs./hr.*	$\frac{h}{h_0}$	$-a$	*Heat balance %*
1	–	–	–	–	–	–	–	–	–
2	775	737	277	3·65	·00535	·0227	0·91	0·126	− 3·5
3	1549	1512	279	7·41	·00444	·0227	0·91	0·124	− 4·4
4	1383	1336	310	5·89	·00442	·0213	0·85	0·132	− 7·3
5	1044	991	282	4·81	·00439	·0203	0·81	0·116	− 4·3
6	852	788	289	3·73	·00432	·0189	0·76	0·115	− 1·7
7	–	–	–	–	–	–	–	–	–
8	–	–	–	–	–	–	–	–	–
9	1782	1764	295	8·17	·00482	·0249	1·00	0·140	− 5·3
10	–	–	–	–	–	–	–	–	–
11	–	–	–	–	–	–	–	–	–
12	1094	973	400	3·33	·00381	·0163	0·65	0·143	+ 4·3
13	1134	1010	408	3·39	·00373	·0160	0·64	0·143	+ 2·2
14	1137	1039	383	3·72	·00377	·0166	0·66	0·136	+ 3·2
15	1257	1168	366	4·36	·00413	·0186	0·74	0·143	− 5·6
16	1344	1241	394	4·31	·00418	·0186	0·74	0·155	− 7·0
17	1264	1152	402	3·92	·00404	·0177	0·71	0·153	− 0·7
18	1278	1189	366	4·44	·00399	·0181	0·72	0·139	0·0
19	1297	1202	380	4·32	·00395	·0178	0·71	0·142	0·0
20	217	217	132	2·25	·00555	·0227	0·91	0·055	0·0
21	–	238	123	2·65	·00556	·0227	0·91	0·051	+ 4·7
22	–	217	125	2·37	·00568	·0232	0·93	0·053	+ 5·2
23	–	228	122	2·56	·00556	·0228	0·91	0·050	+ 1·7
24	–	217	124	2·40	·00544	·0223	0·89	0·050	+ 5·3
25	–	176	105	2·29	·00599	·0240	0·96	0·046	+ 5·8
26	–	290	105	3·78	·00576	·0256	1·02	0·049	− 8·2
27	–	375	81	6·33	·00469	·0242	0·97	0·035	− 8·4

by Colburn and Drew is equal to $-18N_A c_w / Ah_0$ for the uni-directional diffusion taking place in the column. The heat balances were calculated for a datum of 100°F and are based on 1 lb. of dry air. The balances are expressed as an error in closure defined by

$$\% \text{ error in closure} = \frac{(\text{heat in} - \text{heat out}) \times 100}{\text{latent heat of water evaporated}}$$

A sample calculation (run 13) is as follows :

Dry air rate = 3·34 lb. per hr.

Total vapour entering column
= 0·03 + 5·84 − 0·14
= 5·73 lb. per hr.

Humidity at column inlet
= 5·73/3·34 = 1·716 lb. per lb.

Rate of vaporisation
= make-up rate = 1·16 lb. per hr.
= 0·0644 lb. moles per hr.

Humidity at column exit
= (5·73 + 1·16)/3·34
= 2·063 lb. per lb.

Vapour pressure of water at mean temp. (200·0°F)
= 0·783 atm.

Total pressure in column
= 0·992 atm.

Partial pressure of water in gas phase
— at column inlet = 0·729 atm.
— at column outlet = 0·763 atm.

Log mean driving force
= 0·034 atm.

Mean driving force by graphical integration
= 0·034 atm.

Inside area of column (dry)
= 0·731 sq. ft.

Mass transfer coefficient k_G
= 0·0644/0·034 × 0·731
= 2·59 lb. moles/(hr.) (ft.^{2}) (atm.)

p_{BM} at column inlet
$$= \frac{(0{\cdot}992 - 0{\cdot}729) - (0{\cdot}992 - 0{\cdot}783)}{\ln (0{\cdot}263/0{\cdot}209)}$$
= 0·236 atm.

p_{BM} at column exit
$$= \frac{(0{\cdot}992 - 0{\cdot}763) - (0{\cdot}992 - 0{\cdot}783)}{\ln (0{\cdot}229/0{\cdot}209)}$$
= 0·219 atm.

Mean p_{BM}
= (0·236 + 0·219)/2
= 0·228

Mean $\frac{p_{BM}}{P} = \frac{0{\cdot}228}{0{\cdot}992}$
= 0·230

Mean mass rate of flow W
= 3·34 + 5·73 + 1·16/2
= 9·65 lb. per hr.

Film temp.
— at column inlet = (813 + 200)/2 = 507°F
— at column outlet = (454 + 200)/2 = 327°F
— mean value = (507 + 327)/2 = 417°F

Viscosity at mean film temp.
— water vapour 0·0165 centipoise
— air 0·0252 centipoise
— mixture 0·0185 centipoise
= 0·0448 lb./(ft.) (hr.)
by the method of Bromley and Wilke [3].

Cross-sectional area of column (dry)
= 0·00442 sq. ft.

Mean Reynolds number for gas phase flow
$$= \frac{4W}{\pi d \mu} = 4 \times 9{\cdot}65/3{\cdot}142 \times 0{\cdot}0448 \times (0{\cdot}90/12)$$
$$= 17{\cdot}0 \times \frac{9{\cdot}65}{0{\cdot}0448} = 3662$$

$$D = 1{\cdot}46 \times 10^{-4} T^{2{\cdot}5}/P\,(T + 441)$$
$$= \frac{1{\cdot}46 \times 10^{-4}\,(417 + 460)^{2{\cdot}5}}{0{\cdot}992 \times (417 + 460 + 441)}$$
= 2·55 sq. ft. per hr.

$$k_G RTd/D$$
$$= \frac{2{\cdot}59 \times 0{\cdot}728 \times (417 + 460) \times (0{\cdot}90/12)}{2{\cdot}55}$$
= 48·6

Liquor rate
= 111 lb. per hr.

Correction factor (from Fig. 2)
= 1·048

VOL. 3 1954

$(k_G RTd/D)\,(Re^{-0.83})$ at 77 lb. per hr.
$= 48.6/1.048 \times 908$
$= 0.0511$

Mean molecular weight of gas stream
$= 20.7$

Sc calculated for this run
$= 0.547$

Sc used in calculations
$= 0.55$; $Sc^{2/3} = 0.671$

$(k_G p_{BM} M_m/G)\,Sc^{2/3}$ at a liquor rate of 77 lbs./hr.
$$= \frac{2.59 \times 0.228 \times 20.7 \times 0.00442}{9.65 \times 1.048} \times 0.671$$
$= 0.00358$

$(k_G p_{BM} M_m/G)\,(Sc^{2/3})\,(Re^{0.2}) =$
$= 0.00358 \times 5.16 = 0.0185$

Mass Balance

Total water vapour in

— as humidity in air (3.34×0.008)	0.03 lb. per hr.
— from boiler ($5.84 - 0.14$)	5.70 ,, ,, ,,
— make-up	1.16 ,, ,, ,,
— total	6.89 ,, ,, ,,

Total water vapour out

— condensed product	6.85 lb. per hr.
— in outlet air (3.34×0.022)	0.07 ,, ,, ,,
— total	6.92 ,, ,, ,,

Error in closure
$$= \frac{(6.89 - 6.92)}{1.16} \times 100$$
$= -2.6\%$

Total rate of heat transfer across gas-liquid interface
$= q_T = 1.16 \times 977.7 = 1134$ Btu per hr.

Heat transferred by radiation, using the approximate method of Perry [13, p. 490]
$= 124$ Btu per hr.

Heat transferred by convection
$= 1134 - 124$
$= 1010$ Btu per hr.

Log-mean temperature difference
$$= \frac{(813 - 200) - (454 - 200)}{\ln (613/254)}$$
$= 408°F$

Mean temperature difference by graphical integration $= 400°F$.

h = convection heat transfer coefficient
$= 1010/0.731 \times 408 = 3.39$ Btu/(hr)(sq.ft.) (°F.)

c_s at column inlet
$= 0.246 + 0.483 \times 1.716$
$= 1.075$ Btu/(°F) (lb. of dry air)

c_s at column exit
$= 0.243 + 0.475 \times 2.063$
$= 1.223$ Btu/(°F) (lb. of dry air)

mean value of c_s
$= 1.149$ Btu/(°F) (lb. of dry air)

h/cG
$$= \frac{3.39 \times 0.00442}{1.149 \times 3.34} = 0.00390$$

Liquor rate correction factor (from Fig. 2)
$= 1.045$

h/cG at liquor rate of 77 lb./hr.
$= 0.00390/1.045$
$= 0.00373$

$(h/cG)\,(Pr^{2/3})\,(Re^{0.2})$
$= 0.00373 \times 0.833 \times 5.16 = 0.0160$

$$\frac{h}{h_0} = \frac{0.0160}{0.025} = 0.64$$

$$a = -18\,N_A c_W/Ah_0$$
$$= -\frac{18 \times 0.0644 \times 0.479}{0.731 \times 3.39 \times (0.025/0.0160)} = -0.143$$

Heat Balance—

based on 100°F datum, 1 lb. of dry air

Heat in

— sensible heat of air-vapour stream (713×1.075)	766 Btu
— latent heat of water vapour (1.716×1037)	1779 Btu
— sensible heat in water evaporated (1.16×100)/3.34	35 Btu
total	2580 Btu

Heat out

— sensible heat of air-vapour stream
(354 × 1·223) 433 Btu

— latent heat of water vapour
(2·063 × 1037) 2139 Btu

total 2572 Btu

Error in closure

$$= \frac{2580 - 2572}{2139 - 1779} \times 100$$

$$= + 2{\cdot}2\%$$

Discussion

The effect of varying liquor rate on the mass and heat transfer coefficients was determined from several runs operated at low humidities and at almost constant Reynolds numbers for the gas stream. The results of these runs are shown in Fig. 2 where the dimensionless groups, h/cG and

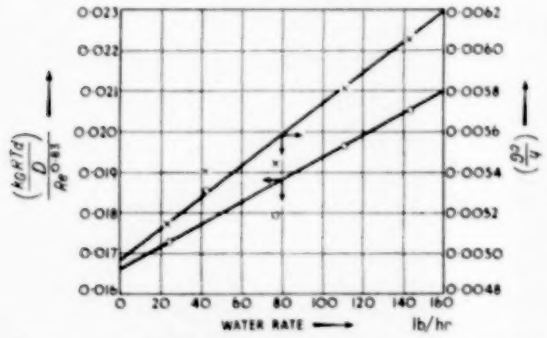

Fig. 2. The influence of the water rate on the mass and heat transfer coefficients.

$k_G RTd/DRe^{0.83}$ are graphed against liquor rate. The liquor rate has a small but appreciable effect on the gas film coefficients of heat and mass transfer.

The results were plotted by several of the methods suggested by previous investigators. The values of dimensionless groups involving k_G or h were corrected by means of Fig. 2 to a standard liquor rate of 77 lb./hr. Gilliland and Sherwood [8] correlated their results by the Nusselt-type equation (7). For a Schmidt number of 0·55 and a liquor rate of 77 lb./hr. the equation may be reduced to

$$(k_G RTd/D)(p_{BM}/P)\, Re^{-0.83} = 0{\cdot}017 \qquad (14)$$

The experimental mass transfer coefficients at low humidities agree with the Gilliland-Sherwood equation, but, as shown in Fig 3, the data at

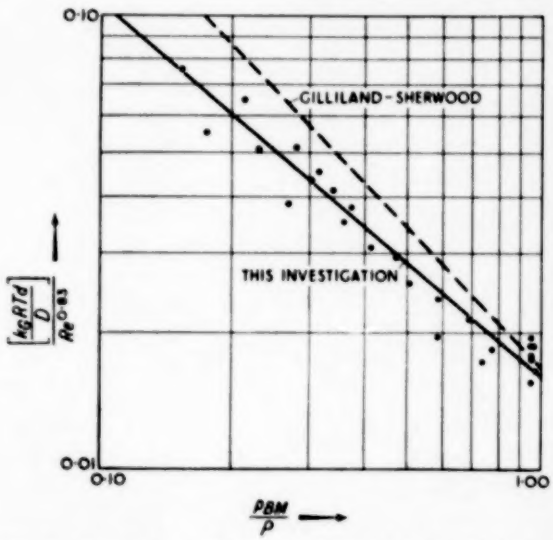

Fig. 3. Comparison of the mass transfer data with the Gilliland-Sherwood equation (14).

high humidities fall consistently below this line. The data at low and high humidities from this investigation were correlated by the method of least squares to give

$$(k_G RTd/D)(p_{BM}/P)^{0.83}\, Re^{-0.83} = 0{\cdot}016 \qquad (15)$$

or

$$(k_G RTd/D)(p_{BM}/P)^{0.83} = 0{\cdot}021\, Re^{0.83} Sc^{0.44} \qquad (16)$$

at a liquor rate of 77 lb./hr. and with a standard deviation of 10%. Comparison of equations (14) and (15) show that the present data do not support the usual procedure of assuming that k_G is inversely proportional to p_{BM}/P. The data were also correlated using viscosities and diffusivities evaluated at the bulk conditions of the air-vapour stream. The equation derived is almost identical to equation (15).

Chilton and Colburn [5] have correlated heat transfer data in an empty tube by plotting a heat transfer factor, $(h/cG)Pr^{2/3}$, against the Reynolds number. Similarly, they correlated mass transfer data by plotting a mass transfer

VOL. 3 1954

factor, $(k_G p_{BM} M_m/G)\, Sc^{2/3}$, against the Reynolds number. Their correlations may be written

$$(h/cG)\, Pr^{2/3} = (k_G p_{BM} M_m/G)\, Sc^{2/3} = 0{\cdot}023\, Re^{-0{\cdot}2} \qquad (17)$$

For a liquor rate of 77 lb./hr. equation (17) becomes

$$(h/cG)\, Pr^{2/3} = (k_G p_{BM} M_m/G)\, Sc^{2/3} = 0{\cdot}026\, Re^{-0{\cdot}2} \qquad (18)$$

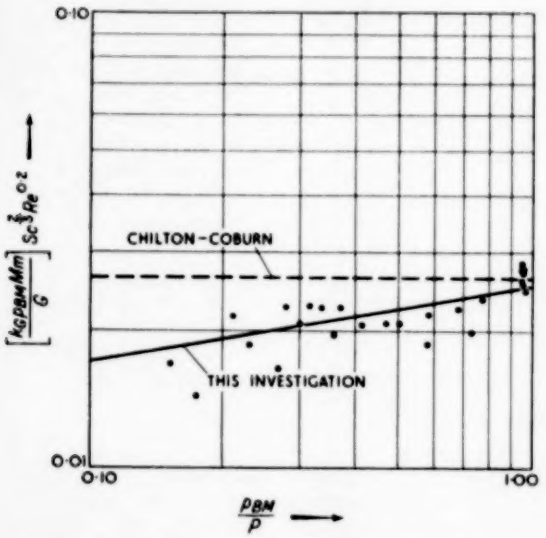

Fig. 4. Comparison of the mass transfer data with the CHILTON-COLBURN equation (18).

The mass transfer data of this investigation have been correlated in Fig. 4 by plotting $(k_G p_{BM} M_m/G)\, Sc^{2/3}\, Re^{0{\cdot}2}$ against p_{BM}/P. The Chilton-Colburn equation (18) is represented by the horizontal line. The data fall consistently below this line at high humidities although the data at low humidities agree with it. The data are best correlated by defining a new mass transfer factor,

$$j_D = (k_G p_{BM} M_m/G)\, Sc^{2/3}\, (p_{BM}/P)^{-0{\cdot}17} \qquad (19)$$

j_D is found to be equal to $0{\cdot}025\, Re^{-0{\cdot}2}$ at 77 lbs./hr. liquor rate. Comparison of equations (18) and (19) show that the present data do not support the CHILTON-COLBURN mass transfer factor at high humidities.

The heat transfer data have been correlated in Fig. 5 by plotting $(h/cG)\, Pr^{2/3}\, Re^{0{\cdot}2}$ against

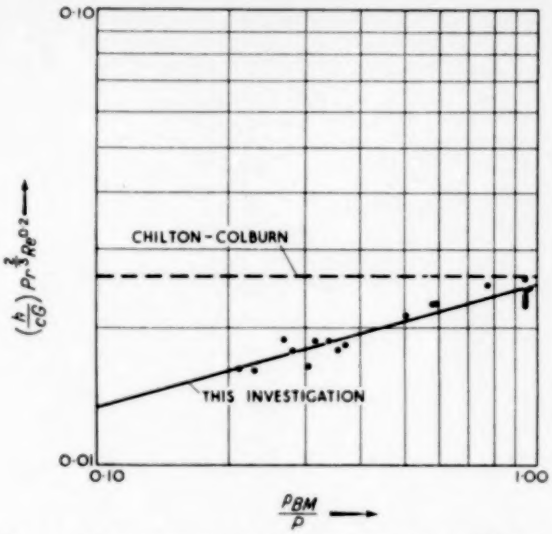

Fig. 5. Comparison of the heat transfer data with the CHILTON-COLBURN equation (18).

p_{BM}/P. The CHILTON-COLBURN equation (18) is represented by the horizontal line. At low humidities the data agree with the CHILTON-COLBURN equation. At high humidities the data fall consistently below the line of equation (18). The data are best represented by defining a new heat transfer factor,

$$j_H = (h/cG)\, Pr^{2/3}\, (p_{BM}/P)^{-0{\cdot}27} \qquad (20)$$

j_H is found to be equal to $0{\cdot}025\, Re^{-0{\cdot}2}$ at 77 lbs./hr.

Both the heat and mass transfer data of the present investigation can be correlated by the one equation

$$j_H = j_D = 0{\cdot}025\, Re^{-0{\cdot}2} \qquad (21)$$

at 77 lb./hr.

The correlations above apply to all the data irrespective of whether the heat balance is positive or negative. Therefore any small temperature gradients in the liquid due to slight heat leakages are negligible.

COLBURN and DREW [6] have proposed a theoretical equation for heat transfer coefficients with simultaneous mass transfer. The effect of the simultaneous mass transfer on the heat transfer coefficient is given by equation (13), where a, in this case, is $-18 N_A c_w/A h_0$. The

ratio h/h_0 is plotted in Fig. 6 as a function of a. The correlation is poor. In particular, runs 2-6 and run 9 show that the correlation in Fig. 5 against p_{BM}/P is superior. The theoretical line of equation (13) is shown in Fig. 6. The predicted effects of a are much smaller than those obtained experimentally.

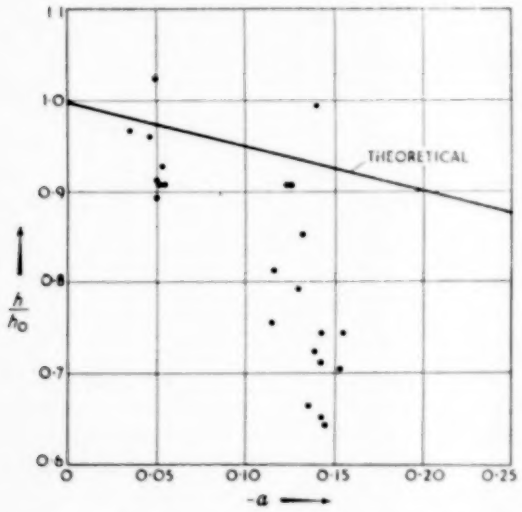

Fig. 6. Comparison of the data with the theoretical equation (13) of Colburn and Drew.

Conclusions

The liquor rate in a wetted-wall column has an appreciable effect on the mass and heat transfer coefficients in the column.

The gas film coefficients of mass transfer in a wetted-wall column vary inversely as the 0·83 power of the ratio p_{BM}/P, and not as the 1·00 power as has previously been assumed on the basis of the film theory. The equations of Gilliland and Sherwood, and of Chilton and Colburn therefore should not be used at high humidities.

The gas film coefficients of heat transfer in an adiabatic wetted-wall column vary as the 0·27 power of the ratio p_{BM}/P and are not independent of this ratio as required by the Chilton-Colburn equation.

The theoretical equation of Colburn and Drew based on the film theory is unable to explain the reduction in the heat transfer coefficient, occurring at high humidities, found in this investigation.

Acknowledgments

Acknowledgment is made to Professor J. P. Baxter, School of Chemical Engineering, N.S.W. University of Technology for helpful discussion and continued interest in this work. The authors are also indebted to Mr. R. Beattie for the construction of the apparatus.

Notation

a = the ratio between the nett sensible heat carried by the diffusing vapours and the heat transferred in the absence of mass transfer
A = the area of the gas-liquid interface, taken as the inside area of the column, when dry, sq. ft.
c = specific heat, Btu/(lb.) (°F.)
c_s = humid heat of the air-vapour mixture, Btu/(lb.) of dry air) (°F)
c_w = specific heat of water vapour, Btu/(lb.) (°F)
c_1, c_2 = the specific heat of diffusing component 1 or 2 respectively, Btu/(lb.) (°F)
d = diameter of column, ft.
D = molecular diffusivity of the diffusing component, sq.ft./hr.
e = base of Naperian logarithms
g = gravitational constant ft./(hr.^{2})
G = mass velocity, lb./(hr.) (ft.^{2})
Gr = modified Grashof number for mass transfer $= (gd^3\rho^2/\mu^2)(M_a T_i/M_i T_a - 1)$
h = convective heat transfer coefficient, Btu/(hr.) (ft.^{2}) (°F)
h_0 = convective heat transfer coefficient in the absence of mass transfer, Btu/(hr.) (ft.^{2}) (°F)
H = humidity, lb. of water vapour per lb. of dry air
j_D = mass transfer factor $= (k_G p_{BM} M_m/G)\, Sc^{2/3} (P_{BM}/P)^{-0.17}$
j_H = heat transfer factor $= (h/cG)\, Pr^{2/3} (p_{BM}/P)^{-0.27}$
k = thermal conductivity, Btu/(hr.) (ft.) (°F)
k_G = the gas film coefficient of mass transfer, lb. moles/(hr.) (ft.^{2}) (atm.)
K_G = the overall mass transfer coefficient, lb. moles/(hr.) (ft.^{2}) (atm.)
M_i = molecular weight at the gas-liquid interface
M_a = the molecular weight of the gas-vapour mixture " far away " from the gas-liquid interface
M_m = the molecular weight of the gas-vapour mixture in the main stream
N_A = the rate of evaporation of water vapour, lb. moles/hr.
Nu = Nusselt number $= hd/k$
P = total pressure, atm.
p_{BM} = the logarithmic mean partial pressure of the non-diffusing gas in the gas film, atm.

VOL. 3 1954

Δp = the driving force for the diffusing vapour, atm.
$\Delta p_{\text{l.m.}}$ = the logarithmic mean between the driving forces at each end of the column, atm.
Pr = Prandtl number = $c\mu/k$
q_C = the rate of heat transfer by convection, Btu/hr.
q_T = the total rate of heat transfer, Btu/hr.
R = gas constant, (ft.^{3}) (atm.)/(lb. mole) ($^\circ$R)
Re = Reynolds number = dG/μ
Sc = Schmidt number = $\mu/\rho D$
St = Stanton number = h/cG
T = absolute temperature, $^\circ$R
T_i = absolute temperature at the gas-liquid interface, $^\circ$R
T_a = absolute temperature "far away" from the gas-liquid interface.
Δt = temperature difference, $^\circ$F
$(\Delta t)_{\text{l.m.}}$ = logarithmic mean temperature difference, $^\circ$F
w_1, w_2 = the rate of diffusion of component 1 or 2 respectively, lb./(hr.) (ft.^{2})
W = mass rate of flow, lb./hr.
x = distance in the direction of diffusion, ft.
μ = viscosity, lb./(hr.) (ft.)
ρ = density, lb./ft.^{3}

References

[1] Barnet, W. I. and Kobe, K. A.; Ind. Eng. Chem. 1941 **33** 436.

[2] Boelter, L. M. K., Gordon, H. S. and Griffin, J. R.; Ind. Eng. Chem. 1946 **38** 596.

[3] Bromley, L. A. and Wilke, C. R.; Ind. Eng. Chem. 1951 **43** 1641.

[4] Cairns, R. C.; Chem. Eng. Sci. 1953 **2** 127.

[5] Chilton, T. H. and Colburn, A. P.; Ind. Eng. Chem. 1934 **26** 1183.

[6] Colburn, A. P. and Drew, T. B.; Trans. Amer. Inst. Chem. Engrs. 1937 **33** 197.

[7] Colburn, A. P. and Hougen, O. A.; Ind. Eng. Chem. 1934 **26** 1178.

[8] Gilliland, E. R. and Sherwood, T. K.; Ind. Eng. Chem. 1934 **26** 516.

[9] Hanks, W. V. and McAdams, W. H.; Ind. Eng. Chem. 1929 **21** 1034.

[10] Hemeon, —.; Thesis in Chem. Eng. M.I.T. 1927.

[11] Hinchley, J. W. and Himus, G. W.; Trans. Inst. Chem. Engrs. (London) 1924 **2** 57.

[12] McAdams, W. H.; Heat Transmission, 2nd. ed., McGraw-Hill Book Co., Inc. N.Y. 1942.

[13] Perry, J. H.; Chemical Engineers' Handbook, 3rd ed., McGraw-Hill Book Co. Inc., N.Y. 1950.

[14] Sherwood, T. K. and Pigford, R. L.; Absorption and Extraction, 2nd ed., McGraw-Hill Book Co. Inc. N.Y. 1952.

[15] Wade, S. H.; Trans. Inst. Chem. Engrs. (London) 1942 **20** 1.

[16] Wenner, R. R.; Thermochemical Calculations, McGraw-Hill Book Co. Inc., N.Y. 1941.

Chemical Engineering Science, 1954, Vol. 3, pp. 110 to 121. Pergamon Press Ltd.

Variables affecting activity of molybdena-alumina hydroforming catalyst in aromatization of cyclohexane

C. G. RUDERSHAUSEN* and C. C. WATSON

University of Wisconsin, Madison, Wisconsin

(*Received* 17 *February* 1954)

Summary—An exploratory study has been made to determine the nature and magnitude of the more obvious variations in the activity of a single batch of catalyst. A pelleted, coprecipitated, gel-type catalyst similar to that used in many commercial catalytic reforming units was studied in a differential reactor.

Apparently the molybdenum oxide promoter was at a higher level of activity when the oxide was in a reduced state, the improvement being directly proportional to the degree of molar reduction of the oxide. Deposition of coke on the catalyst, which reduced activity exponentially, appeared to be a surface-controlled reaction and to involve a dual site mechanism. Increased hydrogen to hydrocarbon molar feed ratios reduced carbon deposition in direct proportion to the associated increase in hydrogen partial pressure, but also reduced conversion because of the lowered reactant partial pressure.

Catalyst regeneration appeared to occur in two distinct steps. In the first step, the rate had a second order dependency on coke concentration. In the second step, for which first-order dependencies on coke concentration and oxygen partial pressure were observed, mass transfer seemed to be the controlling mechanism. No improvement in catalyst activity was noted in the removal of carbon in this second step.

Résumé—Avant d'entreprendre l'étude du mécanisme réactionnel, on a procédé à étude préliminaire de la nature et de la grandeur des variations les plus importantes observables avec une même préparation de catalyseur.

Dans un convertisseur différentiel, on a étudié un catalyseur semblable à celui qui est utilisé dans de nombreuses unités de " reforming " : catalyseur pastillé à partir d'un gel obtenu par coprécipitation.

Il semble que l'activité promotrice de l'oxyde de molybdène est plus élevée quand l'oxyde est dans son état réduit, l'amélioration paraissant directement proportionnelle au degré de réduction molaire de l'oxyde. Le dépôt du coke sur le catalyseur réduisant l'activité exponentiellement semble être une réaction contrôlée par la surface avec un mécanisme faisant appel à deux sites. Avec des alimentations correspondant à un rapport molaire accru de l'hydrogène à l'hydrocarbone, le dépôt de carbone est réduit proportionnellement à l'accroissement de la pression partielle de l'hydrogène, et également à la diminution de la conversion qui est associée à l'abaissement de la pression partielle de l'hydrocarbone.

La régénération du catalyseur paraît s'effectuer en deux étapes : Dans la première, la vitesse dépend de la concentration du coke suivant l'orde deux. Dans la deuxième étape, où l'on observe des relations de premier ordre avec la concentration en coke et la pression partielle de l'oxygène, il semble que le transfert de matière est le mécanisme contrôleur. L'enlèvement du coke dans cette deuxième étape ne s'accompagne pas d'amélioration dans l'activité catalytique.

* Present address : Explosives Department, Eastern Laboratory, E.I. du Pont de Nemours & Co., Gibbstown, New Jersey, U.S.A.

VOL. 3 1954

The investigation was divided into the following studies :

(1) Reduction of catalyst promoter by pretreatment with hydrogen for different lengths of time and in various states of dilution with nitrogen, with and without water vapour addition.

(2) Catalyst fouling by coke deposition during hydrocarbon processing – its effects on catalyst activity, a suggested mechanism of deposition, and its suppression by hydrogen.

(3) Catalyst regeneration – burning rates, degree of regeneration, and mechanism of burning during the later burning stage.

Equipment and Materials

Catalyst

A coprecipitated molybdena-alumina gel-type hydroforming catalyst in the form of $\frac{3}{16}$ in. cylindrical pellets was used. It was obtained as a sample from California Research Corporation, identified by them as CRC-7242, and was similar in chemical composition to that used in many of the catalytic reforming units in the petroleum industry. It was specified as containing approximately 10% molybdena as MoO_3, as having a specific surface in the order of 90 m^2/gm, and as being well below 1% in impurities, chiefly iron and sodium.

Feed

A 98 + mole per cent cyclohexane, purchased from *Shell Chemical Co.*, was distilled in a 30-plate Oldershaw column at a reflux ratio of 7/1, the top 5% and the bottom 5% being discarded. Negligible discrepancy was observed on an analytical infra-red differential spectrum between this feed stock and a sample of very carefully purified cyclohexane.

Reactor

The most significant feature of the equipment was the differential reactor used, that is, a reactor containing only a small catalyst bed which provided conversions generally no greater than 10%. Thus, the temperature and partial pressure variations were most probably either negligible or sufficiently small over the catalyst bed to permit the use of linear approximations.

The 30 grams of catalyst were contained in a 1 in. stainless steel pipe equipped with a preheater spiral to vaporize cyclohexane and to promote mixing and heat transfer. A well, containing thermocouples at levels near the top, at the middle, and near the bottom of the 3 in. high catalyst bed passed axially through the centre of the bed. Because of the large thermal inertia of the aluminium-bronze blocks in which the reactor pipe was contained, the temperature of the catalyst bed could generally be maintained within $\pm$ 1°F.

Feed and Recovery Systems

Cyclohexane was pumped into the reactor by a calibrated assembly consisting of a Zenith gear pump which discharged a heavy oil. This oil displaced mercury which in turn displaced cyclohexane from a high-pressure burette. Copper tubing was used for liquid feed lines. Hydrogen feed was controlled by a needle valve and measured by a high-pressure orifice. In order to eliminate the oxygen contamination, all hydrogen was passed through a stainless steel tube containing quartz chips heated to 1100°F, and then through Drierite, before passing to the reactor.

In the recovery system, ice water was circulated through the liquid product condensers. U-tubes containing Drierite and Ascarite, in that order, were used for water and carbon dioxide determination in product gases. In order to permit complete quantitative determination of carbon, the regeneration gases were passed through a tube of CuO particles held at 300°C, to oxidize any carbon monoxide.

Experimental Procedure

Catalyst Selection

Catalyst pellets from the original sample lot described were selected for the one experimental catalyst bed used throughout the investigation on the basis of their crushing strength. This was considered necessary in the light of previous experiences in which the greater fraction of the pellets in the catalyst bed were observed to soften and crumble. Furthermore, it was also considered desirable because such a selection tended to fix an important variable in the catalyst effectiveness

factor. Thus only pellets were used which withstood a 15-lb. crushing force applied perpendicularly to the cylinder axis. This selection test was passed by only 22% of the pellets in the batch of catalyst sample originally received and which was presumably representative of that commercially used. It has been indicated that it is probably reasonable to assume direct proportionality between crushing strength and density. The pellets in the batch finally selected had densities between 1·47 and 1·70, with an average of 1·56 gm/cc, compared to a density range of between 1·13 and 1·70 for the original batch, with an average density of 1·36 gm/cc.

Reaction Conditions

Studies were made at the following conditions :

Variable	*Range*	*"Standard"*
Catalyst weight, W (gm)	31·2	31·2
Reciprocal space velocity, W/F (gm catalyst/gm mole C_6H_{12}/hr.) . .	5-22	10·4
Pressure (atmabs.)	1·7-7·8	1·7
Temperature (°F)	860-980	940
H_2/C_6H_{12} molar feed ratio, R	0/1-7/1	4·0/1

Run Procedure

The " standard " run consisted of the following operations performed in this order :

(1) Catalyst pretreatment with 100% H_2 at 0·09 scfm. and 1000°F, 15 min.
(2) Hydrocarbon processing, 15 min.
(3) Purge with N_2 at 0·25 scfm., 5 min.
(4) Regeneration with air at 1·7 atmabs. and at 0·025 scfm., 15 min.
(5) Purge with N_2 at 0·25 scfm., 5 min.

The liquid product sample used for the determination of catalyst activity was that obtained during the 3 to 10 min. interval of hydrocarbon processing. As will be noted from Fig. 3, the decline in catalyst activity during this period was still rapid. However, the rate of decline was considerably lower than during the first 3 min., so that reproducibility in sampling was considerably enhanced. The samples were analyzed for benzene concentration by a checked infrared spectrophotometric method.

Determination of Catalyst Activity

Catalyst activity factors were determined by reference to standard curves of conversion, x, vs. reciprocal space velocity, W/F, with temperature as a parameter, as suggested by HOUGEN and WATSON [4]. These curves, illustrated in Fig. 1, were obtained in a single series of runs using the same batch of catalyst which was used throughout the investigation. The "standard" procedure and conditions (except temperature, which was a parameter) were used. Since the " standard " procedure included sampling during the 3 to 10 min. hydrocarbon processing period, the catalyst activity which provided a basis of comparison was by consequence of this procedure integrated over this same time period.

Since

$$\left(\frac{L_{r_1}}{L_{r_2}}\right) = \frac{(W/F)_1}{(W/F)_2}\Bigg)_{x,T,P,} \quad \text{where}$$

L_{r_1} = activity of catalyst under test conditions ;

L_{r_2} = activity of catalyst under standard conditions ; activity considered unity;

$(W/F)_1$ = standard reciprocal space velocity at x, T, P (from standard curves) ;

$(W/F)_2$ = experimental reciprocal space velocity at x, T, P ;

x, T, P = conversion, temperature, and pressure, respectively ;

$$\left(L_r\,(=L_{r_1}) = \frac{(W/F)\text{ std.}}{(W/F)\text{ exptl.}}\right)_{x,T,P,}$$

The difference between uncorrected plots of conversion vs. reciprocal space velocity, and plots corrected to a standard carbon concentration is also illustrated in Fig. 1. These plots, as they have been used in this study and as generally used for the determination of catalyst activity, apply to a standard process period. Hence, each point represents a different integrated catalyst activity because of the varying coke concentration on the catalyst resulting from the variations in operating temperature and in the conversion corresponding to the different feed rates. However

VOL. 3 1954

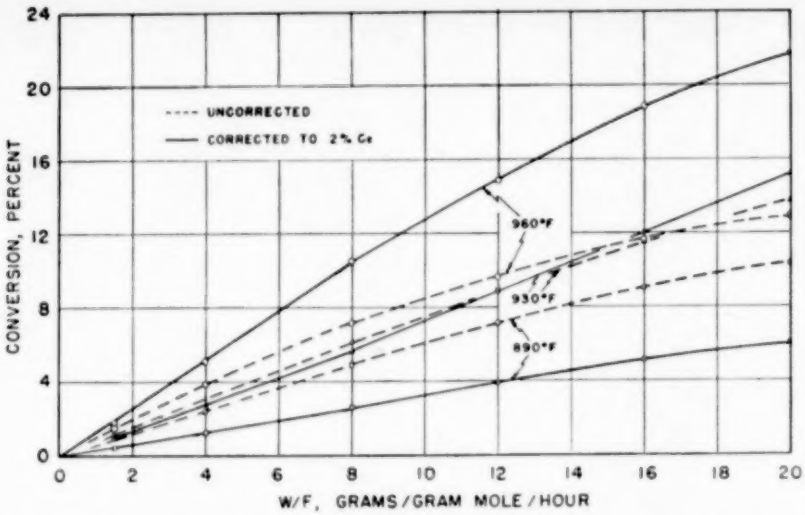

Fig. 1. Conversion vs. W/F : contrast between uncorrected curves and curves corrected to constant catalyst carbon concentration (P = 1·7 atmabs.; R = 4·0/1 molar feed ratio.)

at the lower conversions and reciprocal space velocities, nearly linear relationships generally apply. Thus the error is usually not serious in this range. It is obvious from the curves shown in Fig. 1 that a larger discrepancy is introduced in directly comparing catalyst activity at different temperature levels using the uncorrected curves. This results from the fact that uncorrected isotherms refer to the catalyst at substantially different levels of activity because of the appreciably different carbon concentrations at the different temperatures.

It is also desirable to observe the correction to a common coke concentration in obtaining reaction velocity constants and enthalpies of activation. It is often preferable to obtain the more meaningful values referring to the clean catalyst from a plot corrected to zero coke concentration. The conversions for the clean catalyst at a given temperature would be obtained by extrapolation.

Catalyst Pretreatment

A striking increase in the activity of the catalyst was observed to result from a hydrogen pretreatment, and this was accompanied by the evolution of appreciable quantities of water. It has been tentatively suggested that the molybdenum promoter was reduced to a lower and more catalytically active state of oxidation than that in which it was left after the catalyst regeneration with air.

The following reaction seemed to be a plausible description [6] :

$$5MoO_3 + 8H_2 \longrightarrow Mo_5O_7 + 8H_2O.$$

The quantity of water evolved in pretreatment was in good agreement with that calculated by assuming the molybdena to be present entirely as MoO_3 after regeneration and to be completely reduced to Mo_5O_7 during an extended hydrogen pretreatment.

The data showed a 10% increase in activity with a fivefold increase in hydrogen flow rate during pretreatment, from 0·018 scfm. to 0·090 scfm. At the lower of these flow rates, the reduction in hydrogen partial pressure over the bed at the point of maximum rate of water evolution was practically negligible.

The effect of the length of the pretreatment on catalyst activity is shown in Fig. 2. The greater percentage of the improvement in activity occurred during the early period of pretreatment. The fact that the curve plotting the degree of

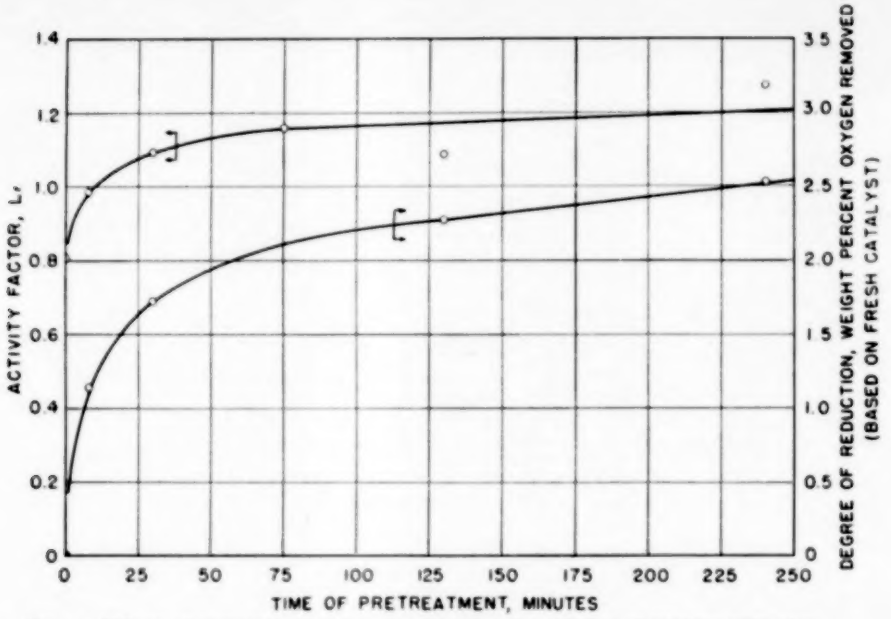

Fig. 2. Effects of pretreatment time on activity and on degree of catalyst reduction.

reduction (defined as the weight per cent oxygen removed, based on fresh catalyst) was of the same shape suggested the linear relationship between activity and the degree of reduction, shown graphically in Fig. 3.

Changes in the degree of reduction were also accomplished by varying the concentration of water vapour in the pretreatment gas between 0 and 2 mole per cent while holding pretreatment time constant. While the rate of reduction was considerably reduced by the added water vapour, the activity was again observed to be a linear function of the degree of reduction, as also shown in Fig. 3. Possibly water was adsorbed by active sites and thus tended to diminish the accessibility of the active sites for reduction. In hydrocarbon processing, water may then have been rapidly displaced from the active sites by the preferentially adsorbed hydrocarbons so that the changes in activity were a reflection only of the changes in the degrees of reduction. Thus, Fig. 3 also shows that the relationships between activity and degree of reduction effected by both methods coincide. Chemisorption of water at these temperatures has been evidenced in the dehydrogenation of butane on chromia-alumina catalysts ;

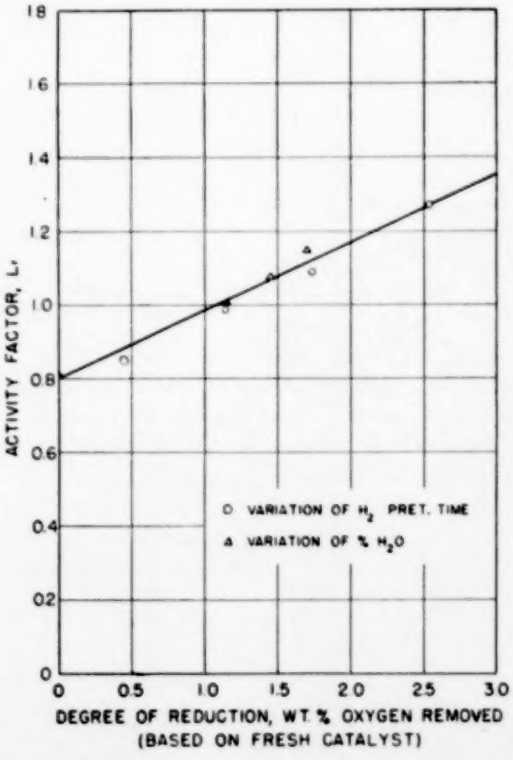

Fig. 3. Activity factor vs. degree of catalyst reduction.

VOL. 3 1954

and present data on the molybdena-alumina catalyst used in this work indicates that the surface of the lower oxide is saturated with chemisorbed water [9].

The effect of the concentration of hydrogen in the pretreatment gas diluted with nitrogen was also observed. The activity increased only a few per cent for an increase in hydrogen concentration from 25 to 100 mole per cent. At 0% hydrogen, the effect was the same as that of no pretreatment. No data were obtained at concentrations between 0% and 25% hydrogen.

The reduction of molybdenum oxides has been mentioned as taking place during hydrocarbon processing in commercial hydroforming for production of high-octane motor fuel [3]. The final metal oxide at the completion of the 4½ hr. hydrocarbon processing period has been suggested to be approximately Mo_2O_3. This reference states that the reduction of the molybdena results in a decline (not an increase) in catalyst activity. Herrington and Rideal [5] have attributed the promoter action of an alumina supported catalyst to the stabilization of the MoO_2 produced during the hydrogen pretreatment. The reaction under test was the aromatization of a paraffin. Using a chromia-alumina catalyst in the dehydrogenation of butane, Stevens [8] observed an appreciable decline in catalyst activity with the reduction of the chromium oxide promoter and observed a corresponding increase in catalyst activity with oxidation of the chromium oxide. He was able to relate the effects on the catalyst activity to the partial pressures of hydrogen and oxygen and the time of treatment for the reduction-oxidation cycle.

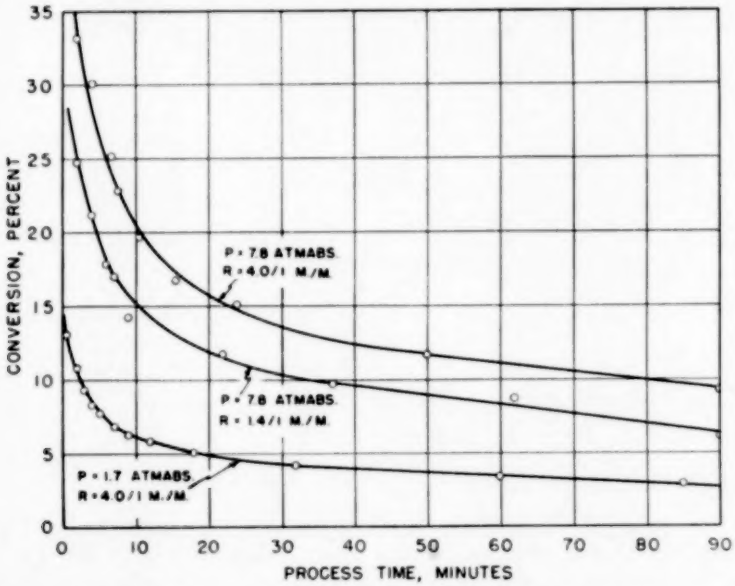

Fig. 4. Conversion vs. process time at various conditions of total pressure and H_2/C_6H_{12} molar feed ratio (all other conditions "standard").

Hydrocarbon Processing

Nature of Carbon Deposition

The initially rapid decline in conversion with process time is shown in Fig. 4 and is reflected in the plots of activity vs. process time and vs. carbon deposition, Fig. 5. Process time and carbon deposition are shown to affect activity exponentially. As implied here, carbon deposition increased exponentially with time. Within the experimental error, the rate of carbon deposition could be described as

$$\frac{dCc}{d\theta} = \frac{K}{Cc}, \text{ where}$$

$\frac{dCc}{d\theta}$ = rate of carbon deposition,

Cc = concentration of carbon on the catalyst, and

K = a constant.

Voorhies [10] observed the same relationship in his work with both natural and synthetic cracking catalysts in both fixed and fluidized beds using a gas-oil feed. Because a postulated diffusion-controlled mechanism, wherein the coke represents the resistance, would imply a rate of carbon deposition inversely proportional to the coke concentration, and because of the low temperature coefficient of carbon deposition which he observed (a 200°F increase in temperature in the 900°F vicinity approximately doubled the carbon formation rate), he suggested that a diffusion mechanism might be controlling the carbon deposition. However, the temperature coefficient observed for the system used here was nearly ten times greater. This appeared to rule out the possibility that the controlling mechanism for this system was diffusion and suggested a reaction-controlled mechanism.

A frequently advanced hypothesis of coke formation is the irregular "polymerization" of unsaturated by-products to form polymers which tend to be preferentially adsorbed and then to be progressively dehydrogenated. In the light of this hypothesis, a suggested reconciliation of the high temperature coefficient to the inverse proportionality of the rate to the concentration of carbon on the catalyst is indicated by the following analysis suggested by Villiers-Fisher [9]:

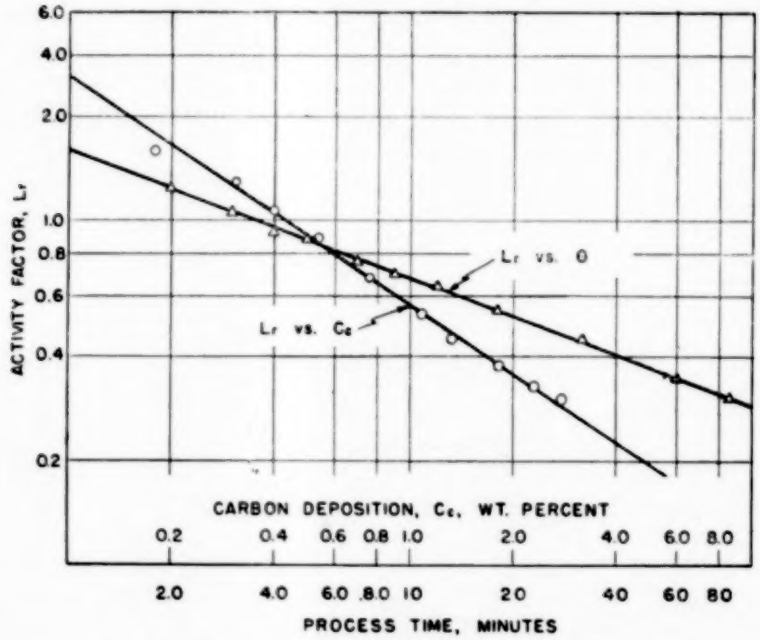

Fig. 5. Decline in activity with process time and with carbon deposition ("standard" conditions, except process time).

Assume that the reaction taking place in coke formation is

$$A_n + A \longrightarrow A_{n+1}, \text{ where}$$

A_n = adsorbed coke molecule (postulated to be unsaturated);

A = adsorbed unsaturate molecule to be added;

A_{n+1} = adsorbed larger coke molecule.

VOL. 3 1954

Neglecting the reverse reaction and assuming that the mechanism of the indicated reaction involves reaction of an activated unsaturate on one active site with the " coke unsaturate " on an adjacent active site, the rate of reaction is expressed as

$$r = \frac{Ca_A a_{A_n}}{(1 + K_A a_A + K_{HC} a_{HC} + K_{A_n} a_{A_n})^2},$$

where

C = a constant at the given reaction conditions ;

a = thermodynamic activity ;

K = adsorption equilibrium constant of subscript ;

HC = adsorbed hydrocarbons not participating in reactions of coke formation.

Assuming (1) that $(K_{A_n} a_{A_n}) >> (1 + K_A a_A + K_{HC} a_{HC})$ on the basis that the coke is probably much more strongly adsorbed than the unsaturates or other hydrocarbons ; (2) that the coke can be considered in terms of thermodynamic activity as shown in the rate equation ; and (3) that the activity of the unsaturate additives remains reasonably constant on the basis of the reasonably constant conversion observed during the run beyond the initial processing period, the rate equation then simplifies to

$$r = \frac{C'}{a_{A_n}}. \qquad \text{Here}$$

r = rate of coke deposition $\sim \dfrac{dCc}{d\theta}$;

a_{A_n} = activity of coke $\sim Cc$, coke concentration ;

C' = a constant $\sim K$, another constant,

and the equation is equivalent to the rate equation originally indicated by the data,

$$\frac{dCc}{d\theta} = \frac{K}{Cc}.$$

This analysis indicates that perhaps the coke deposition was controlled by a dual site surface reaction mechanism.

Coke deposition was observed to increase only about 50% with a fourfold increase in conversion at 940°F (from approximately 4% to 16% conversion) and a corresponding increase in reciprocal space velocity, W/F (from 5 and 22 gm/gm mole/-hr.). While a definite relationship was shown between coke deposition and aromatization activity, as described earlier, it is possible that coke formation, presumably a very irregular reaction, was promoted in part by sites which did not effect aromatization. Conceivably, the relatively slight increase in coke deposition with conversion might have been the result of the promotion of certain side reactions producing unsaturates, which by their condensation contributed to coke formation. These side reactions may have been promoted, at least in part, by the site systems responsible for aromatization. The rate of coke deposition may also have been increased by the higher concentration of unsaturate intermediates of the principal reaction, the concentration of these intermediates being a function of the conversion.

The hypothesis of the compound site system for coke formation may be further supported by the fact that aromatization catalyst activity was definitely diminished by small concentrations of water in the feed, but the activity for coke formation apparently remained relatively uninhibited. On the other hand, this might have been a result of competitive active site adsorption in which the coke and its intermediates competed against water more successfully than the cyclohexane.

Again, in the aging of the catalyst, the increase in coke formation activity was about four times the increase in aromatization activity. On the other hand, this might possibly be explained in terms of specifically unobserved phenomena which occurred during the early hydrocarbon processing period. During this period the initial carbon deposition was relatively large, and yet the sample on which aromatization activity was based was not taken during this initial period but rather during the 3 to 10 min. period.

Heinemann [2] cites evidence which might be interpreted as lending further support to the hypothesis of the compound site system in coke formation. In the dehydrogenation of methylcyclopentane using a chromia-alumina catalyst,

he observed that the effect of adding a small quantity of benzene to the feed was to reduce the coke deposition to approximately a third of its original level without appreciably diminishing the conversion. This might have implied the poisoning of sites active in carbon formation, suggesting a separate site system for the dehydrogenation and for the coke formation.

Hydrogen Addition

The effect of hydrogen addition with the hydrocarbon feed is shown in Fig. 6. Carbon deposition was found to decrease linearly with hydrogen partial pressure, showing the suppression of coke formation, apparently by saturation of olefinic precursors in proportion to the hydrogen partial pressure. Conversion, however, decreased linearly with increased hydrogen partial pressure because of the correspondingly reduced reactant partial pressure. Although the curves shown in Fig. 7 obviously apply specifically to the " standard " conditions and the physical system used in this particular investigation, they illustrate very strikingly the favourable effect of hydrogen addition on the one hand, namely, the diminished coke deposition and the associated higher catalyst activity ; and the unfavourable effect on the other hand, namely, the decreased conversion due to decreased reactant partial pressure.

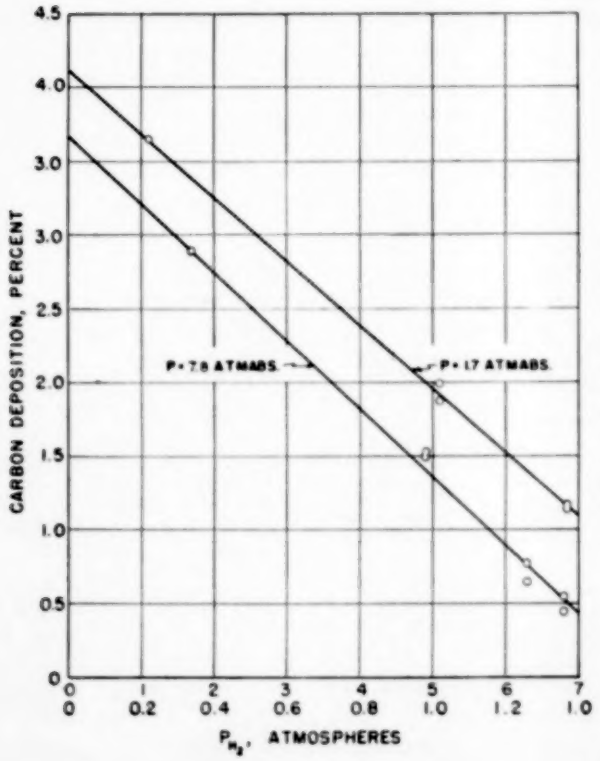

Fig. 6. Effect of partial pressure of hydrogen on carbon deposition ("standard" conditions, except total pressure and H_2/C_6H_{12} molar feed ratio).

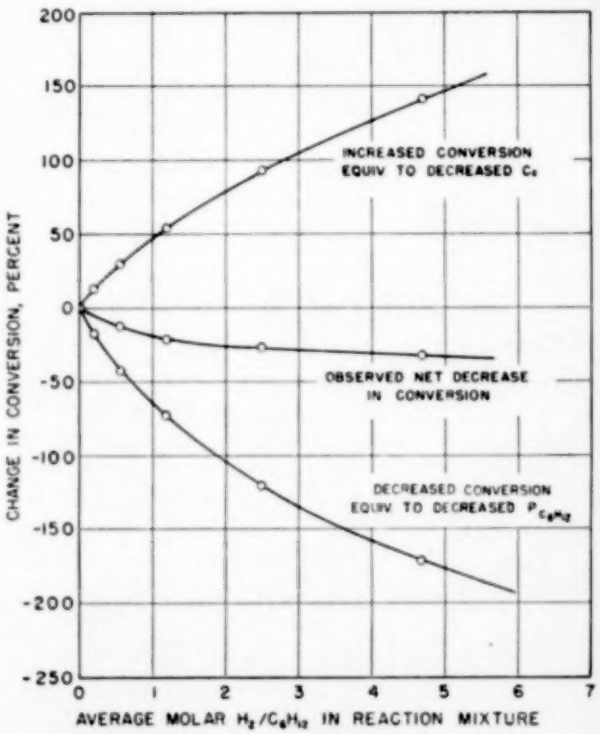

Fig. 7. Change in conversion vs. average H_2/C_6H_{12} in reaction mixture (all conditions "standard" except H_2/C_6H_{12} molar feed ratio).

REGENERATION

The evolution rates at various levels of original total carbon deposition are shown in Fig. 8. As will be noted, two distinctly different rates of carbon evolution were involved. The primary burning occurred at a high rate, and at its

VOL. 3 1954

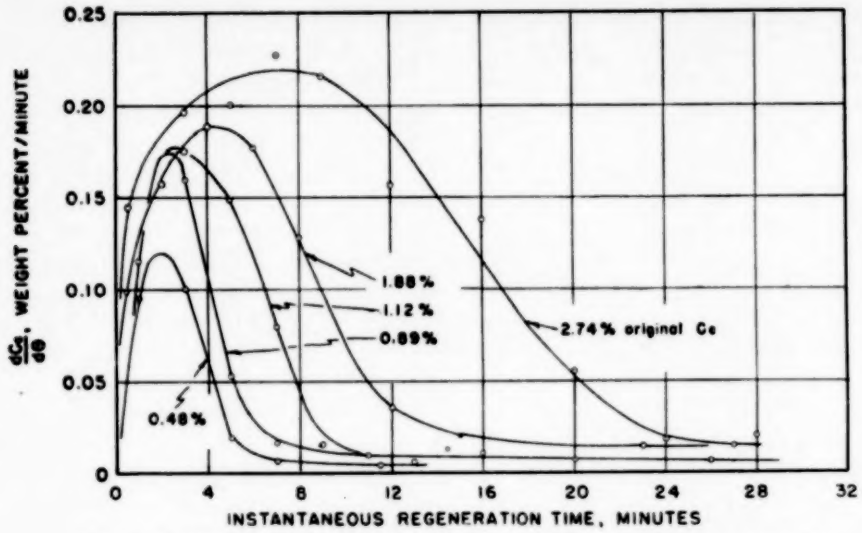

Fig. 8. Carbon evolution rates at various levels of original total carbon deposition.

completion, the rate decreased abruptly, being followed by a secondary burning which occurred at a much lower rate. This suggested that coke was first removed from the more accessible surfaces of the catalyst during the primary burning period, and that the remainder of the coke burned off at a far lower rate from the less accessible surfaces of the catalyst.

The rate of carbon evolution as a function of the instantaneous carbon concentration on the catalyst is shown in Fig. 9. The data were obtained from a single regeneration four hours in duration, which probably implied the removal of very nearly all the carbon from the catalyst. Thus, values of instantaneous total carbon concentrations were probably reasonably accurate representations. Again, two distinctly different carbon rates appear to be indicated.

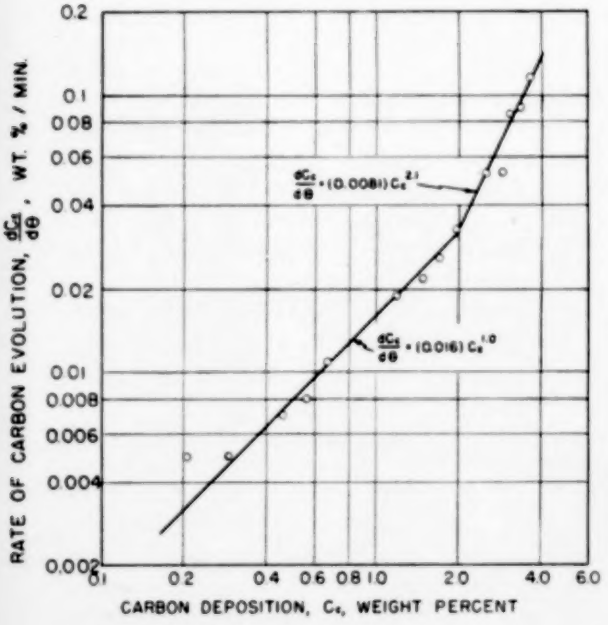

Fig. 9. Rates of carbon evolution during regeneration vs. carbon concentration on catalyst.

Primary Burning

Not much significance could be attached to the actual shapes of the primary burning rate curves, mainly because neither temperature nor oxygen partial pressure was held constant during the earlier stages of regeneration. At maximum burning rates, catalyst bed temperature would increase by more or than 100°F and oxygen partial pressure would decrease by about 50%.

The regeneration time required to achieve completion of the primary burning is shown in Fig. 10. This plot was obtained from the rate vs. time data shown in Fig. 8, the primary burning being considered completed at a final

carbon evolution rate of 0·025% carbon on catalyst per minute. Total time to achieve completion of the primary burning was directly proportional to the total quantity of carbon removed during the primary burning.

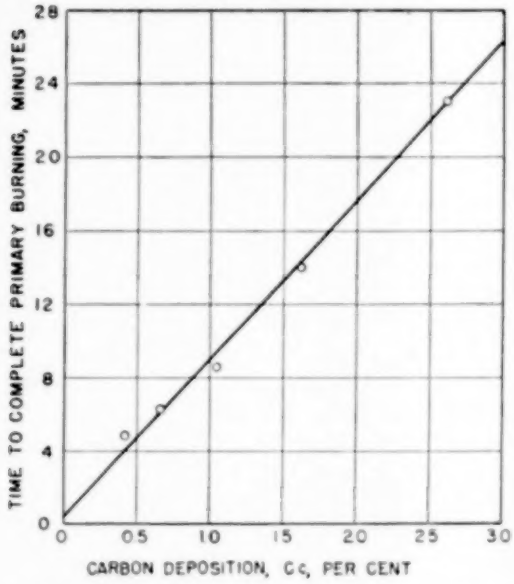

Fig. 10. Regeneration time required to complete primary burning vs. total carbon deposition.

The first segment of the plot of carbon evolution rate vs. carbon concentration indicates that the primary burning had second-order dependency on instantaneous carbon concentration, although this result was somewhat fortuitous inasmuch as catalyst bed temperature was higher during the earlier part of the primary burning period, as mentioned before. DART and co-workers [1] have indicated such second-order dependency in the regeneration of cracking catalysts.

Secondary Burning

The segment representing the secondary burning suggested first order dependency on instantaneous carbon concentration and refers to essentially constant temperature and oxygen partial pressure. The secondary burning rate was also shown to have first-order dependency on oxygen partial pressure. An approximately fivefold increase in carbon evolution rate was obtained by the use of pure oxygen rather than air.

The effect of catalyst activity on regeneration beyond the primary burning period was virtually negligible. After first regenerating with air for the standard 15-min. period, the catalyst was further regenerated with pure oxygen for variable lengths of time between 0 and 60 min., carbon being evolved at a constant rate over this entire range. During the 60-min. pure-oxygen regeneration, 25% additional carbon was removed, based on the carbon removed during the standard 15-min. air regeneration, yet activity was the same as that for the catalyst not regenerated beyond this standard air regeneration. This was taken as further evidence in support of the hypothesis that during secondary burning, carbon was removed from relatively inaccessible areas within the catalyst pellet. These areas, because of their comparative inaccessibility, contributed so little to the over-all effectiveness of the catalyst that no increase in activity was shown, even early in the run.

In view of these observations, it appeared possible that the mechanism of secondary burning was diffusion-controlled. The burning may have been progressive toward the interior of the pellet ; or it may have taken place in the smaller and more inaccessible pores.

Assuming a mass-transfer controlling mechanism, SEADER [7] has suggested a further analysis of this secondary burning by considering the cylinder as consisting either of an infinite slab or an infinite cylinder. Burning of the coke in the cylindrical pellet was assumed to occur at a continuously receding boundary area. Equations were derived ; and using these, resistance to mass transfer at the surface of the catalyst pellet appeared to be negligible, as indicated by a correlation with the data. Similarly, all terms except those designating the carbon concentration on the catalyst were probably constant. Thus these equations predicted that the carbon evolution rate could be related as follows :
For the slab,

$$\frac{dCc}{d\theta} = k \frac{1}{Cc_0 - Cc};$$

and for the infinite cylinder,

$$\frac{dCc}{d\theta} = k \frac{1}{\ln \frac{Cc_0}{Cc}} \; ; \quad \text{where}$$

$\frac{dCc}{d\theta}$ = rate of carbon evolution, per cent carbon on catalyst (based on weight of fresh catalyst) per minute ;

Cc_0 = original carbon concentration (includes primary carbon) per cent, based on weight of fresh catalyst ;

Cc = instantaneous carbon concentration, per cent, based on weight of fresh catalyst.

Indeed, plots of $dCc/d\theta$ vs. $1/(Cc_0 - Cc)$ and $dCc/d\theta$ vs. $1/\ln (Cc_0/Cc)$ both resulted in straight lines.

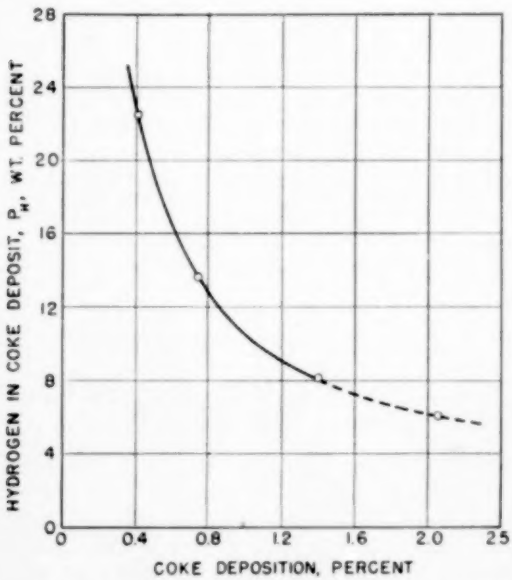

Fig. 11. Hydrogen concentration in coke vs. degree of coke deposition ("standard" conditions except process time).

Coke Composition

The composition of the coke deposit as it varied with the degree of deposition is shown in Fig. 11. The decline of hydrogen content with the degree of deposition was anticipated in view of the fact that the degree of deposition was varied by changes in total processing time, thus not only varying the degree of coke deposition, but the degree of dehydrogenation of the coke. The hydrogen content in the coke was found to decrease exponentially with process time.

Acknowledgments

The equipment used in this study was constructed by John M. Woods. The co-operation and assistance of various graduate and undergraduate students as well as of several staff members is much appreciated. Financial support by the Wisconsin Alumni Research Foundation and by the *American Cyanamid Company* is also gratefully acknowledged.

References

[1] Dart, J. C., Savage, T. and Kirkbride, C. G.; Chem. Eng. Prog. 1949 **45** 102.

[2] Heinemann, H.; Ind. Eng. Chem. 1951 **43** 2098.

[3] Hill, L. R., Vincent, G. A. and Everett, E. F.; Trans. Amer. Inst. Chem. Engrs. 1946 **42** 611.

[4] Hougen, O. A. and Watson, K. M. : Chemical Process Principles, Vol. III, Wiley 1947.

[5] Herrington, E. F. G. and Rideal, E. K.; Proc. Roy. Soc. 1945 A **184** 434.

[6] Jacobson, C. C.; Encyclopedia of Chemical Reactions, Vol. IV, Reinhold 1951.

[7] Seader, J. D.; Personal communications, 1952.

[8] Stevens, W. F.; Ph.D. Thesis, University of Wisconsin 1949.

[9] Villiers-Fisher, J.; Personal communications, 1952.

[10] Voorhies, A., Jr.; Ind. Eng. Chem. 1945 **37** 318.

Chemical Engineering Science, 1954, Vol. 3, pp. 122 to 142. Pergamon Press Ltd.

Mass transfer between isobutanol and water in a spray-column

P. M. HEERTJES, W. A. HOLVE and H. TALSMA*

The University of Technology, Laboratory for Chemical Engineering, Delft, Holland

(*Received* 11 *March* 1954)

Summary—A study of the rate of mass transfer across a liquid boundary beween a discontinuous and a continuous phase, using a binary mixture and a droplet system has been made.

Because of differences in density and movement of the drops the continuous phase appeared to be thoroughly mixed. This resulted in a nearly constant concentration independent of the height of the column.

For the continuous phase a relation for the partial mass transfer coefficient k_c in the form $k_c d_d/D = Sh = h\, Re_d^{\frac{1}{2}}\, Sc_c^{\frac{1}{3}}$ has been used.

Satisfactory correlation of the experimental results could be obtained with this equation. The constant h in the above relation appeared to be a function of the relative interfacial velocity which in turn is a function of the viscosities of the drops and the surrounding fluids. Following the concept of HADAMARD this function is taken as $\eta_c/\eta_c+\eta_d$.

This picture of the mechanism is representative of the situation, when the circulation in the drop is not restricted by interfacial tension.

For transfer to the discontinuous phase the unsteady state equation of KRONIG and BRINK, considering the occurrence of internal droplet circulation, was shown to express fairly adequately the experimental results for free rise of isobutanol droplets. Water drops showed a divergence from the Kronig-line possibly due to the " floating " effect of water droplets in isobutanol.

Résumé—Les auteurs ont étudié la vitesse du transport de matière, à travers une surface limite entre deux liquides, vers les phases continue et discontinue en utilisant un mélange binaire et un système à gouttes.

Par suite de la différence en densité et du mouvement des gouttes la phase continue se révélait intimement mélangée d'où résultait une concentration presque constante indépendant de la hauteur de la colonne.

Pour la phase continue, on a utilisé une relation, pour le coefficient partiel du transport de matière k_c, sous la forme de

$$\frac{k_c\, d_d}{D} = Sh = h\, Re_d^{\frac{1}{2}}\, Sc_c^{\frac{1}{3}}$$

Cette équation permettait d'obtenir une corrélation satisfaisante avec les résultats expérimentaux. La constante h dans la relation susnommée paraissait être une fonction de la vitesse relative se produisant à la surface limite. Cette vitesse est une fonction des viscosités des gouttes et des liquides envirronnants. Basée sur la conception de HADAMARD, cette fonction s'écrit comme

$$\frac{\eta_c}{\eta_c + \eta_d}$$

Cette présentation du mécanisme est représentative quand la circulation dans la goutte n'est pas limitée par la tension à la surface limite.

Pour la transmission à al phase discontinue, on prouve que l'équation de KRONIG et BRINK – équation qui tient compte de la présence d'une circulation interne dans la goutte – exprime de façon assez efficace les résultats expérimentaux en cas d'un vol libre de gouttes d'isobutanol. Les gouttes d'eau présentent une déviation de la courbe de KRONIG. Cette déviation est causée probablement par le phénomène de " flottaison " manifesté par les gouttes d'eau dans isobutanol.

* Part of the thesis for Ph.D. of H. TALSMA, presented at the University of Technology, Delft (1953).

VOL. 3 1954

INTRODUCTION

For the study of the mass transfer between two liquids a partially miscible binary system was chosen, because if equilibrium at the interface can be assumed, the interfacial concentration is then only a function of the temperature, being the saturation concentration. A spray column was finally used, because in that case the interfacial area can easily be calculated. Other types of apparatus with known areas such as the wetted wall column and the horizontal extractor showed disadvantages over the spray column. In the wetted wall column the film at the wall is easily disturbed ; in the horizontal extractor a stationary condition is only very slowly reached in the viscous region of flow, moreover small differences in density caused layer formation, which hindered the experiments very considerably.†

The known interfacial concentration makes possible the calculation of a partial mass transfer coefficient, the advantages of which are apparent.

The spray-column resembles technical extraction apparatus more closely than the others mentioned.

The study to be given here can be regarded as an introductory study to the problems of real extraction. As far as known to the present authors, SHERWOOD [1] and LICHT and CONWAY [2] have used the known interfacial area of a spray column in their extraction calculations whereas COLBURN and WELSH [3] and LADDHA and SMITH [4] have used a binary system.

METHOD AND APPARATUS USED

In Fig. 1 a diagrammatic sketch of the apparatus used to contact the one phase in droplet form countercurrently with the other is given. As shown, the apparatus is set up for contacting the heavier water droplets falling through isobutanol as the continuous phase. The description will be based on this type of contact. The apparatus could easily be changed for isobutanol drops rising in water as the continuous phase.

The head tanks for both the water (*A*) and the isobutanol (*B*) were heavy walled glass containers of 60 litre capacity supported 3 metres above the floor. A constant head for the flow meters was maintained by the method of Mariotte, whereby an open capillary, with its tip placed near the bottom of the otherwise sealed container insured that the pressure in the horizontal plane with the tip was constant and about equal to that of the atmosphere.

Provisions were made for filling the vats from supply vessels by air pressure and for venting during the time of filling. The capillary and vent of the water head tank were provided with dust filters and those of the isobutanol head tank were connected with a $CaCl_2$ drying tube and a jar of NaOH in series to prevent the absorption of atmospheric moisture in the dry isobutanol.

By syphoning action the liquids were led via their respective capillary flow meters (*C* and *D*) and control valves to the column distributors. The water stream was fed to the upper distribution chamber (*E*) and then to the eight thick walled capillaries (*F*) which had been cut from the same length of capillary tubing. The capillaries each 18 centimetres long, with an I.D. of 0·1 cm and an O.D. of 0·6 cm were arranged symmetrically around a 4 centimetre diameter circle in a rubber stopper which snugly fits the experimental column of average diameter 7·3 cm. A short section of rubber tubing connecting each capillary with the distribution chamber, permitted individual closure by screw clamps (*G*).

After passage through the column, which varied in length from less than 1 cm to 128 cm, the drops were collected by the lower conical section and rolled into the narrowed neck where the interfacial position (*H*) was held 1 cm below the constriction by adjustment of the overflow leg. The water streamed through this leg and by means of a vent at the highest point overflowed smoothly into the discharge line. Here a three way cock was provided for taking individual samples during the collection of the composite sample over a material balance period.

Isobutanol, the continuous phase, was discharged directly under the rubber ring joining the lower distributor to the column through four evenly spaced headers (*I*). From this annular space, it flowed smoothly and without undue disturbance under the circumference and into the column proper.

Provisions for sampling the isobutanol discharge from the column were the same as described above for the water phase.

For the investigation of rising isobutanol droplets, the whole column was simply inverted and the necessary changes made in the flowmeter capillaries for measuring the new flows.

All flow lines were provided with vent valves at the highest points to permit easy removal of air bubbles and prevent possible blocking of flow. In addition both lines contained valves for sampling the inlet streams. An Anschutz thermometer, accurate to 0·05°C was placed in the line by each flow meter for determining the entering stream temperatures and one installed in the column for the determination of the temperature under which the mass transfer took place. The surrounding room temperature was kept as constant as possible between 20 and 21°C.

† To be published elsewhere.

After the start up, a time sufficient for the continuous phase to displace four times the content of the column was taken to reach dynamic equilibrium, as was proved by experience. This " run in " time varied from 3-48 hours. During this period the head of the flowmeter for isobutanol (ΔH_i) and for water (ΔH_w) the temperature of the isobutanol (t_i) and water stream (t_w) and in the column (t_k) were read at regular intervals and if need be readjusted. After reaching steady state conditions the following experimental data were taken during the material balance period :

1. The time of fall of the droplets from each capillary (θ_{cap} in sec) as a mean of 15 determinations taken from the moment the drop left the capillary up to the moment it passed the brim of the column.

2. Number of droplets escaping from a capillary per second (A_{cap}). This number was determined at low water rates by measuring the time necessary to form 20 drops, five times per capillary. If A_{cap} is larger than 2 a stroboscope was used, determining for each capillary three successive frequencies at which the drop seems to be at

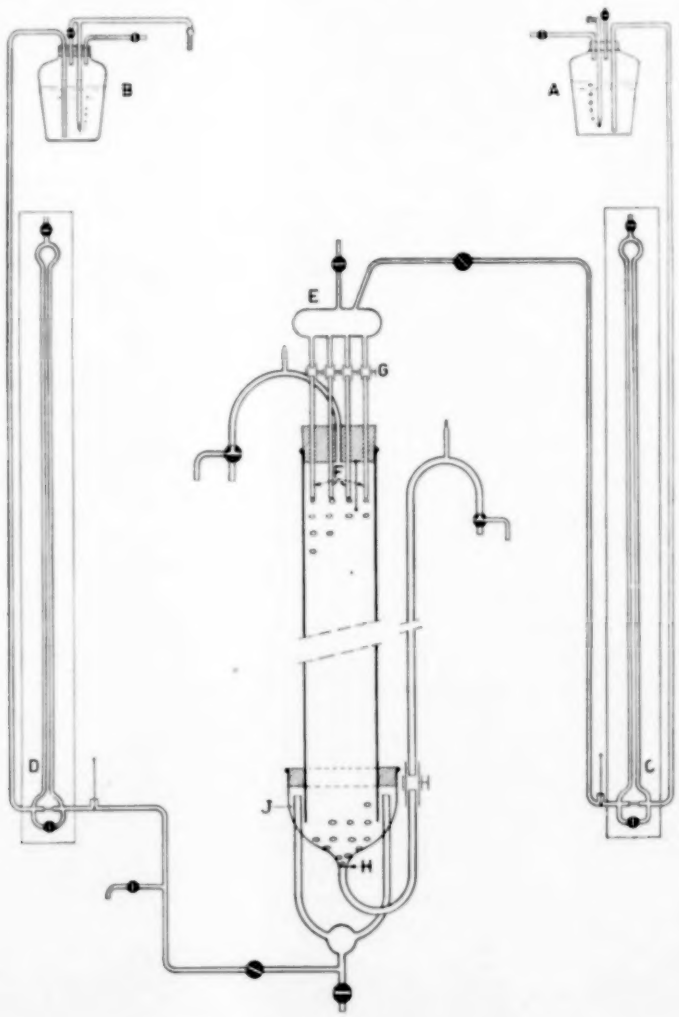

Fig. 1. Sketch of the extraction apparatus.

VOL. 3 1954

rest, and taking their greatest common measure.

3. The temperatures t_i, t_w, t_k and the heads of the flowmeters ΔH_i and ΔH_w at 2 minutes interval (in some experiments 3 minutes).

4. Five timed volume samples, collected in tared flasks, of each exit stream.

After the end of the experiment, the flow of the capillaries was shut off by closing the screw clamps and then immediately closing the continuous phase control valve and the overflow leg. The column was then drained at a velocity of 2 ml/sec while at least six representative 200 ml interval samples were taken of the content. Finally a sample of the entering isobutanol stream was taken and after reweighing the material balance sample flasks, all sample flasks were sealed with paraffin wax to await analysis.

ANALYSIS

The amount of water in isobutanol was determined by means of the Karl-Fischer reagent by a slightly modified titration method as described by MITCHELL and SMITH [5]. The two-solution technique was used [6].

The amount of isobutanol in water was found by determining the carbon content by combustion with oxygen over copper oxide at 750°C and determining the amount of carbon dioxide formed by adsorption in NaOH-asbestos (Ascarite) and weighing. This method will be described elsewhere.

The water used was distilled water. The isobutanol was obtained by distillation of a commercial product in a column with sieve-plates; boiling point 108·1°C at 760 mm Hg, $n_D^{20} = 1{\cdot}3959$, water content < than 0·05%

EVALUATION OF THE DATA OBTAINED

From the measurements collected the following data could be obtained :

1. The amount of the discontinuous phase entering the column (Q_{1d} in cm³/sec) from the mean readings of the capillary flowmeter. A correction for deviations of the temperature as shown by the mean temperature measured is used.

2. The number of drops per sec (A in number/sec found as the sum of A_{cap} for the eight capillaries).

3. The initial volume of one drop (V_1 in cm³) from $V_1 = \frac{Q_{1d}}{A}$. It may be noted that even with the same capillary and with the same flow rate the drop volume is not always the same. In particular for water drops in isobutanol the deviations are large. Therefore A has to be determined in every experiment.

4. The amount of the continuous phase entering the column (Q_{1c} in cm³/sec) from the mean readings of the capillary flowmeter.

5. The amount of the discontinuous phase leaving the column (Q_{2d} in cm³/sec) from the time necesssary to fill the ample flasks of known volume as a mean.

6. The end volume of the drop (V_2 in cm³) from $V_2 = \frac{Q_{2d}}{A}$.

7. The amount of the continuous phase leaving the column (Q_{2c} in cm³/sec) from the amount in the material balance flask and the 5 sample flasks, divided by the total time of one experiment.

From these data and with the aid of the properties of the mixtures some important variables governing the mass transfer can be derived.

(*a*) *Diameter and surface of a drop*

Very shortly after leaving the capillary the drop takes the form of an oblate ellipsoid. If α and β denote half of the short axis and half of the long axis respectively the surface O of this ellipsoid of volume V is given by :

$$O = 2\pi \sqrt[3]{\left(\frac{3V}{4\pi}\frac{\alpha}{\beta}\right)^2} \left(1 + \frac{\alpha^2}{\beta^2} \cdot \frac{1}{\sqrt{1 - \frac{\alpha^2}{\beta^2}}} \ln \frac{1 + \sqrt{1 - \frac{\alpha^2}{\beta^2}}}{\frac{\alpha}{\beta}}\right)$$

By a photographic method the relation between V and $\frac{\alpha}{\beta}$ has been determined both for water and isobutanol and is given graphically in Fig. 2.

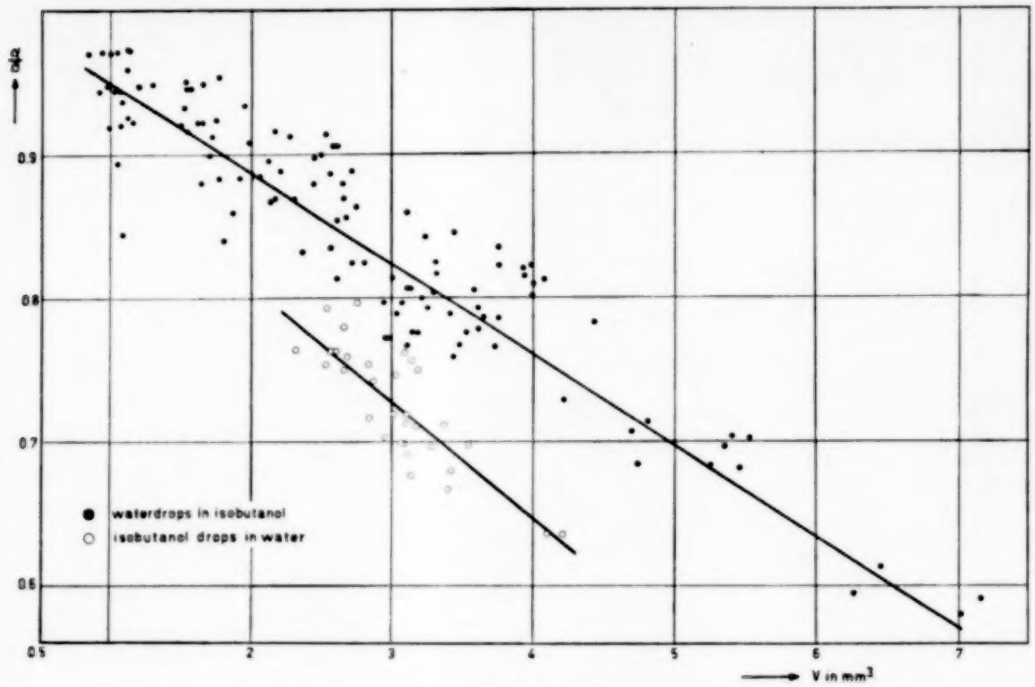

Fig. 2. The relation between $\frac{\alpha}{\beta}$ and the volume V for water and isobutanol drops.

Assuming a linear relation between V and $\frac{\alpha}{\beta}$, by the method of the least squares the following relations have been found :

" water " drops : $\frac{\alpha}{\beta} = 1{\cdot}01 - 0{\cdot}0643\ V$

" isobutanol " drops : $\frac{\alpha}{\beta} = 0{\cdot}97 - 0{\cdot}0806\ V$

These relations are given as lines in Fig. 2. With the aid of these equations the relation of O to V has been calculated and is given in Fig. 3 for both " water " and " isobutanol " drops. With the aid of these lines the surface of the drop could be found for every calculated volume.

Each drop changes in volume during the rise or fall. To describe the mass transport to the continuous phase a mean surface $\bar{O}$ has to be used. As will be seen later the conditions for the use of HIXON's mean surface

$$\bar{O} = \frac{O_1^{3/2} - O_2^{3/2}}{3(O_1^{1/2} - O_2^{1/2})},$$

except as far as the constancy of $\frac{\alpha}{\beta}$ is concerned, are fulfilled, although the change in volume is 33% at the maximum. The use of an arithmetic mean surface $\bar{O} = \frac{O_1 + O_2}{2}$ showed deviations of only 0·4% at the maximum with the surface calculated according to HIXON. For convenience therefore the arithmetic mean has been used.

A mean drop radius (r_d in cm) has been introduced, being defined by $\bar{O} = 4\pi r_d^2$. The diameter $d_d = 2\, r_d$.

(*b*) *Total amount of drops, P.*

The total amount of drops present in the column is found by adding the products of $A_{cap.} \times \theta_{cap.}$ of the eight capillaries. The total exchanging surface in the column is then represented by : PO ; the mean time of fall or ascent (θ) by

VOL. 3 1954

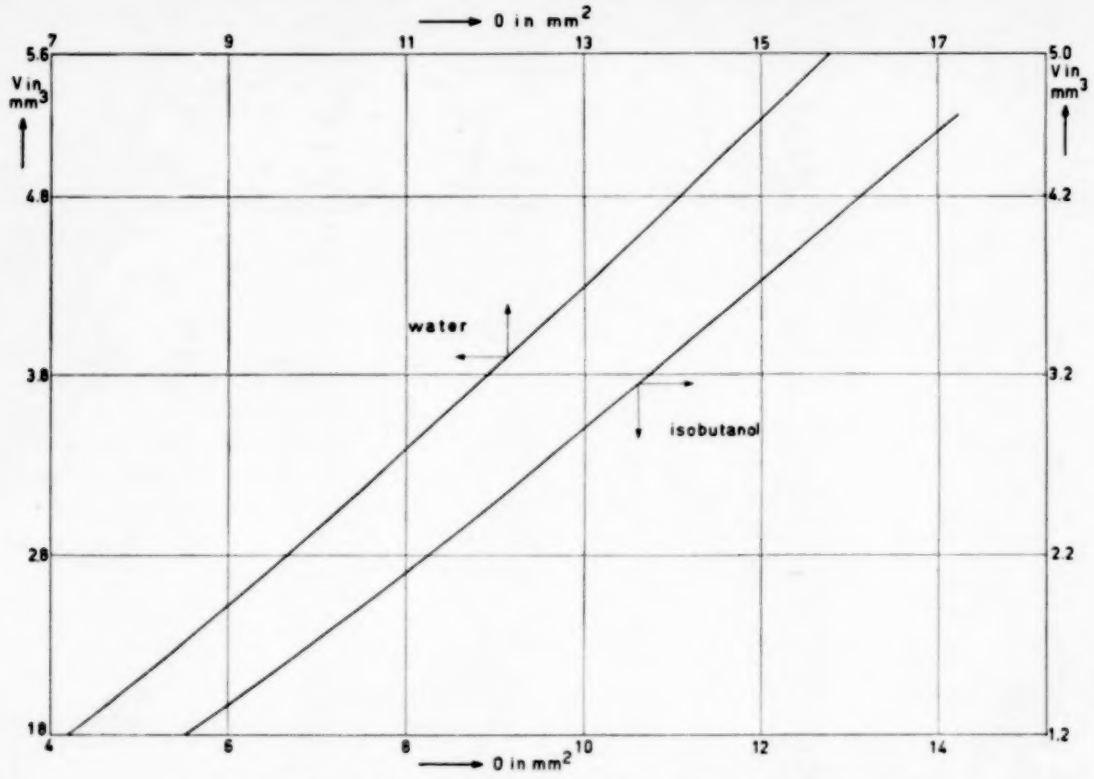

Fig. 3. The relation of the surface of the ellipsoid drops (O) and their volume (V).

$\theta = \frac{P}{A}$; and the mean velocity of the drops v_D by $v_D = \frac{L}{\theta}$ in which L is the length of the column (cm).

(*c*) *The column concentration* y_k.

During the experiments it could be observed that in the continuous phase mixing occurred. At the outset, for the calculation of the mass transport the concentrations of the entering and leaving continuous phase were used to calculate the partial mass transfer coefficients. A closer examination, however, proved that this was not correct. By filling the column for $\frac{7}{8}$ of its height with isobutanol (with 2% water) and by bringing in a small layer of isobutanol with 0·2% water coloured with Sudan III, which did not mix with the denser first layer, and by introducing water drops into the column in the coloured layer, within a quarter of an hour the two ixobutanol layers were thoroughly mixed (same colour intensity). It was therefore possible that on this mixing effect, no appreciable concentration gradient was present, except around the drops. This indeed proved to be the case. Therefore, for every experiment the column concentration was actually measured at different heights, as described. Some of the results are graphically represented in Fig. 4, for water as the continuous phase (upper Fig.) and for isobutanol as the continuous phase (lower Fig.) giving the column concentration as a function of position in the column. (It may be remarked that water is introduced at the top end of the column, isobutanol at the lower end, both with a concentration = 0). In this figure the concentration of the exit stream is also given as points on the $L = 0$ abscissa, respectively $L = 63$ abscissa.

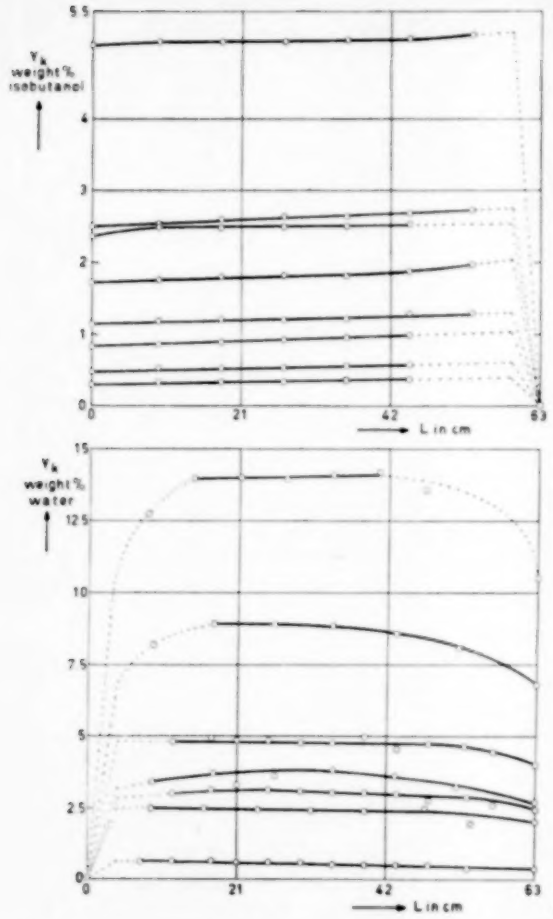

Fig. 4. The mean column concentration (y_k) at different heights for water (upper fig.) and for isobutanol (lower fig.) as the continuous phase.

It is clear from Fig. 4 that the column concentration is fairly constant over the whole height of the column. For isobutanol as the continuous phase this concentration is about 1·25 times the exit stream concentration and independent of the flow rate (different heights denote different flow rates). To this may be added that at a low continuous isobutanol rate a horizontal plane caused by a difference in refractive index could easily be observed in the neighbourhood of the capillary tips. For water as a continuous phase the column concentration is also constant and almost equal to the exit concentration. Apparently during the " run in " period, owing to mixing and aided by the way the capillaries are placed, a cylinder of fairly constant concentration is formed.

The continuous isobutanol phase in the steady state (again aided by the manner of introduction) flows along the wall in a thin " layer," mixes with some of the heavier liquid core, and leaves the apparatus at a lower concentration than this cylinder-liquid.

For water, which has a lower viscosity than isobutanol, this mixing is more intense, and water leaves the column at a concentration almost equal to that of the column.

The concentration of the continuous phase in the column (y_k) will be given as a mean arithmetic concentration calculated from the data measured. It will be given in weight percentage of the component present in the lowest concentration.

VOL. 3 1954

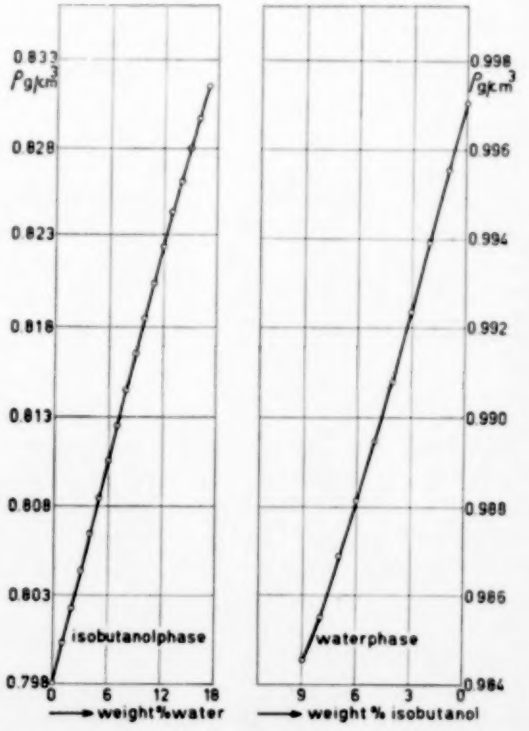

Fig. 5. The densities of mixtures of isobutanol and water at 25°C.

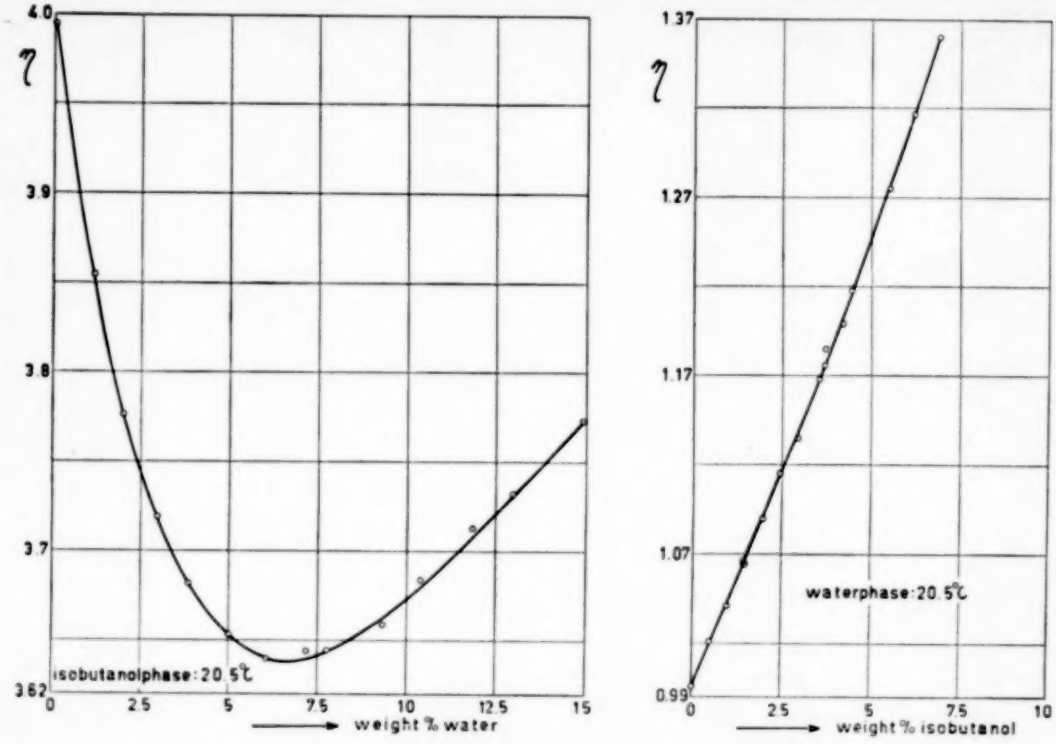

Fig. 6. The viscosities of mixtures of isobutanol and water at 20·5°C.

(*d*) *The density of mixtures of isobutanol and water*

The knowledge of the densities of the mixtures was necessary for the evaluation of the results. They were determined at 25·0°C and given graphically in Fig. 5 as a function of the amount (weight %) of water present in isobutanol and of the amount (weight %) of isobutanol present in water.

Circumstances made it necessary for these densities to be determined at 25°C. The other experiments were carried out at about 20°C. The densities found were corrected by means of the equation :

$$\frac{1}{\rho_{m,t}} = \frac{1}{\rho_{m,25}} + (1-q)\left(\frac{1}{\rho_{w,t}} - \frac{1}{\rho_{w,25}}\right) + q\left(\frac{1}{\rho_{i,t}} - \frac{1}{\rho_{i,25}}\right),$$

in which q = weight fraction of isobutanol, m denotes the mixture, w : water, i : isobutanol and t : the temperature.

The densities of the pure components at different temperatures have been taken from the literature.

The calculated values are accurate enough to be used and a redetermination of the densities at 20°C has not been undertaken.

(*e*) *The viscosity of mixtures of isobutanol and water*

The viscosities of the mixtures of isobutanol and water have been determined with an Ostwald viscometer and calculated by means of the equation : $\eta = i\,\rho\,\theta - \frac{i'\rho}{\theta}$ in which η = viscosity which will be expressed in centipoises, θ the time of emptying, ρ the density, i and i' constants of the apparatus.

The constant i' was calculated from the dimension of the viscosimeter ; i was determined with solutions of cane sugar in distilled water, and checked on solutions of glycerol in distilled water and on distilled water.

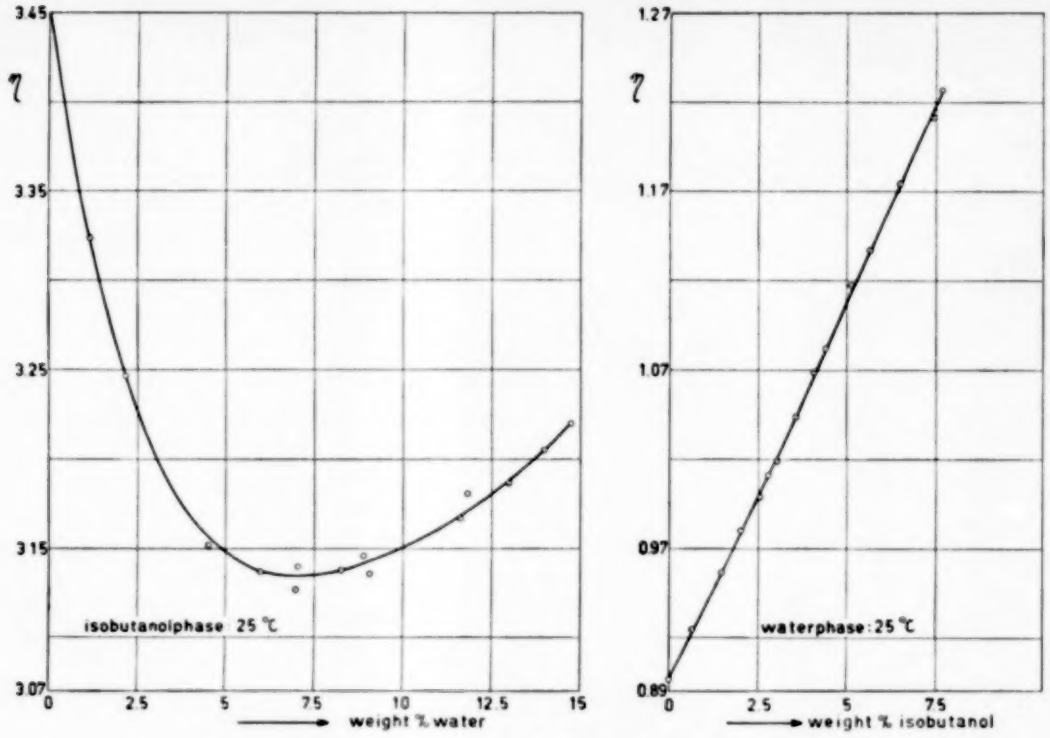

Fig. 7. The viscosities of mixtures of isobutanol and water at 25·0°C.

The viscosities found are presented in Fig. 6 for 20·5°C and in Fig. 7 for 25°C.

A linear interpolation between the two temperatures was used for the temperature of ca. 20·6°C of the column.

(*f*) *Mutual solubility of isobutanol and water*

In the calculations it has been assumed that equilibrium exists, at the interface between the drops and the continuous phase. Therefore the mutual solubility of isobutanol and water had to be known. The determinations were made in two different ways. The water content in saturated isobutanol solutions was determined by shaking isobutanol and water for 24 hours at constant temperature and by titrating the isobutanol phase after settling.

For the water phase the temperature of formation of two phases on heating solutions of known composition was determined. The criterion was the first formation of a slight turbidity. The results obtained are given in Fig. 8. For the isobutanol content of water slightly lower values than obtained by MICHELS [7] have been found. Use of the method described for the isobutanol phase gives values lying close to those of MICHELS.

(*g*) *The diffusivities of isobutanol and water*

The diffusivities of water in isobutanol (D_w in cm²/sec) and of isobutanol in water (D_i in cm²/sec) were determined with a *Schlieren* method. The apparatus used was that of WIENER [8] as improved by THOVERT [9] and LAMM [10]. Assuming that a linear relation exists between the refractive index and the concentration, the following have been found at 20°C as mean values over the whole concentration range involved :

$$D_w = (2{\cdot}0 \pm 0{\cdot}4)\ 10^{-6}\ \text{cm}^2/\text{sec}$$
$$D_i = (6{\cdot}0 \pm 0{\cdot}5)\ 10^{-6}\ \text{cm}^2/\text{sec}^*$$

* These values were determined by courtesy of Prof. H. KRAMERS by L. M. HAMAKER.

VOL. 3 1954

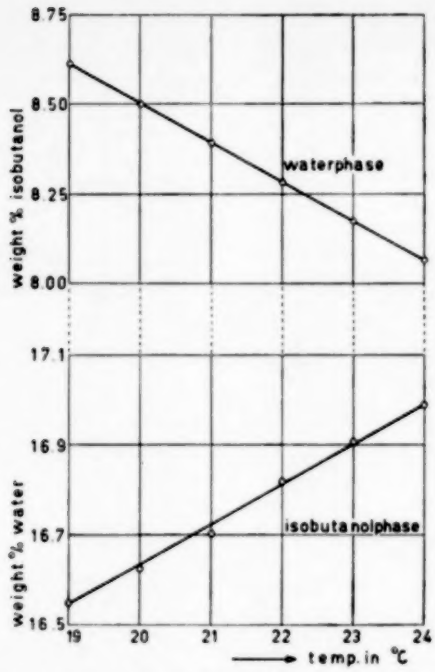

Fig. 8. The mutual solubility of isobutanol and water as a function of the temperature.

The rather large inaccuracy was caused by the fact that the container was not absolutely plane-parallel and moreover that the air temperature was not thermostatically controlled.

Measurements with a better apparatus are not yet finished.

(*h*) *Partial mass transfer coefficient in the continuous phase* (k_c)

The amount of substance (water if isobutanol is the continuous phase, isobutanol if water is the continuous phase) transported in unit time (seconds) from the drops to the continuous phase can be found from the concentrations of exit and entering streams and the quantities.

The concentrations are denoted for the continuous phase by y in weight %, for the discontinuous phase by x, also in weight %.

The subscript 1 refers to the entering stream, the subscript 2 to the leaving stream, subscript c to the continuous phase, subscript d to the discontinuous phase, subscript k for the column, subscript s to the surface of the drops. Therefore thə amount of substance transported in unit time, expressed in g/sec is :

$$\frac{1}{100}(y_2 \rho_{2c} Q_{2c} - y_1 \rho_{1c} Q_{1c}).$$

As has been shown the concentration in the continuous phase can be taken as constant. Denoting the surface concentration by y_s (weight %), the driving force for the mass transport in the whole continuous phase is :

$$\frac{1}{100}(y_s \rho_{sc} - y_k \rho_k) \qquad \text{in g/cm}^3$$

A partial mass transfer coefficient for the continuous phase therefore in this case can be given and defined as :

$$k_c = \frac{y_2 \rho_{2c} Q_{2c} - y_1 \rho_{1c} Q_{1c}}{P\bar{O}\,(y_s \rho_{sc} - y_k \rho_k)}$$

in which $P\bar{O}$ is the surface of all the drops present, k_c is therefore expressed in cm/sec.

(*i*) *Dimensionless groups used*

For the description and correlation of the mass transport in the discontinuous phase the dimensionless groups :

$$\epsilon = \frac{x_s \rho_{sd} - \overline{x_2 \rho_{2d}}}{x_s \rho_{sd} - x_1 \rho_{1d}} \quad \text{and} \quad \frac{D\theta}{r^2_d};$$

for the continuous phase the Reynolds number : $Re_d = \frac{v_d d_d \rho_c}{\eta_c}$, the Schmidt number : $Sc_c = \frac{\eta_c}{\rho_c D}$ and the Sherwood number : $Sh = \frac{k_c d_d}{D}$ are used. ρ_c and η_c are determined at the column temperature t_k and the column concentration y_k; x_s and y_s at the temperature t_k.

RESULTS

The results of the experiments have been evaluated in the manner described.

To save space the experimental figures will not be presented. For readers interested in the actual measurements the data are to be had in tabular form from the first-mentioned author.

DISCUSSION OF RESULTS

A. *Mass transfer in the discontinuous phase*

To study the results obtained in Fig. 9 for isobutanol drops and in Fig. 10 for water drops $\frac{D\theta}{r_d^2}$ is plotted against $\log \frac{x_s \rho_{sd} - \overline{x_2 \rho_{2d}}}{x_s \rho_{sd} - x_1 \rho_{1d}}$ for three cases, viz. :

1. *Mass transfer in the sphere by diffusion only*

According e.g. to NEWMAN [11] assuming a constant boundary concentration and uniform initial concentration the equation of this line, which will be called the diffusion line, is :

$$\epsilon = \frac{x_s \rho_{sd} - \overline{x_2 \rho_{2d}}}{x_s \rho_{sd} - x_1 \rho_{1d}} = \frac{6}{\pi} \sum_{n=1}^{\infty} \frac{1}{n^2} e^{-n^2 \pi^2 \frac{D\theta}{r_d^2}}.$$

An approximation of this line for a short time of contact, can be found by using HIGBIE's equation [12] for diffusion from a plane surface in an infinite thick layer and integrating over the time, which yields :

$$\epsilon = 1 - \frac{6}{\sqrt{\pi}} \sqrt{\frac{D\theta}{r_d^2}}.$$

This equation is somewhat easier to handle, but gives too high a mass transport because a plane area is assumed and the concentration in the centre of the sphere is taken constant and equal to the initial concentration. For $\frac{D\theta}{r_d^2}$ values of $6 \cdot 10^{-4}$ and $70 \cdot 10^{-4}$ the differences are 0·1 and 3% respectively for the fraction of the possible amount taken up. This second line is not shown. Moreover the diffusion line is not shown in Fig. 10.

2. *Mass transfer by diffusion and circulating*

Using the stream function of HADAMARD [13] in a liquid sphere moving under the influence of gravity in a continuous medium, neglecting the quadratic velocity terms, KRONIG and BRINK [14] have calculated the mass transport in a liquid sphere by diffusion and circulation. The limiting assumptions made were :

1. The sphere has a uniform initial concentration and the surface concentration remains constant ;

2. The time of circulation (the time which a liquid particle following a stream line needs to reach its starting point) is small compared with the diffusion-time (the time necessary to reduce $x_s \rho_{sd} - \overline{x_2 \rho_{2d}}$ to $\frac{1}{e} (x_s \rho_{sd} - x_1 \rho_{1d})$;

3. As for HADAMARD the interfacial tension is zero.

The equation given is :

$$\epsilon = \frac{x_s \rho_{sd} - \overline{x_2 \rho_{d2}}}{x_s \rho_{sd} - x_1 \rho_{1d}} = \frac{3}{8} \sum_{n=1}^{\infty} A_n^2 e^{-\mu_n 16 \frac{D\theta}{r^2 d}}$$

In the original paper only two values for A and μ are given. The first part of the line is curved rather strongly, and for this part more terms are needed. By courtesy of Prof. R. KRONIG some more terms have been calculated by L. VAN DEN BRANDELER and are presented in Table 1.

Table 1

n	A	μ
1	1·33	1·678
2	0·60	8·48
3	0·36	21·10
4	0·35	38·5
5	0·28	63·0
6	0·22	89·8
7	0·16	123·8

For $\theta = 0$, there has been no mass transfer. Therefore

$$\frac{3}{8} \sum_{n=1}^{\infty} A_n^2 = 1.$$

As can be calculated :

$$\frac{3}{8} \sum_{n=1}^{7} A_n^2 = 0{\cdot}95.$$

For

$$\frac{D\theta}{r_d^2} > 70 \cdot 10^{-4},$$

the fifth term already can be neglected.

The above equation is plotted in Fig. 9 and 10 as the " Kronig " line.

3. *The experimental data*

Comparing the experimental data with the two theoretical curves it must be kept in mind that

VOL. 3 1954

certain conditions postulated in the derivation of these lines are not fulfilled in the experiments, viz. :

1. The drops are not spheres ;
2. The interfacial tension although small (2 dyne/cm) is not zero ;
3. The velocity region lies outside the Stokes' region as is shown by Re_d and by the ellipsoid form of the drops ;
4. During the formation and during the confluence mass transfer also takes place (called entry-effect and end-effect) ;
5. The diffusivities used are mean values and taken as constant ;
6. Heat effects accompany the process.

The results with isobutanol drops—As is clear from Fig. 9 with the exception of the points for very short columns (low $\frac{D\theta}{r_d^2}$ values) a curve can be drawn through the experimental points. This experimental curve lies lower than both the diffusion curve and the Kronig curve. This means a higher rate of mass transfer caused by the entry- and end-effects. An extrapolation to $\frac{D\theta}{r_d^2} = 0$, in order to determine the sum of entry- and end-effects however is not permissible, because the experiments were carried out with varying amount of drops and varying time of drop formation (θ_v) ; therefore with varying entry effects.

For $\theta_v \to \infty$. $\log \epsilon \to -\infty$; for
$\theta_v \to 0$, $\log \epsilon \to 0$.

The end effect will depend among other things on the amount of drops. The behaviour discussed is confirmed for the lower column lengths. The extraction as carried out gives a bundle of lines starting at different ordinates (sum of both effects) and having a different slope, the line lying closest to the $\frac{D\theta}{r_d^2}$ axis (small θ_v) having the greatest negative slope.

This can be seen in Table 2, where the slopes of the connecting lines are given as a function of θ_v for each value of the time for two experiments with different column lengths ($L = 3{\cdot}5$ and $34{\cdot}8$ cm) but with equal θ_v and equal continuous rates.

Table 2

θ_v *in sec.*	*slope*
1	− 28·4
$\frac{1}{2}$	− 28·6
$\frac{1}{3}$	− 39·3
$\frac{1}{4}$	− 53·0

Apparently at higher values of $\frac{D\theta}{r_d^2}$ for the times of formation used the bundle of curves coincide to one curve.

Although an extrapolation to $\theta = 0$ ($L = 0$) is therefore not permitted, a rough estimate (found by extrapolation) indicates that under the experimental conditions used for $L = 0$ $\log \epsilon = -0{\cdot}1$, indicating that the sum of entry- and end-effects amounts to about 20% of the maximum possible mass transfer.

In view of the fairly constant entry- and end-effects for high $\frac{D\theta}{r_d^2}$ values, a decision can be taken as to what is happening in the drops by displacement of the experimental line. A vertical displacement of the lines from the ordinate 0, − 0·1 to 0·0 would include the assumption that the drop leaves the capillary with a uniform initial concentration and a constant end effect. A uniform initial concentration in the drop is approximated by short times of formation, causing turbulence in the drops.

A horizontal displacement includes the assumption that the end effect, which would necessitate a vertical displacement, is small compared with the entry-effect and that the drop leaves the capillary with a concentration distribution equal to that in a rising or falling drop. Although this is not very likely, it will be clear that without further information about entry- and end-effects a definite decision about the displacement to be undertaken cannot be made. The following procedure has therefore been adopted. At the highest values of $\frac{D\theta}{r_d^2}$ obtained the slope of

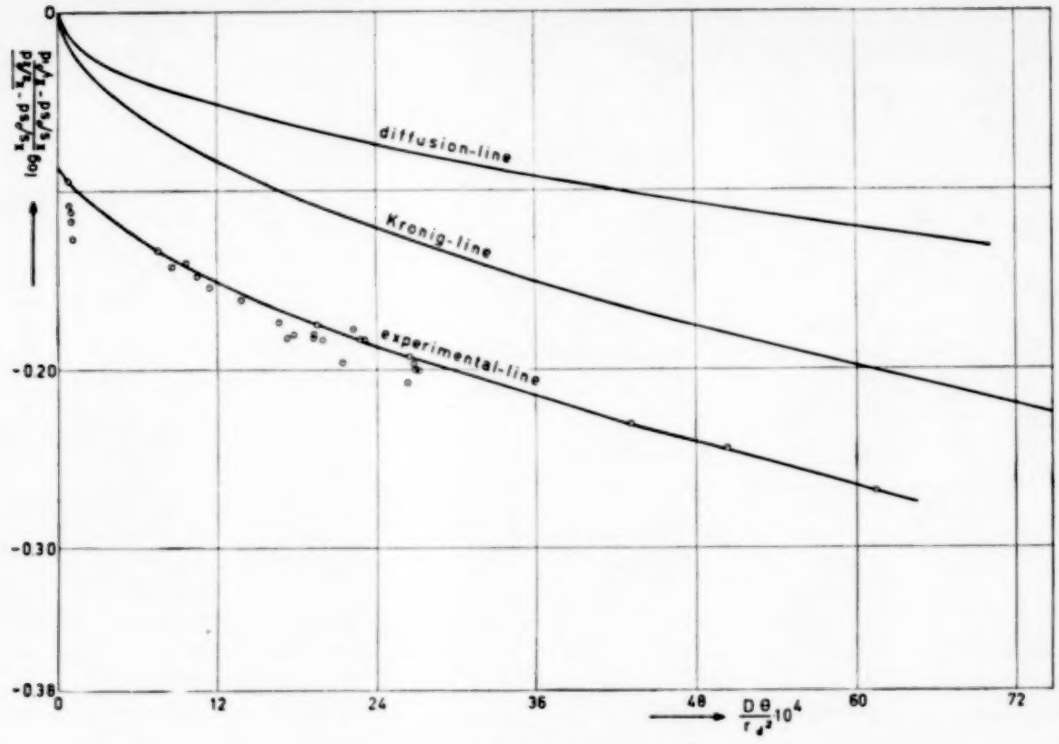

Fig. 9. Mass transfer into isobutanol drops.

the three lines have been determined for equal values of $\frac{D\theta}{r^2_d}$ (vertical displacement) and for equal values of log ϵ (horizontal displacement). The results are collected in Table 3.

Including the deviations from theory 1, 2, 3 and 5 mentioned earlier, and observing that the drops are of such a size that the interfacial tension cannot influence the movement in the drops very strongly (see later), it can be concluded from the figures given, that in isobutanol drops ascending in a water phase the transport of water in the drops takes place by diffusion and circulation in agreement with the predictions of KRONIG and BRINK. The greater negative slope of the experimental line compared with the Kronig line may be caused by a different stream pattern caused by the ellipsoid form of the drops under the

Table 3

Displacement	*Vertical*			*Horizontal*		
Line	*Diff.*	*Kronig*	*Exper.*	*Diff.*	*Kronig*	*Exper.*
Region $D\theta/r^2_d \cdot 10^4$	50-60	50-60	50-60	230-240	90-100	50-60
Slope $\Delta \log \epsilon / \Delta\, D\theta/r^2_d$	− 11·3	− 18·7	− 20	− 6·0	− 15·4	− 20

VOL. 3 1954

experimental conditions. In the derivation of the Kronig line the quadratic velocity terms have been neglected.

The results with water drops—The results with the water drops have been investigated in a similar way to those with the isobutanol drops. As can be seen in Fig. 10 the results with water drops seem to be quite different. The results for the different column lengths cannot be represented by one line. Moreover, as can be seen, for the greater column lengths, on increasing the rate of the discontinuous phase (and therefore decreasing the time of formation of the drops (θ_v) and increasing the volume V of the drop and decreasing the falling time and therefore $\left(\frac{D\theta}{r^2_d}\right)$ the ratio ϵ first increases (as could be expected and has been confirmed for the isobutanol drops) but then decreases very strongly which is quite unexpected. This has been found for both the 34·1 cm as for the 62·8 cm column as shown by the drawn lines. Because on decreasing θ_v the ratio ϵ for both the entry-effect and the exchange during the flight increases, the cause of the abnormal behaviour must be found in the end-effect. During the experiments it has been observed that the water drops float for some time on the interface before coalescence. For the isobutanol drops a similar effect is far less pronounced. According to MAHAJAN [15] the residence time of falling water drops at the interface can be 8 sec in a medium of a viscosity of 4 cp. This behaviour of the water drops – in the opinion of the present authors caused more by the interfacial tension than by viscosity – gives the explanation of the effect found. On increasing the amount of drops, coalescence cannot take place rapidly enough, and the drops are forced through the interface with an amount of the continuous phase. This amount of the continuous phase increases with the amount of the drops and causes too high an exit concentration. Therefore the mass transfer found will be too high.

This drag-effect will increase with decreasing area of the interface in the neck, and probably with increasing η_e. On the other hand an interface of small area has been chosen to decrease the mass transport from this interface to both phases separated. It may be remarked that very great differences in concentration could be observed in the water discharge line, while these were absent in the case of the isobutanol drops.

The drag effect decreases also with smaller column length, which could be caused by a lower isobutanol concentration. Experiments to verify this have till now not been very convincing.

In view of the above it is even dangerous to draw an experimental line through the points representing experiments with long θ_v for comparison with the Kronig line. However, for the longest column also starting from the largest θ_v used, in the first instance the ratio ϵ increases on decreasing θ_v. Therefore these points have been compared with the Kronig line, which for this purpose has been displaced in a vertical direction and given in Fig. 10 as the dotted line. From this it can be concluded that in the falling water drops material is also transferred by diffusion and by circulation. A very rough extrapolation of the experiments last mentioned shows a sum of entry- and end-effects of about 35% of the maximum possible, which is 1·8 times that of isobutanol.

The discontinuous entry-effect—As follows from the foregoing paragraph a quantitative knowledge about the discontinuous entry- and end-effects is necessary for a more detailed evaluation of the results. Several attempts have been made to measure this effect.

First of all the behaviour of the liquid in the drop during formation was investigated with isobutanol drops coloured blue with cobalt chloride. Above a certain water content the blue colour changes to pale pink. By means of this colour change it could be proved that drops formed in 1·3 sec or in shorter times showed a very marked circulation. If the time of formation was larger than 1·5 sec no circulation occurred. A marked pink zone was found in the lower part of the drop in which a vertical thin blue channel lying in the axis of the capillary was visible. The upper part was blue with the exception of a very thin film at the interface with the continuous water phase. During the formation the horizontal dividing plane moved upward with a velocity dependent on the velocity of formation.

Moreover on ascending, blue-coloured

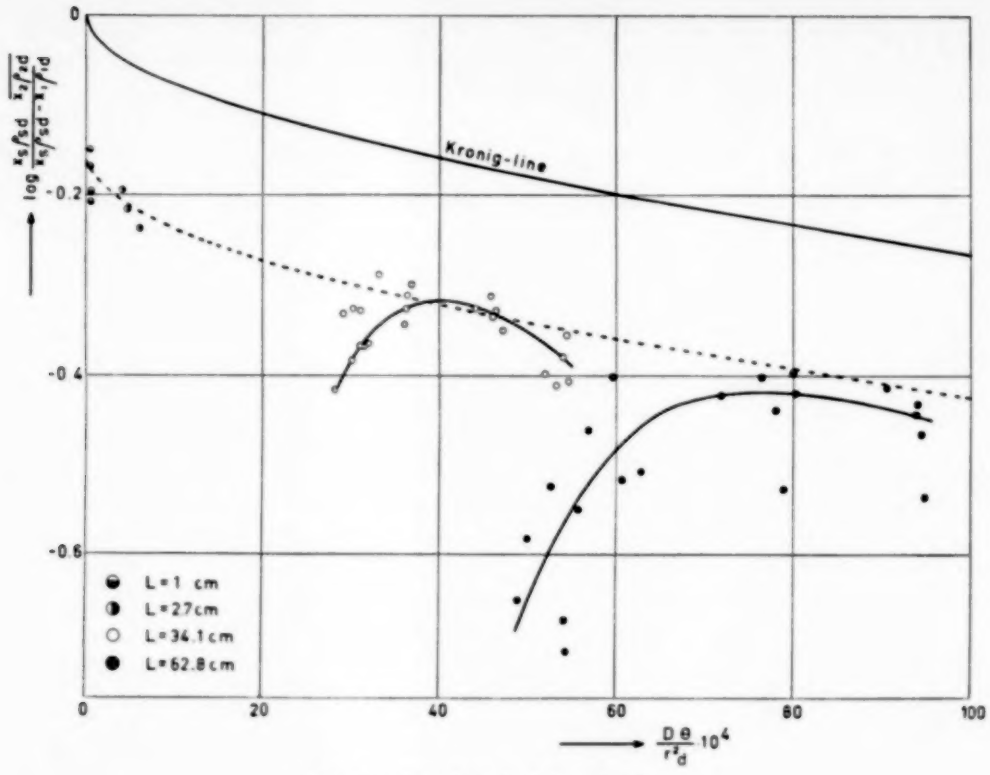

Fig. 10. Mass transfer into water drops.

isobutanol drops gradually changed their colour to pink in the whole drop, with a blue ring in the equatorial plane which disappeared last of all. This is in agreement with the theory of HADAMARD which demands that in a sphere with circulation a ring in the equatorial plane on a distance of $\frac{1}{2}\sqrt{2} \cdot r_d = 0{\cdot}71\, r_d$ from the centre is at rest. This again proves circulation in the isobutanol drops.

Although the time of formation in our experiments is shorter than 1·5 sec, an attempt to calculate the order of magnitude of the mass transfer during formation have been carried out under the following assumptions : diffusion takes place only ; the velocity of diffusion is small compared with the velocity of growing ; the drop is formed by introducing a constant amount of liquid (as in the experiments) of constant concentration (c_0 in moles/cm³) in the centre of the drop ; the drop is a sphere with constant boundary concentration (c_s in moles/cm³).

Applying HIGBIE's equation for the rate of transport (R) at the time θ in moles per sec per cm², $R = (c_s - c_0)\sqrt{\frac{D}{\theta\pi}}$ from a flat surface with a constant concentration (c_s) into a layer of infinite thickness having concentration c_0 at time $\theta = 0$, we obtain for the total rate of mass transfer (R') at timeθ in moles per sec to the inside of a drop :

$$R' = \int_0^O (c_s - c_0)\sqrt{\frac{D}{\theta\pi}} \cdot dO.$$

As $O^{2/3} = p_1 V_\theta = p_2 \theta$, in which p_1 and p_2 are constants the integration gives for the rate of mass transfer under consideration :

$$R' = 4\, p_2^{2/3}(c_s - c_0) \cdot \theta^{1/6}\sqrt{\frac{D}{\pi}}.$$

The mass transfer to the drop during the time

VOL. 3 1954

of formation θ_v therefore is, expressed in moles :

$$\int_0^{\theta_v} R'\,d\theta = \int_0^{\theta_v} 4\,p_2^{2/3}(c_s - c_0)\,\theta^{1/6}\sqrt{\frac{D}{\pi}}\,.\,d\theta =$$

$$= \frac{24}{7}\,p_2^{2/3}(c_s - c_0)\,\theta_v^{7/6}\sqrt{\frac{D}{\pi}}$$

$$= \frac{24}{7}\cdot\frac{p_1}{p_2^{1/3}}\,.\,V_\theta\,.\,(c_s - c_0)\,.\,\theta_v^{1/6}\sqrt{\frac{D}{\pi}}$$

This mass transfer can also be expressed as $(\bar{c}_\theta - c_0)\,V_\theta$. Therefore :

$$(\bar{c}_\theta - c_0)V_\theta = \frac{24}{7}\cdot\frac{p_1}{p_2^{1/3}}\,.\,(c_s - c_0)\,.\,V_\theta\theta_v^{1/6}\sqrt{\frac{D}{\pi}}\,.$$

By expressing p_1 and p_2 in d_θ (diameter of the sphere at time θ_v) and by rearranging one obtains :

$$\frac{\bar{c}_\theta - c_0}{c_s - c_0} = \frac{\overline{x_2\,\rho_{2d}} - x_1\,\rho_{1d}}{x_s\,\rho_{sd} - x_1\,\rho_{1d}} = 1 - \epsilon = \frac{20\,.\,6}{d_\theta}\cdot\sqrt{\frac{D\theta_v}{\pi}}$$

In Table 4 the experimental results for very short columns for water (1-5) and for isobutanol (71-76) have been collected together with the values calculated from the above equation.

Table 4

No. of experiment	θ_v *in sec.*	$\frac{\theta_v^{\frac{1}{2}}}{d_\theta}$ *in* $sec^{\frac{1}{2}}\,cm^{-1}$	$1-\epsilon$	
			found	*calculated*
71	0·24	2·47	0·196	0·0405
72	0·32	3·12	0·221	0·0513
73	0·38	3·52	0·228	0·0579
74	0·49	3·91	0·236	0·0642
75	0·89	5·61	0·253	0·0921
1	0·24	2·38	0·291	0·0676
2	0·34	2·92	0·319	0·0829
3	0·63	4·16	0·363	0·1182
4	1·18	5·90	0·380	0·1677

As in the equation $(1 - \epsilon)$ for the experiments increases with increasing $\theta_v^{\frac{1}{2}}\,.\,d_\theta^{-1}$ but not linearly. Moreover, the values found are much higher, which is easily understood because : the end effect still exists ; there will be some mass transfer in the short column ; circulation in the drop for the small θ_v used has been proved ; part of the drop after it has been released adheres to the capillary and finally surface oscillations caused by the release of the drop may occur.

A study of the entry- and end-effects must be made in a different way. Until now no success was met in this respect. Formation of drops 1 mm above the liquid surface and comparing those with drops formed 1 mm beneath the surface met with no success at all since a fall even over so short a distance in air caused deformation of the drops and in all cases a very strong turbulence in and around the drops. During these experiments in some cases a small bubble of air was trapped in the water drop. Photographically it was found that the bubble was always in the equatorial plane while the maximum distance of this bubble from the centre was found to be 0·6 r_d. This proves the circulation of the liquid in the water drops.

Experiments are now being pursued in a different direction.

B. *Mass transfer from the drops to the continuous phase*

The mass transfer from drops to the continuous phase is governed by two factors : (*a*) diffusion from the interface perpendicular to the direction of flow and (*b*) the liquid velocity along the surface of the sphere. It may be remarked that in our experiments only the immediate surroundings of the drops have to be included in the observations because of the mixing effect observed.

For a moving solid sphere the velocity at the interface can be assumed to be zero in respect to the sphere. In such a case, in view of the magnitude of the diffusion coefficients, mass transfer takes place mainly perpendicular to the surface and not over the surface. Therefore the concentration gradient in the direction of flow is small compared with that perpendicular to the direction of flow.

For a falling fluid sphere in which circulation takes place, the interface moves in respect to the centre of the sphere, if this centre is considered at rest. This implies that the top of the sphere in the direction of flow always meets fresh liquid. During the flow past the sphere mass is transferred into the stream from the interface by

diffusion and a concentration gradient is built up in the direction of flow as well as perpendicular to the direction of flow. Mass is transported mainly over the surface of the sphere in the direction of flow and leaves the sphere at the bottomside if the velocities are large compared with the diffusivities.

If the circulation in the fluid drop is limited by the fact that either η_d is not small compared with η_c or that the drop diameter becomes smaller than the critical diameter d_{cr}, defined by BOND and NEWTON [16] as :

$$d_{cr} = 2\sqrt{\frac{\gamma}{(\rho_d - \rho_c)\,g}},$$

the velocity at the interface in the continuous phase will accordingly diminish. In such cases the type of mass transfer from a fluid sphere can change gradually to that from a solid sphere.

The partial mass transfer coefficient for both types of mass transfer must depend in different ways on Re_d and Sc_c.

The correlation found so far in the literature takes the form $Sh = f + h\,Re_d^{\,b}\,Sc_c^{\,a}$. For a solid sphere, f which is the Sherwood number when there is no flow past the sphere, can be calculated from the theory as being 2·0.

For a solid sphere FRÖSSLING [17] found semi empirically $h = 0{\cdot}552$, $b = \frac{1}{2}$, $a = 1/3$. For gas bubbles PIETERS and VAN KREVELEN [18] found $f = 0$, $h = 1{\cdot}1$, $b = \frac{1}{2}$, $a = \frac{1}{2}$. For heat transfer from a solid sphere with constant surface temperature to a continuous medium RANZ [19] derived : $Nu = 2 + 0{\cdot}60\,Re_d^{0{\cdot}5}\,Pr^{1/3}$ which using either the Lewis or Chilton-Colburn analogy yields a mass transfer equation of the Frössling type.

For potential flow across a solid (or any other) sphere BOUSSINESQ [20] derived an equation for heat transfer : $Nu = 1{\cdot}13\,Pe^{0{\cdot}5} = 1{\cdot}13\,Re^{0{\cdot}5}\,Pr^{0{\cdot}5}$ or an analogy for mass transfer $Sh = 1{\cdot}13\,Re^{0{\cdot}5}\,Sc^{0{\cdot}5}$ (Pe = Peclet number).

The same type of equation can be derived by using the Higbie concept of mass transfer and assuming either potential flow across a solid sphere or using HADAMARD's stream function for the continuous phase, yielding : $Sh = h\,Re_d^{\,0{\cdot}5}\,Sc_c^{\,0{\cdot}5}$ in which h depends on the thickness of layer around the sphere in which a concentration gradient exists.

It seems quite safe to neglect f for the regions investigated. Moreover, in view of what has been said, the power of the Reynolds number can be assumed to be 0·5 in first approximation. For mass transfer from moving spheres to the continuous phase the following equation can then be given : $Sh = h\,Re_d^{\,0{\cdot}5}\,Sc_c^{\,a}$. Both h and a will depend on the circulation in and therefore outside the sphere. A measure for the type of flow will be the ratio between the liquid velocity at the interface of the sphere in an equatorial plane perpendicular to the direction of the undisturbed flow, to the velocity of the undisturbed flow, if the centre of the sphere is thought to be at rest.

For the Stokes' region of flow this ratio can be found from the Hadamard stream function and appears to be :

$$\frac{\eta_c}{2\,(\eta_c + \eta_d)}.$$

Although the Reynolds number indicates that the experiments have been carried out outside the Stokes' region, the ratio $\frac{\eta_c}{\eta_c + \eta_d}$ is taken as governing the magnitudes of both h and a.

For the experiments to be described however only a small variation of the Schmidt number was possible in each case. In view of the above and of the results discussed later a will be taken as 0·5, making h the only variable. An eventual variation in a will therefore manifest itself in h.

In Fig. 11 Sh as calculated has been plotted against $Re_d^{\frac{1}{2}}\,Sc_c^{\frac{1}{2}}$ with the exception of two experiments (see below). Excluding the experiments in which y_k was not measured but only calculated, for the three sets of points by means of the method of the least squares three straight lines are drawn which have the following equations :

isobutanol, $L = 62{\cdot}8$ cm : $Sh = -137 + 0{\cdot}98\,Re_d^{\frac{1}{2}}\,Sc_c^{\frac{1}{2}}$
isobutanol, $L = 34{\cdot}1$ cm : $Sh = -78 + 0{\cdot}96\,Re_d^{\frac{1}{2}}\,Sc_c^{\frac{1}{2}}$
water, $L = 62{\cdot}8$ cm : $Sh = -44 + 0{\cdot}80\,Re_d^{\frac{1}{2}}\,Sc_c^{\frac{1}{2}}$

The negative value found for f has no real significance, because an extrapolation of the lines

VOL. 3 1954

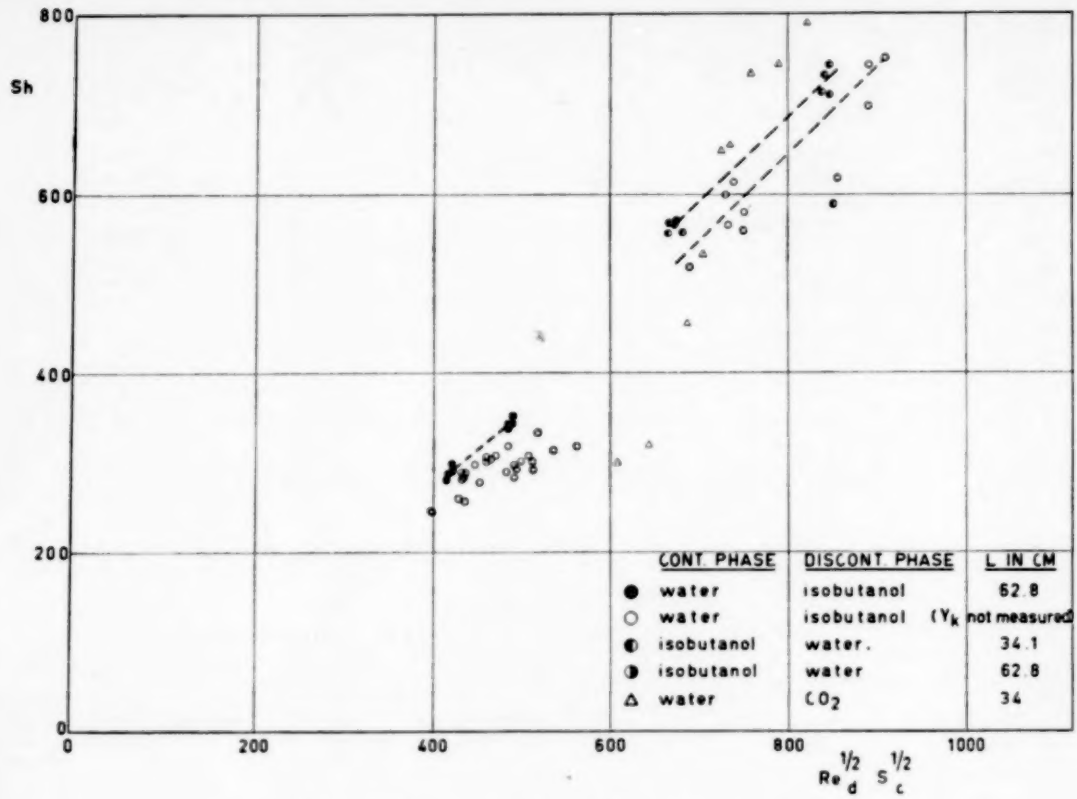

Fig. 11. *Sh* as a function of $Re_d^{\frac{1}{2}} Sc_c^{\frac{1}{2}}$ for the continuous phase.

found to $Re_d = 0$ is not permissible, because the number of experiments and the regions are rather small; moreover the line may be curved for smaller values of $Re_d\, Sc_c$.

A better method of determining the constant h is to neglect f and to determine h as the slope of the line drawn through every point and the origin (see below).

In Fig. 11 some experiments of GUYER and PFISTER [21] as carried out with CO_2 bubbles in water have also been included. Their experiments enable one to calculate *Sh* and $\frac{vd_d}{D} = Re_d\, Sc_c$, if it may be assumed that the resistance in the gas phase can be neglected compared with that in the liquid phase and moreover that the CO_2 concentration in the bulk of the continuous phase is zero.

In the experiments in question a slight influence of y_k on *Sh* can be observed, in this sense that h decreases with increasing y_k as measured. The value for y_k is a mean value of the core and of the stream along the wall which has a lower concentration. The mean value used for y_k therefore will be somewhat too low, which will manifest itself in a Sherwood number that is too low.

The influence will be larger if y_k is near y_s. This is clearly seen in the two experiments which have been excluded from Fig. 11 (see before). Here y_k as calculated was 12·9 and 13·8. A fairly small increase to 13·7 and 14·1 respectively would bring the Sherwood number on the line calculated.

Also for the continuous phase entry- and an end-effect will be present. These effects however will be smaller than for the discontinuous phase. In view of the concentration distribution in the column during formation and during coalescence the driving force will not be far from $(y_s - y_k)$.

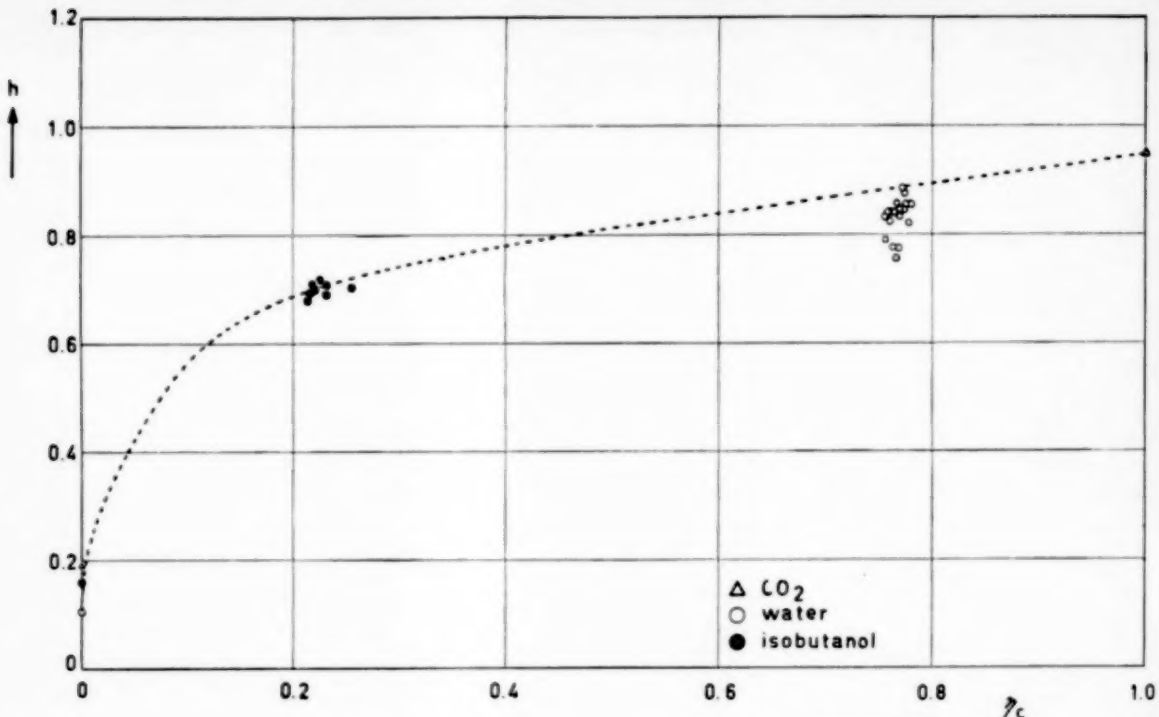

Fig. 12. The factor h as a function of $\frac{\eta_c}{\eta_d + \eta_c}$.

Near the capillaries a marked concentration gradient has been found outside the exchange region, moreover the same was the case near the inlet of the continuous phase. For isobutanol as the continuous phase the stagnant layer beneath the inlet had a concentration of 15%, which must be compared with $y_s = 16{\cdot}6\%$. The product for partial mass transfer and surface will be small for the entry- and end-effects compared with that for the rising and falling drops. Therefore the partial mass transfer as calculated will be somewhat larger than that actually existing. The relative difference will become larger if the column is shorter and will disappear with a column of infinite height.

The equations as found for the Sherwood number for isobutanol confirm this. This can also be concluded from the experiments using water as a continuous phase. Even for the very short column this tendency is present, although the stability of this phase is very poor owing to the influence of the entering and leaving stream.

To compare the mass transfer from solid spheres, isobutanol and water drops and CO_2 bubbles to a continuous phase in Fig. 12, the factor h as described ($h = Sh/Re_d^{\frac{1}{3}} Sc_c^{\frac{1}{3}}$) is plotted against $\frac{\eta_c}{\eta_c + \eta_d}$, for the isobutanol and water drops and for the CO_2 bubbles with total circulation, as well as the values which would follow if in these cases the drops behaved as solid spheres in which case h according to the Frössling equation would be $0{\cdot}552/Sc_c^{1/6}$. The values used in this last case are given in Table 5.

In Fig. 12 only these experiments have been

Table 5

Discontinuous phase	Sc_c	$0{\cdot}522/S_c^{1/6}$	h
CO_2	570	0·19	0·96
isobutanol	1790	0·16	0·70
water	23600	0·10	0·85

VOL. 3 1954

Table 6

Lit.	*Dis-continuous phase*	*Continuous phase*	η_d/η_c	γ *dyne/cm*	$\Delta\rho$ *g/cm³*	d_{cr} *in cm*	d_{cr} *in cm measured*
16	air	waterglass	10^{-7}	104	1·69	0·5	0·33
16	air	golden syrup	10^{-6}	91	1·48	0·5	0·33
16	air	water	0·018	73	1·0	0·5	0·33
21	CO_2	water	0·015	73	1·0	0·5	0·35 (?)

included in which the velocity at the drop surface was at the maximum possible, therefore for drops with total internal circulation, for which $d_d > d_{cr}$.

From the experiments of GUYER and PFISTER it can be calculated that an increase in d_d, goes parallel with an increase in $Sh/(Re_d\,Sc_c)^{\frac{1}{2}}$. Starting from 0·49 for drops of 0·18 cm, for drops of about 0·47 cm and larger $Sh/Re_d^{\frac{1}{2}}\,Sc_c^{\frac{1}{3}}$ becomes constant (*ca.* 0·96). The critical diameter in this case would be of the order of 0·35 cm. Some other values as given in the literature are collected in Table 6 in which the critical diameters as calculated from $d_{cr} = 2\sqrt{\frac{\gamma}{\Delta\rho\,.\,g}}$ have also been collected.

For the isobutanol drops (0·15-0·18 cm) and the water drops (0·17-0·22 cm) the calculated $d_{cr} = 0{\cdot}2$ cm. In view of the fact that the calculated data seem somewhat high because the experiments lie outside the Stokes' region, complete internal circulation has also been assumed in these drops.

The results discussed permit the conclusion that for mass transfer from CO_2, isobutanol and water drops to a continuous phase the Sherwood number is directly proportional to $Re_d^{0{\cdot}5}$.

The data given in Table 5 indicate that in these cases Sh is also directly proportional to $Sc_c^{0{\cdot}5}$ and h therefore a real constant independent of Re_d and Sc_c.

Starting from solid spheres (or spheres which behave as such, like a liquid drop in a gas) the proportionality constant h based on $Sh = h\,Re_d^{0{\cdot}5}\,Sc_c^{0{\cdot}5}$ increases rapidly on increasing the ratio $\frac{\eta_c}{\eta_c+\eta_d}$, that is on decreasing η_d from ∞ to 0, if the maximum internal circulation is possible.

Between zero and a certain value >0 of $\frac{\eta_c}{\eta_c+\eta_d}$ which might be very close to zero, h will depend on the Schmidt number as follows from the foregoing. In these cases $h = h'\,(Sc)_c^{-m}$, in which h' and m (varying from 1/6 to 0) are real constants. Both h and h' and also m, are a function of $\frac{\eta_c}{\eta_c+\eta_d}$. For $\eta_d = \infty$, h' reaches the value 0·552 and m the value of 1/6.

The value of $\frac{\eta_c}{\eta_c+\eta_d}$ at which m becomes zero is not yet known. As said above this value might be very close to zero.

If the condition that the diameter of the drop is larger than the critical diameter is not fulfilled, the constant h will be lower than that found for drops with the maximum internal circulation. The limiting case is that the drops become so small that no circulation at all will occur, in which case the drop will behave as if solid.

Part of the experimental work has been carried out by D. FLEMMING, R. E. LITAN, P. L. SLEVEN and A. M. A. J. TIELENS as partial fulfilment for the examination for Chemical Engineer.

The authors should like to thank at this place Prof. H. KRAMERS and Prof. R. VAN DE LAAR KRONIG for valuable discussions on parts of the work.

NOTATION

a = power of Sc_c
A = number of drops per sec
A_n = constant in n^{th} term of a series
b = power of Re_d
c = concentration in moles/cm³
d = diameter of drop in cm
D = diffusion coefficient in cm²/sec

f = Sherwood number in stagnant medium
g = acceleration of gravity, cm/sec^2
h, h' = proportionality constants
ΔH = head of flow meter in cm of liquid
i, i' = constants
k = partial mass transfer coefficient in cm/sec
m = power of Sc_c
n = index of refraction
Nu = Nusselt number
O = surface of drops in cm^2
P = amount of drops
Pe = Peclet number
Pr = Prandtl number
p_1, p_2 = constants
q = weight fraction isobutanol
Q = amount of continuous and discontinuous phase in cm^3/sec
r = radius of drop in cm
R = velocity of mass transport in moles/sec cm^2
R' = rate of mass transfer in moles/sec per drop
Re_d = Reynolds number $\frac{v_d\, d_d\, \rho_c}{\eta_c}$
Sc_c = Schmidt number $\frac{\eta_c}{\rho_c\, D}$
Sh = Sherwood number $\frac{k_c\, d_d}{D}$
t = temperature in °C
v = velocity of drop in cm/sec
V = volume of drop in cm^3
x = concentration of substance in smallest amount present in discontinuous phase in weight %
y = concentration of substance in smallest amount present in continuous phase weight %
α = half short axis of ellipsoid in cm
β = half long axis of ellipsoid in cm
γ = surface tension in dyne/cm
ϵ = ratio $\frac{x_s\, \rho_{sd} - x_2\, \rho_{2d}}{x_s\, \rho_{sd} - x_1\, \rho_{1d}}$
η = viscosity in poise
θ = time in sec
μ_n = constant in n^{th} term of a series
ρ = density in g/cm^3

Subscripts

c = of the continuous phase
cap. = per capillary
cr = critical
d = of the discontinuous phase
k = of the column
i = of isobutanol
m = of the mixture
s = at the surface of a drop
t = at temperature t
v = after formation of the drop
w = of water
θ = at time θ
0 = at time zero
1 = of the entering stream
2 = of the exit stream

REFERENCES

[1] SHERWOOD, T. K., EVANS, J. E. and LONGCOR, J. V. A.; Trans. Amer. Inst. Chem. Engrs. 1939 **35** 597 ; Ind. Eng. Chem. 1939 **31** 1144.

[2] LICHT, W. and CONWAY, J. B.; Ind. Eng. Chem. 1950 **42** 1151.

[3] COLBURN, A. P. and WELSH, D. G.; Trans. Amer. Inst. Chem. Engrs. 1942 **38** 179.

[4] LADDHA, G. S. and SMITH, J. M.; Chem. Eng. Prog. 1950 **46** 195.

[5] MITCHELL, J. and SMITH, D. M.; Aquametry, New-York, 1948.

[6] JOHANSSON, A.; Svensk Papperstidn, 1947 **50** nr. 11 B, 124.

[7] MICHELS, A.; Arch. Neerland, Series III a, 1923 **6** 127.

[8] WIENER, O.; Ann. Phys. Chem. 1893 **49** 105.

[9] THOVERT, M. J.; Ann. Phys. (9th series) 1914 **2** 369 ; Ann. Chim. Phys. (7th series) 1902 **26** 366.

[10] LAMM, O.; Z. Phys. Chem. 1928 A **138** 313.

[11] NEWMAN, A. B.; Trans. Amer. Inst. Chem. Engrs. 1931 **27** 310.

[12] HIGBIE, R.; Trans. Amer. Inst. Chem. Engrs. 1935 **31** 365.

[13] HADAMARD, J.; Comptes Rendus 1911 **152** 1735.

[14] KRONIG, R. and BRINK, J. C.; Appl. Sci. Res. 1950 A **2** 142.

[15] MAHAJAN, L. D.; Phil. Mag. [7] 1930 **10** 383.

[16] BOND, W. N. and NEWTON, D. A.; Phil. Mag. [7] 1928 **5** 794.

[17] FRÖSSLING, N.; Gerl. Beitr. Geophys. 1938 **52** 170.

[18] PIETERS, H. A. J. and VAN KREVELEN, D. W.; The wet purification of coal gas and similar gases by the Staatsmijnen-Otto process, Amsterdam, 1946, p. 28.

[19] RANZ, W. E.; Chem. Eng. Prog. 1952 **48** 247.

[20] BOUSSINESQ, J.; J. Math. [6] 1905 **1** 285.

[21] GUYER, A. and PFISTER, X.; Helv. Chim. A 1946 **29** 1173, 1400.

VOL. 3 1954

Book review

Fourth Symposium on Combustion. Baillière Tindall and Cox, London. 1953. xx + 926 pp. 56s.

Combustion research has been expanding rapidly during recent years. Whereas 400 people attended the Third Symposium in 1948, more than 700 were attracted to the Fourth Symposium at M.I.T. in September 1952. The scope of the Fourth Symposium was deliberately limited to the physical aspects of combustion, especially flame phenomena and turbulence. Despite this restriction, 112 papers, more than in the Third Symposium, were finally accepted and published in this account of the proceedings.

A new feature of this series of Symposia, is the inclusion of nine invited survey papers, which occupy the first 113 pages of this volume. These reviews increase considerably the value of the book to the general reader. Their subjects illustrate the scope of the Symposium, dealing with limits of inflammability; ignition; burning velocity measurements; laminar flame structure; instabilities such as cellular flames; quenching, flashback, and blowoff; turbulent flames; burning of fuel jets; and flame stabilisation by baffles placed in the stream.

The largest group of papers, 50 in all, falls under the heading of laminar combustion and detonation waves. Theoretical analysis has become possible for more simple flames while there is experimental work on the effects of pressure and inert diluents with increased precision in the measurement of temperature profiles and burning velocities. The papers on premixed turbulent flames show how the concept of the wrinkled flame front is being refined. In the more applied section, although the main impetus comes from problems arising in rocket and jet engines, there are about a dozen papers concerned with the burning of fuel jets and droplets relevant to furnace combustion.

The amount of space devoted to discussion, about 2%, is rather limited; only a fifth of the papers receive any comments but these are usually pertinent and concise. The book contains a large number of diagrams and photographs. The production and binding are excellent, and as the result of a subsidy, the price is exceptionally low. It can be warmly recommended to all concerned with combustion problems.

J. C. Lee.

Conference on Oxidation Processes (Amsterdam)

A Joint Conference of the Institution of Chemical Engineers and Chemical Engineering Group of the Society of the Chemical Industry in London with the Royal Institution of Engineers (Chemical Engineering Group of the Netherlands) and the Royal Netherlands Chemical Society (Section for Chemical Technology) on Oxidation Processes, was held in Amsterdam on 6th, 7th and 8th May, 1954. The papers presented at the Conference are given below. Arrangements for publication of these papers, together with the relevant discussions, through the medium of *Chemical Engineering Science*, are now being discussed.

The BASF-process for production of acetylene by partial oxidation of gaseous hydrocarbons by E. Bartholomé, Ammoniaklabatorium der Badischen Analin- & Soda-Fabrik A.G., Ludwigshafen a. Rhein, Germany.

Oxygen processes in the steel industry by W. J. B. Chater, The British Oxygen Company Ltd., Morden Factory Estate, London.

The provision of oxygen for industrial processes by A. M. Clark, The British Oxygen Company Ltd., Morden Factory Estate, London.

The development of a process for the manufacture of p-tertiary-butyl-benzoic acid by R. M. Cole, A. W. Fairbairn and K. D. Detling, Shell Development Company, Emeryville, California, U.S.A.

The use of oxygen in gasification by F. J. Dent, West Midlands Gas Board, Birmingham, England.

The air oxidation of mixtures of benzene and cyclohexane to phenol by M. B. Donald and J. R. Grover, Ramsay Laboratory of Chemical Engineering, University College, London.

Preparation of cumene hydroperoxide by J. P. Fortuin and H. I. Waterman, Laboratory of Chemical Engineering, Delft Technological University, Holland.

Nitric acid oxidation design in the manufacture of adipic acid from cyclohexanol and cyclohexanone by A. F. Lindsay, Imperial Chemical Industries Ltd., Dyestuffs Division, Billingham, Co. Durham, England.

Oxidations carried out by means of vanadium oxide catalysts by J. Mars and D. W. van Krevelen, Staatsmijnen in Limburg, Central Laboratory, Geleen, Holland.

The mechanism of liquid-phase oxidation by G. H. Twigg, The Distillers Company Ltd., Great Burgh, Epsom, Surrey, England.

Herstellung synthetsicher Fettsauren durch Oxydation von Paraffinischen Kohlenwasserstoffen mit Molekularem Sauerstoff by G. Wietzel.

VOL.
3
1954